UNIVERSIDADE FEDERAL DO PARANÁ

FÁBIO BERTON

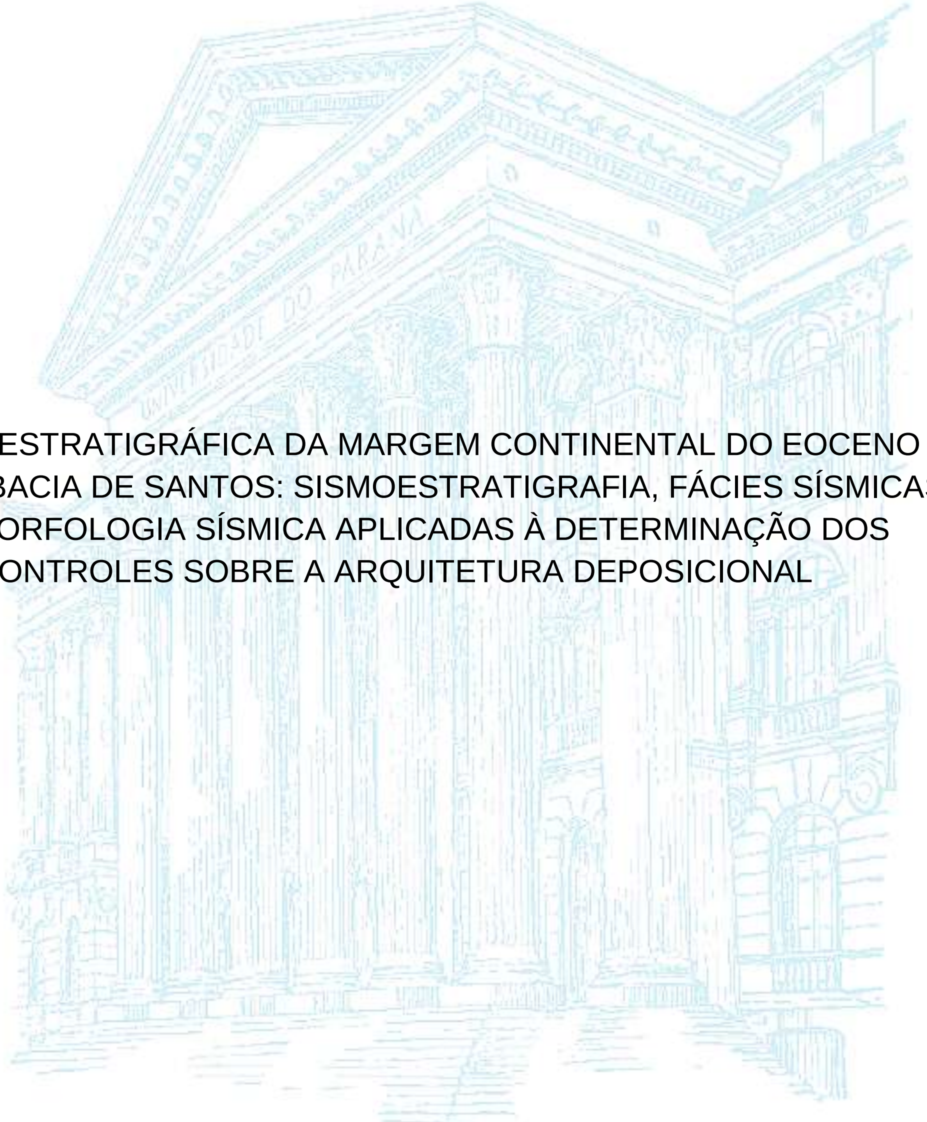

EVOLUÇÃO ESTRATIGRÁFICA DA MARGEM CONTINENTAL DO EOCENO NO NORTE DA BACIA DE SANTOS: SISMOESTRATIGRAFIA, FÁCIES SÍSMICAS E GEOMORFOLOGIA SÍSMICA APLICADAS À DETERMINAÇÃO DOS CONTROLES SOBRE A ARQUITETURA DEPOSICIONAL

CURITIBA

2016

FÁBIO BERTON

EVOLUÇÃO ESTRATIGRÁFICA DA MARGEM CONTINENTAL DO EOCENO NO NORTE DA BACIA DE SANTOS: SISMOESTRATIGRAFIA, FÁCIES SÍSMICAS E GEOMORFOLOGIA SÍSMICA APLICADAS À DETERMINAÇÃO DOS CONTROLES SOBRE A ARQUITETURA DEPOSICIONAL

Dissertação apresentada como requisito à obtenção do grau de Mestre em Geologia, no Programa de Pós-Graduação em Geologia, Setor de Ciências da Terra, Universidade Federal do Paraná.

Orientador: Prof. Dr. Fernando Farias Vesely

CURITIBA

2016

B547e Berton, Fábio

Evolução estratigráfica da margem continental do eoceno no norte da bacia de Santos : sismoestratigrafia, fácies sísmicas e geomorfologia sísmica aplicadas à determinação dos controles sobre a arquitetura deposicional/ Fábio Berton. – Curitiba, 2016.

114 f. : il. color. ; 30 cm.

Dissertação - Universidade Federal do Paraná, Setor de Ciências da Terra, Programa de Pós-graduação em Geologia, 2016.

Orientador: Fernando Farias Vesely .
Bibliografia: p. 100-114.

1. Geologia estratigráfica. 2. Sedimentos (geologia). 3. Transporte de massa. I. Universidade Federal do Paraná. II.Vesely, Fernando Farias. III. Título.

CDD: 551.36

TERMO DE APROVAÇÃO

FÁBIO BERTON

"Evolução estratigráfica da margem continental do Eoceno no norte da Bacia de Santos: sismoestratigrafia, fácies sísmicas e geomorfologia sísmica aplicadas à determinação dos controles sobre a arquitetura deposicional."

Dissertação de Mestrado aprovada como requisito parcial para obtenção do grau de Mestre no Programa de Pós-Graduação em Geologia, área de concentração em Geologia Exploratória, da Universidade Federal do Paraná. Comissão formada por:

Prof. Dr. Mario Luis Assine - Unesp

Prof. Dr. Rodolfo José Angulo - UFPR

Prof. Dr. Fernando Farias Vesely - UFPR
Presidente

Curitiba, 18 de dezembro de 2015.

DEDICATÓRIA

Dedico este trabalho a Renata Zanella: nenhum desafio é demais com você ao meu lado.

AGRADECIMENTOS

Agradeço ao meu orientador, Prof. Dr. Fernando F. Vesely pela paciência, dedicação e amizade ao longo dos últimos anos.

Agradeço à Universidade Federal do Paraná (UFPR), pela infraestrutura, apoio e oportunidades desde meu ingresso na graduação, em 2008.

Agradeço à estrutura e excelente ambiente de trabalho oferecido pelo Laboratório de Análise de Bacias (LABAP), assim como à Profa. Dra. Bárbara Trzaskos e aos colegas de laboratório Amanda Carvalho, Danielle Schemiko, Leonardo Barão, Matheus Eler, Mérolyn Rodrigues e Thammy Mottin pela amizade e companheirismo.

Agradeço o apoio financeiro da Agência Nacional do Petróleo, Gás Natural e Biocombustíveis – ANP – , da Financiadora de Estudos e Projetos – FINEP – e do Ministério da Ciência, Tecnologia e Inovação – MCTI por meio do Programa de Recursos Humanos da ANP para o Setor Petróleo e Gás – PRH-ANP/MCTI.

Agradeço o esforço das professoras Maria José J. de S. Ponte e Renata B.G. Valt para manter a ótima qualidade do programa.

Agradeço ao Programa de Pós-Graduação em Geologia de UFPR e a todos seus membros, em especial agradeço pela dedicação do funcionário Kazutoshi Milton Matsugano.

Agradeço também ao Banco de Dados de Exploração e Produção da Agência Nacional do Petróleo, Gás Natural e Biocombustíveis (BDEP-ANP) pelo fornecimento do banco de dados de excelente qualidade.

Agradeço as correções e sugestões para a melhoria do trabalho, dos professores Dr. Rodolfo José Angulo e Dr. Mario Luis Assine.

Agradeço aos meus pais, Carmen e Marcos, por toda uma vida de apoio e incentivo. Minhas conquistas também são suas.

Por fim, agradeço à minha companheira e amiga, Renata Zanella. De me fazer sorrir nas dificuldades até as discussões sobre ciência no final do dia, lhe agradeço por estar presente em todos os momentos. Obrigado pelo seu apoio inestimável.

Nullius in verba

Lema da Royal Society

RESUMO

A estratigrafia de sequências tem sido utilizada com sucesso na análise estratigráfica em subsuperfície, mas quando aplicada em conjunto com técnicas mais modernas de análise do dado sísmico se mostra mais confiável para o estudo das condições ambientais durante a deposição, da arquitetura deposicional e estudo da gênese de elementos deposicionais e feições erosivas. Dentre estas técnicas, se destacam a análise de trajetórias de migração da margem da plataforma, a identificação de fácies sísmicas e a geomorfologia sísmica. O objeto de estudo deste trabalho é o intervalo eoceno no norte da Bacia de Santos, formado em um período de aporte sedimentar alto e de predomínio de rebaixamentos do nível de base. O objetivo é utilizar em conjunto técnicas clássicas e modernas da sismoestratigrafia para determinar como estas condições afetaram a arquitetura deposicional e o transporte de sedimentos para o ambiente marinho profundo em uma margem passiva, assim como analisar as mudanças ambientais no final do período que alteraram o estilo deposicional na bacia. Como resultado do alto aporte sedimentar, foram formadas geometrias progradantes, que registram migração da margem da plataforma de até 30 km em direção à bacia. As principais fácies sísmicas identificadas correspondem a deltas de margem de plataforma e clinoformas de talude com trajetórias descendentes e *topsets* truncados, aos quais ocorrem associados turbiditos arenosos, depósitos de transporte em massa (DTMs) e depósitos continentais a plataformais. Os últimos, formados em períodos de subida do nível de base e agradação na plataforma, são truncados na sua terminação distal por cicatrizes de escorregamento no talude, às quais se encontram associados os DTMs. Portanto, a gênese dos DTMs está relacionada ao colapso gravitacional do talude. Os turbiditos arenosos, compostos por sistemas de canais submarinos e espraiamentos frontais, estão associados aos deltas de margem de plataforma, que constituem as principais fontes dos fluxos de turbidez. Na estratigrafia de sequências foram determinadas sete sequências deposicionais compostas por tratos de sistemas de regressão forçada e de mar baixo, que refletem um período em que, mesmo em momentos de subida do nível do mar, o aporte de sedimentos foi alto o suficiente para resultar em regressões normais. Cartas cronoestratigráficas mostram que a deposição de turbiditos foi abundante em todo o intervalo, o que indica que o principal controle para a formação destes depósitos foi o alto aporte sedimentar. Os DTMs, por outro lado, ocorrem na transição de regressões normais para regressões forçadas, e seu volume é proporcional à espessura dos depósitos de *topset* formados antes do colapso do talude. A mudança do estilo deposicional no final do período está associada a mudanças tectônicas e climáticas que afetaram o aporte sedimentar para a bacia. Como consequência, as geometrias progradantes dão lugar a registros transgressivos do Oligoceno. A transição do Eoceno para o Oligoceno no norte da bacia é uma superfície de afogamento onde são observadas feições erosivas relacionadas à ação de correntes de fundo de alta energia recém-estabelecidas sob as novas condições ambientais.

Palavras-chave: estratigrafia de sequências; turbiditos; depósitos de transporte em massa; trato de sistemas de regressão forçada; *comet marks*

ABSTRACT

Sequence stratigraphy have been successfully applied in the stratigraphic analysis of subsurface deposits, but when applied altogether with modern techniques of analysis of seismic data, it becomes a more reliable tool for the determination of environmental conditions during deposition, depositional architecture, and studies about the genesis of depositional elements and erosive features. Amongst these techniques, studies of shelf-margin trajectory, identification of seismic facies and seismic geomorphology can be pointed as key complementary tools. The target of the present study is the Eocene interval in north Santos Basin, deposited during a period of high sediment supply and mainly base-level falls. The scope is to determine how these conditions affected depositional architecture and sediment supply to deep-marine environments, as well as to analyze the environmental changes in the end of the period, which affected the depositional style in the basin. As a result of the environmental conditions, essentially prograding geometries were formed, registering a shelf-break migration that reaches 30 km basinward. The main identified facies correspond to shelf-margin deltas and slope-accretion clinoforms with descendant trajectories and truncated topsets. Sand-rich turbidites, mass-transport deposits (MTDs) and continental to shelfal deposits are associated to the clinoforms. Shelfal deposits, formed during periods of base level rise and aggradation on the shelf, are truncated in their distal domain by slump scars. MTDs are associated with these scars, and their genesis is related to slope gravitational collapse. Sand-rich turbidites, composed by submarine channels and frontal splays, are associated to shelf-margin deltas, as these are the main source for turbiditic flows. Seven depositional sequences were defined in the sequence-stratigraphic analysis, mainly composed by falling-stage and lowstand systems tracts, reflecting a period in which, even in moments of base level rise, sediment supply was high enough to result in normal regressions. Chronostratigraphic charts show that turbidite deposition was abundant during the whole interval, indicating that the main control for formation of these deposits was the high sediment supply. MTDs, on the other hand, occur in the transition between a normal regression and the onset of forced regression, and their volumes are proportional to the thickness of pre-slump topset deposits. Changes of depositional style in the end of the period are related to tectonic and climatic changes that affected the sediment supply to the basin. As a consequence, the prograding geometries gave place to transgressive records. Eocene-Oligocene transition in north Santos Basin is seismically expressed as a drowning surface with bottom-current-related erosive features, formed in a context of recently-established high energy flows under the new environmental conditions.

Keywords: sequence stratigraphy; turbidites; mass-transport deposits; falling-stage systems tract; comet marks

LISTA DE FIGURAS

Figura 1: Modelo de tratos de sistemas deposicionais, onde o principal momento de transporte de sedimentos para o ambiente marinho profundo ocorre durante o trato de sistemas de regressão forçada 4

Figura 2: Mapa de localização da Bacia de Santos, com localização da área de estudo e dos campos produtores de petróleo 7

Figura 3: Carta estratigráfica da fase drifte da Bacia de Santos, com destaque à Progradação Juréia e ao intervalo eoceno 8

Figura A1: Mapa de localização da Bacia de Santos, e carta estratigráfica da fase pós-rifte da bacia, com indicações do principais eventos de inundação, da progradação Juréia e do intervalo eoceno 14

Figura A2: Mapa de localização da área de estudo e dos dados utilizados 17

Figura A3: Interpretação das principais superfícies estratigráficas relacionadas ao intervalo eoceno em seção sísmica *dip* 18

Figura A4: Seção sísmica *dip* com interpretação das superfícies limítrofes do intervalo eoceno e das sete fácies sísmicas identificadas no intervalo 19

Figura A5: Esquema de classificação de clinoformas com base em sua geometria 20

Figura A6: Interpretação de deltas de margem de plataforma em sísmica 3D 20

Figura A7: Seções sísmicas *dip* com interpretação das geometrias de clinoformas de talude. Foram representadas clinoformas tangenciais oblíquas (A e B), clinoformas sigmoides de alto ângulo (C e D) e clinoformas complexas sigmoides-oblíquas de alto ângulo (D e E) 22

Figura A8: Seção sísmica *dip* com interpretação de deltas de margem de plataforma, clinoformas tangenciais oblíquas, refletores de *bottomset* e turbiditos arenosos, interceptados pelo poço projetado à direita 25

Figura A9: Horizontes sísmicos mostrando sistemas de canais e espraiamentos frontais submarinos que compõem os turbiditos na área de estudo (A, B, E e F), e interpretação de canais submarinos e leques turbidíticos do Golfo do México 26

Figura A10: Seções sísmicas *strike* e *dip* com interpretação de depósitos de transporte em massa, interceptados no poço projetado à direita. Notar a presença de falhas e dobras abertas. Abaixo, interpretação de cicatriz de escorregamento, depósito de transporte em massa e blocos de composição arenosa 28

Figura A11: Seção sísmica *dip* com interpretação dos dois principais depósitos de transporte em massa da área de estudo (MTD 1 e MTD 2), e mapas de isópacas de cada depósito 29

Figura A12: Horizonte sísmico correspondente à principal cicatriz de escorregamento da área, truncando depósitos de *topset*. Notar o desenvolvimento de cânions que atuaram como pontos preferenciais ao transporte de sedimentos para o mar profundo 30

Figura A13: Refletores de *topset* com padrão de migração das terminações em *onlap* em direção ao continente, e truncados em sua terminação distal por cicatriz de escorregamento 31

Figura A14: Seção sísmica *dip* com interpretação das associações de fácies sísmicas geneticamente relacionadas 32

Figura B1: Mapa de localização da Bacia de Santos na margem sudeste brasileira e carta estratigráfica da fase drifte 52

Figura B2: Seção sísmica regional da Bacia de Santos, com interpretação das principais superfícies cronoestratigráficas 53

Figura B3: Mapa de localização da área de estudo e dados utilizados no artigo 54

Figura B4: Seção sísmica *dip* com interpretação das principais fácies sísmicas identificadas, correspondendo a deltas de margem de plataforma (A), clinoformas tangenciais oblíquas (B), clinoformas sigmoides (C), depósitos continentais a plataformais (D), e depósitos de transporte em massa (E) 56

Figura B5: Seção sísmica *dip* e interpretação de deltas de margem de plataforma, clinoformas de talude, refletores de *bottomset* e turbiditos arenosos, interceptados pelo poço projetado à direita 58

Figura B6: Seções sísmicas *strike* e *dip* com interpretação de depósitos de transporte em massa, interceptados no poço projetado à direita. Abaixo, interpretação de cicatriz de escorregamento, depósito de transporte em massa e blocos de composição arenosa .. 60

Figura B7: Seção sísmica *dip* com interpretação dos dois principais depósitos de transporte em massa da área de estudo, e mapas de isópacas para cada depósito 61

Figura B8: Seção sísmica *dip* com interpretação das sete principais sequências e seus respectivos limites de sequências do intervalo eoceno 63

Figura B9: Seções sísmicas *dip* com interpretação das principais sequências do intervalo eoceno e trajetórias de migração da margem da plataforma 64

Figura B10: Mapas de migração da quebra da plataforma para cada sequência 65

Figura B11: Diagrama de Wheeler com representação das sequências e limites de sequências, e projeção de ocorrências de turbiditos arenosos e depósitos de transporte em massa 68

Figura B12: Seção sísmica *dip* com interpretação dos tratos de sistemas deposicionais de regressão forçada e de mar baixo no intervalo eoceno 70

Figura B13: Modelo conceitual da instabilidade do talude e geração de depósitos de transporte em massa, e interpretação da superfície basal de regressão forçada 74

Figura C1: Mapa de localização da Bacia de Santos e carta estratigráfica da fase drifte da bacia, com destaque às principais progradações durante a fase de progradações Juréia (setas em verde) e à transgressão na transição do Eoceno para o Oligoceno (seta vermelha) 87

Figura C2: Seção sísmica 2D *dip* com interpretação das principais superfícies estratigráficas regionais, e indicação das principais progradações do Paleógeno e da transgressão no limite Eoceno-Oligoceno 88

Figura C3: Mapa de localização da área de estudo e projeção dos dados sísmicos utilizados na pesquisa 89

Figura C4: Indicação de *comet marks* (setas em azul) em seções sísmicas 2D *strike* e *dip*. Notar as ocorrências de deltas de margem de plataforma e clinoformas de talude sotopostos 91

Figura C5: *Comet marks* observadas em *inline* do volume sísmico 3D, e visões em planta e perspectiva das feições em horizonte sísmico (amplitude e decomposição espectral), com interpretação da direção das paleocorrentes 92

Figura C6: Interpretação das formas e do preenchimento das *comet marks* em seções sobre o horizonte sísmico, e morfologia de uma feição 93

Figura C7: Interpretação de chaminés de gás a partir de deltas de margem de plataforma do Eoceno, e modelo de geração de *pockmarks* no leito submarino a partir da ascensão de gás 94

Figura C8: Interpretação de *comet marks* em horizonte sísmico (decomposição espectral) e diagrama de rosetas mostrando a direção das paleocorrentes 97

Figura C9: Modelo conceitual do desenvolvimento de *comet marks* a partir da ação de correntes de fundo sobre *pockmarks* originadas pela ascensão de gás 98

LISTA DE ABREVIATURAS

ANP – Agência Nacional do Petróleo, Gás Natural e Biocombustíveis

BDEP – Banco de Dados de Exploração e Produção

BSFR – basal surface of forced regression

DTM – depósito de transporte em massa

ETM – Eocene thermal maximum

FSST – falling-stage systems tract

LST – lowstand systems tract

MTD – mass-transport deposit

NRM – nível relativo do mar

NE – nordeste/northeast

NW – noroeste/northwest

SB – sequence boundary

SE – sudeste/southeast

SW – sudoeste/southwest

TWT – two-way-time

LISTA DE UNIDADES

km – quilômetro/kilometer

km^2 – quilômetro quadrado/square kilometer

m – metro/meter

Ma – milhões de anos

$m\ s^{-1}$ – meters per second

ms – milissegundo/millisecond

My – million years

SUMÁRIO

1. INTRODUÇÃO 1

1.1 Estrutura da Dissertação 1

1.2 Análise do Problema e Motivação da Pesquisa 3

1.3 Objetivos 5

1.4 Contexto Geológico e Localização 6

2. RESULTADOS E DISCUSSÕES 11

2.1 Seismic expression of depositional elements associated with a strongly progradational shelf margin: northern Santos Basin, southeastern Brazil ……..... 11

2.1.1 ABSTRACT ……………..…………………………………………………………... 12

2.1.2 INTRODUCTION …………………………………………………………………... 13

2.1.3 REGIONAL SETTING …………………………………………………………….. 14

2.1.4 DATASET AND METHODS ………………………………………………………… 16

2.1.5 SEISMIC FACIES ………………………………………………………………….. 17

2.1.5.1 Shelf-margin deltas (facies A) ………………………………………………… 20

2.1.5.2 Oblique (tangential) shelf-margin clinoforms (facies B) …………..………… 21

2.1.5.3 Sigmoidal slope clinoforms (facies C) ……………………………………… 23

2.1.5.4 Complex sigmoidal-oblique clinoforms (facies D) ...………..……………..... 23

2.1.5.5 Sand-rich turbidites (facies E) …………………………………………….... 24

2.1.5.6 Mass-transport deposits (facies F) ………………………………………….. 27

2.1.5.7 Continental to shelfal deposits (facies G) …………………………………… 30

2.1.5.8 Seismic facies associations ………………………………………………... 31

2.1.6 DISCUSSION …………………………………………………………………… 33

2.1.7 CONCLUSIONS ……………………………………………………………… 37

2.1.8 ACKNOWLEDGEMENTS ………………………………………………………… 38

2.1.9 REFERENCES ……………………………………………………………….. 39

2.2 Base-level and sediment-supply controls on shelf-margin growth and deep water depositional systems: Eocene clinoforms from northern Santos Basin, offshore Brazil ……………………………………………………………………….. 48

2.2.1 ABSTRACT …………………………………………………………………… 49

2.2.2 INTRODUCTION ………………………………………………………….... 50

2.2.3 GEOLOGICAL SETTING …………………………………………………… 51

2.2.4 DATABASE AND METHODS ……………………………………………… 54

2.2.5 SEISMIC FACIES: DESCRIPTION AND INTERPRETATION ………………….. 55

2.2.5.1 Facies A – shelf-margin deltas …………………………………………... 55

2.2.5.2 Facies B – oblique (tangential) shelf-margin clinoforms ………………… 57

2.2.5.3 Facies C – sigmoidal shelf-margin clinoforms …………………………….. 59

2.2.5.4 Facies D – continental to shelfal deposits ………………………………….. 59

2.2.5.5 Facies E – mass-transport deposits (MTDs) ……………………………….. 60

2.2.6 SEQUENCE STRATIGRAPHY ……………………....................................... 62

2.2.6.1 Sequence E31 62

2.2.6.2 Sequence E32 64

2.2.6.3 Sequence E41 65

2.2.6.4 Sequence E42 65

2.2.6.5 Sequence E51 66

2.2.6.6 Sequence E52 66

2.2.6.7 Sequence E60 67

2.2.6.8 Synthesis of the interpreted stratigraphic evolution 67

2.2.7 DISCUSSION 69

2.2.8 CONCLUSIONS 73

2.2.9 ACKNOWLEDGEMENTS 75

2.2.10 REFERENCES 75

2.3 Seismic expression of buried bottom-current-related comet marks developed in an outer shelf and upper slope – Eocene-Oligocene transition in northern Santos Basin, SE Brazil 83

2.3.1 ABSTRACT 84

2.3.2 INTRODUCTION 85

2.3.3 GEOLOGICAL SETTING 86

2.3.4 DATASET AND METHODS 89

2.3.5 SEISMIC EXPRESSION OF COMET MARKS 90

2.3.6 GAS-ESCAPE CONDUCTS ……………………………………………….............. 94

2.3.7 DISCUSSION 95

2.3.8 CONCLUSIONS 99

2.3.9 ACKNOWLEDGEMENTS 100

2.3.10 REFERENCES 100

3. CONSIDERAÇÕES FINAIS 107

REFERÊNCIAS BIBLIOGRÁFICAS 109

1. INTRODUÇÃO

O estudo de subsuperfície de depósitos de plataforma, talude e de ambientes marinhos profundos tem grande importância para o entendimento dos processos atuantes no preenchimento de uma bacia em determinado intervalo estratigráfico. Em geologia do petróleo, o uso dos dados sísmicos e dos conceitos clássicos da estratigrafia de sequências é comum na fase exploratória destes depósitos. Técnicas auxiliares à sismoestratigrafia permitem maior detalhamento de feições deposicionais que auxiliam a interpretação geológica e a determinação das condições ambientais ao longo da deposição.

Neste trabalho, a análise de sismofácies em conjunto com a caracterização de elementos deposicionais e da geomorfologia sísmica com uso de dados sísmicos é aplicada no estudo de sequências deposicionais do intervalo eoceno no norte da Bacia de Santos para a análise dos controles atuantes na construção da arquitetura deposicional na margem continental. Desta forma, é possível estabelecer as condições ambientais ao longo do intervalo, e determinar como as variações do nível relativo do mar e a entrada de sedimentos na bacia condicionaram a deposição. Com a aplicação destas técnicas em conjunto, são avaliados os controles sobre a arquitetura deposicional e geração de turbiditos e depósitos de transporte em massa em um intervalo com condições específicas de alto aporte sedimentar e predomínio de rebaixamentos do nível de base.

1.1 Estrutura da Dissertação

Esta dissertação é composta por uma introdução da pesquisa, três artigos científicos e uma conclusão integrada dos resultados do trabalho. Na introdução são feitas considerações que abrangem os três artigos como um todo, a respeito da análise do problema e motivação da pesquisa, objetivos do trabalho, e contexto geológico regional e discussão de trabalhos anteriores. Da mesma maneira, a conclusão da dissertação abrange de forma integrada os artigos. Os materiais e métodos auxiliares à estratigrafia de sequências são explicados em cada artigo separadamente, devido às diferenças de dados utilizados e técnicas aplicadas em cada trabalho. As referências bibliográficas apresentadas ao final da dissertação tratam apenas das publicações citadas nos capítulos introdutórios e de conclusão da dissertação. As publicações citadas ao longo dos artigos encontram-se ao final de seus respectivos textos.

O primeiro artigo, intitulado "*Seismic expression of depositional elements associated with a strongly progradational shelf margin: northern Santos Basin, southeastern Brazil*", trata da caracterização e interpretação da arquitetura e das relações genéticas entre elementos deposicionais e feições erosivas do intervalo eoceno, utilizando como base a análise de fácies sísmicas, a geomorfologia sísmica e a análise de trajetórias de migração da margem da plataforma. O artigo tem como objetivo determinar as condições ambientais e os processos sedimentares atuantes ao longo do intervalo.

O segundo artigo, "*Base-level and sediment-supply controls on shelf-margin growth and deep water depositional systems: Eocene clinoforms from northern Santos Basin, offshore Brazil*", é complementar ao primeiro, utilizando as interpretações das características ambientais do intervalo com base na análise de fácies sísmicas como base para a aplicação da estratigrafia de sequências. Este artigo tem como objetivo analisar os controles das variações do nível de base e do suprimento sedimentar sobre a acresção da margem da plataforma e geração de turbiditos e depósitos de transporte em massa.

O terceiro artigo, de título "*Seismic expression of buried bottom-current-related comet marks developed in an outer shelf and upper slope – Eocene-Oligocene transition in northern Santos Basin, SE Brazil*" trata da ação de correntes de fundo termohalinas sobre a região da plataforma e talude na transição do Eoceno para o Oligoceno. O artigo tem como objetivo a caracterização sísmica (2D e 3D) de estruturas erosivas relacionadas a correntes de fundo, e a avaliação das mudanças climáticas que afetaram o suprimento sedimentar e as variações do nível de base no período.

1.2 Análise do Problema e Motivação da Pesquisa

Os turbiditos têm grande importância como reservatórios de petróleo de ambiente marinho profundo em margens passivas (Mutti *et al.*, 2007), e historicamente constituem os reservatórios produtores mais importantes do Brasil (Della Fávera, 2000; Mohriak, 2003), com reservas nas bacias de Campos, Santos e Espírito Santo (e.g. Pereira & Macedo, 1990; Carminatti *et al.*, 2000; Arienti *et al.*, 2009). Recentemente, depósitos de transporte em massa (DTMs) também têm sido avaliados como potenciais reservatórios ou selos para sistemas petrolíferos (e.g. Moscardelli & Wood, 2008; Gamberi *et al.*, 2011; Posamentier & Martinsen, 2011; Alves *et al.*, 2014). Assim, se torna necessária a compreensão da arquitetura interna e externa destes depósitos, de suas formas de ocorrência, de sua associação com depósitos de plataforma e talude, e dos controles geológicos que influenciam na deposição, visando a avaliação da previsibilidade de ocorrência na bacia. Para tanto, são aplicadas técnicas da estratigrafia de sequências em conjunto com ferramentas auxiliares na análise e interpretação dos dados sísmicos.

A formação de sequências e tratos de sistemas deposicionais é controlada pela ação conjunta das variações do espaço de acomodação e da taxa de sedimentação na bacia, sendo importante a avaliação destes controles sobre a arquitetura deposicional e para a predição da ocorrência de turbiditos e depósitos de transporte em massa (Johannessen & Steel, 2005). Modelos clássicos da estratigrafia de sequências afirmam que o principal momento de transferência de sedimentos para o mar profundo ocorre durante o trato de sistemas de regressão forçada, quando os pontos de descarga dos sistemas fluvio-deltaicos se aproximam da margem da plataforma (Fig.1; e.g. Vail *et al.*, 1977; Posamentier & Vail, 1988; Catuneanu, 2002; Catuneanu, 2006).

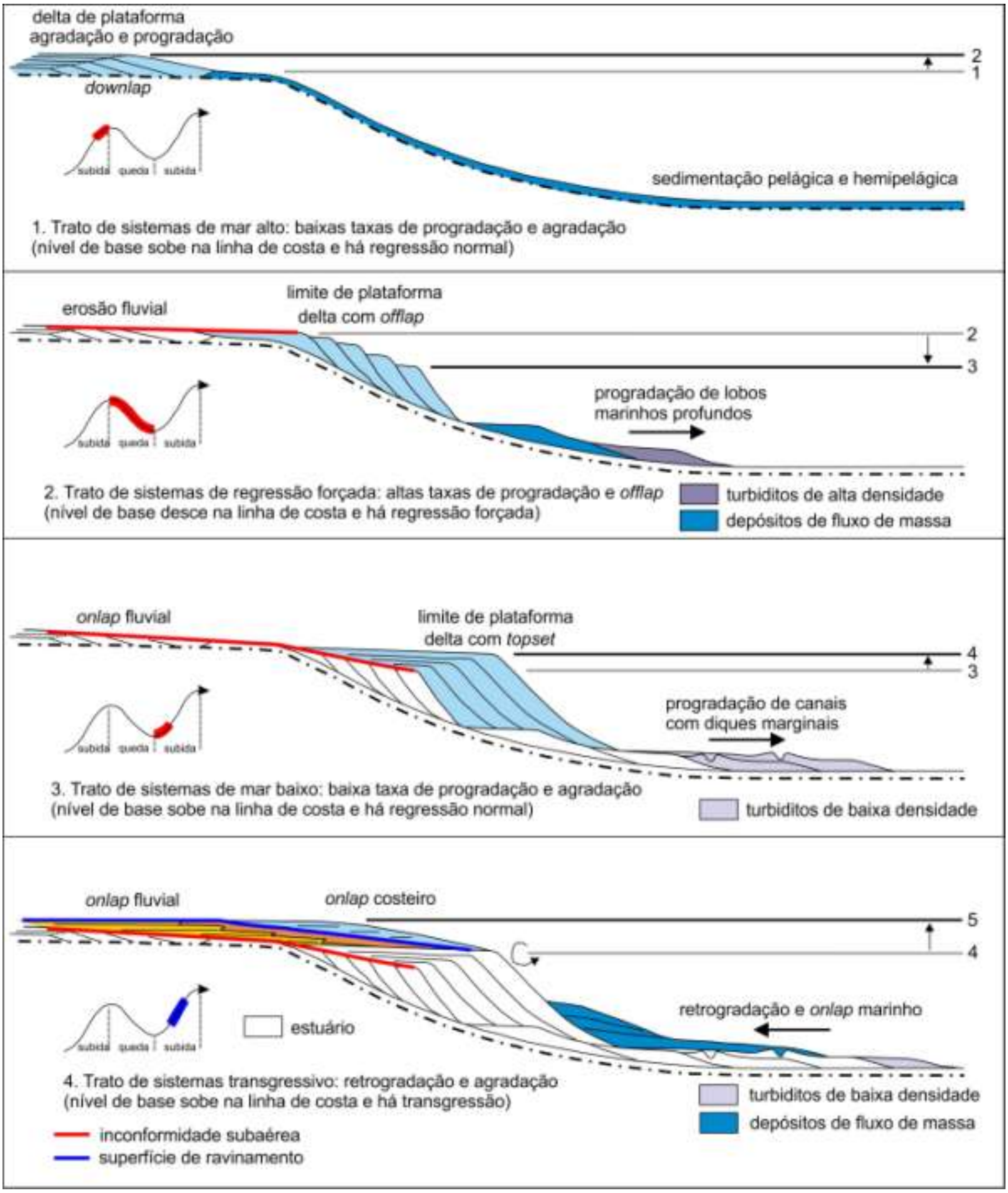

Figura 1: Modelo clássico de tratos de sistemas deposicionais, com interpretação da arquitetura deposicional e estilos de transferência de sedimentos para o ambiente marinho profundo de tratos de sistemas de mar alto (1), trato de sistemas de regressão forçada (2), trato de sistemas de mar baixo (3), e trato de sistemas transgressivo (4). Neste modelo, o principal momento de geração de turbiditos e depósitos de transporte em massa ocorre durante o trato de sistemas de regressão forçada (2), quando as desembocaduras fluviais se aproximam da margem da plataforma. Figura traduzida de Catuneanu (2006).

Nos ambientes marinhos profundos, este modelo implica em uma forte influência das variações do nível relativo do mar na geração de turbiditos arenosos e depósitos de transporte em massa (e.g. Walker, 1990; Posamentier & Allen, 1999; Muto & Steel, 2002; Helland-Hansen & Hampson, 2009). Assim, variações no espaço de acomodação na plataforma seriam o principal controle na sedimentação marinha profunda (Catuneanu *et al.*, 2009).

O intervalo Eoceno no norte da Bacia de Santos foi escolhido como um estudo de caso ideal para a avaliação dos controles descritos acima, devido à deposição em condições de alto aporte sedimentar influenciado por condições tectônicas e climáticas específicas, e de predomínio de extensivas fases de regressão forçada. Portanto, o intervalo apresenta condições favoráveis à deposição de turbiditos e depósitos de transporte em massa no ambiente marinho profundo. As características deposicionais resultaram em um intervalo de arquitetura essencialmente progradante, com o desenvolvimento de clinoformas de talude de alto ângulo bem definidas, às quais ocorrem associados turbiditos arenosos e depósitos de transporte em massa de matriz argilosa. A área dispõe de dados sísmicos de boa resolução, permitindo a interpretação de fácies sísmicas que auxiliam no entendimento das condições ambientais durante a deposição, assim como a aplicação dos conceitos da estratigrafia de sequências.

1.3 Objetivos

Os objetivos da pesquisa são a determinação da evolução estratigráfica do intervalo eoceno no norte da Bacia de Santos, dos efeitos das condições ambientais durante a deposição sobre a arquitetura deposicional, e dos controles e *timing* na geração de turbiditos e depósitos de transporte em massa, utilizando os conceitos e técnicas relacionados à estratigrafia de sequências. Para que estes objetivos sejam alcançados, foram estabelecidos objetivos específicos:

- interpretação de elementos deposicionais em subsuperfície para análise da arquitetura deposicional e determinação das condições deposicionais ao longo do intervalo;
- determinação da evolução estratigráfica do intervalo, estabelecendo os principais momentos de geração de turbiditos e DTMs em relação às condições do NRM e da sedimentação na bacia;
- avaliação das mudanças nas condições ambientais que interromperam a geração de turbiditos e depósitos de transporte em massa no Eoceno da Bacia de Santos.

1.4 Contexto Geológico e Localização

A Bacia de Santos está distribuída em uma área de aproximadamente 270.000 km² sobre o platô de São Paulo, na margem continental do sudeste do Brasil, delimitada a norte pelo Alto de Cabo Frio e a sul pelo Alto de Florianópolis (Fig. 2; Mohriak, 2012). A área geográfica da bacia encontra-se dentro dos limites dos mares territoriais dos estados do Rio de Janeiro, São Paulo, Paraná e Santa Catarina (Fig. 2), ultrapassando a cota batimétrica de 3000 m.

A área de estudo se localiza na porção norte da bacia, distante aproximadamente 150 km da cidade do Rio de Janeiro (Fig. 2). O embasamento data do Neocomiano, representado por derrames basálticos associados aos processos de abertura do Oceano Atlântico Sul. Moreira *et al.* (2007) dividem o arcabouço cronolitoestratigráfico em três supersequências: rifte, pós-rifte ou transicional (Mohriak, 2003) e drifte (Fig. 3).

A fase rifte (Barremiano a Aptiano) é marcada por vulcanismo básico e deposição vulcanossedimentar em ambientes continentais. O vulcanismo na fase inicial da bacia está associado ao contexto tectônico de afinamento litosférico, com geração de falhamentos lístricos normais no embasamento e formação de hemigrábens (Mohriak, 2012), que atuaram como depocentros para a sedimentação de arenitos imaturos e conglomerados associados a leques aluviais que progradavam para lagos rasos em porções proximais (Pereira *et al.*, 1986). Nas porções distais havia deposição de calcirruditos e folhelhos depositados em ambiente anóxico, sendo estes os principais geradores de petróleo na bacia (Chang *et al.*, 2008). O topo da fase rifte é delimitado por discordância regional do Aptiano (118-120 Ma; Modica & Brush, 2004).

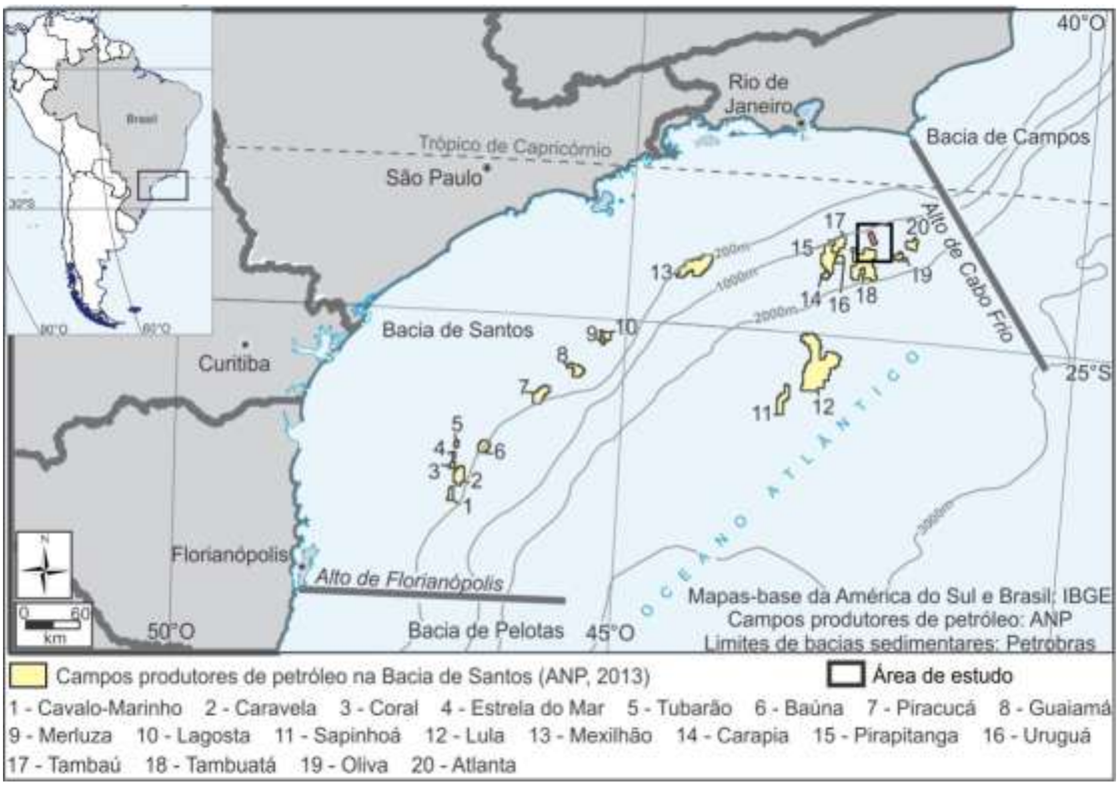

Figura 2: Localização da Bacia de Santos na margem sudeste do Brasil, e localização da área de estudo na região norte da bacia.

A fase transicional ou de golfo, de idade Aptiana, é caracterizada pelo desenvolvimento de uma bacia restrita com períodos de alta salinidade (Williams & Hubbard, 1984). Na sua base ocorrem rochas siliciclásticas e carbonáticas depositadas sobre a discordância regional (Mohriak, 2012), sendo os carbonatos desta fase as principais rochas reservatório da bacia (Chang *et al.*, 2008). Acima da sucessão basal foram depositados evaporitos compostos predominantemente por halita e anidrita, com ocorrências de sais solúveis como taquidrita, carnalita e silvinita (Moreira *et al.*, 2007).

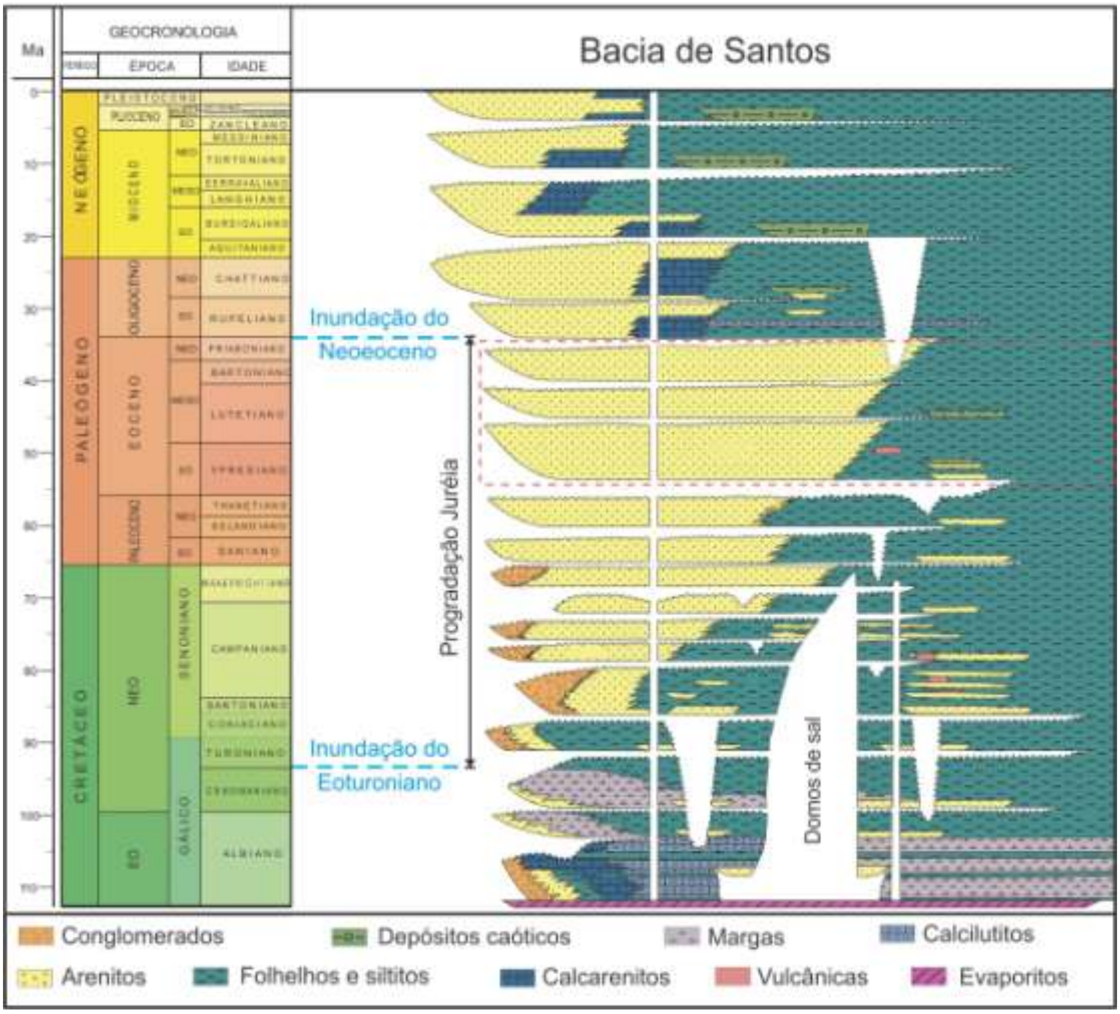

Figura 3: Carta estratigráfica da fase drifte da Bacia de Santos, com indicação da fase de progradações Juréia. O intervalo eoceno está delimitado pelo tracejado em vermelho. Figura modificada de Moreira *et al.* (2007).

Segundo Dias (2008), a geração de grandes acumulações de sal durante a abertura do Atlântico Sul pode ser explicada pelo desenvolvimento de um ambiente com baixa circulação de águas marinhas e clima árido/semiárido. No caso, esta restrição seria ocasionada por uma muralha vulcânica que atuaria como barreira à entrada de água do mar. A movimentação desses evaporitos devido à carga sedimentar e à inclinação da bacia na fase drifte originou importantes estruturas (Sombra *et al.*, 1990) e favoreceu a geração de trapas de petróleo (Chang *et al.*, 2008). Dentre estas estruturas, Contreras *et al.* (2010) destacam a formação de domos de sal que deformam as sucessões sobrepostas, e a geração de falhas lístricas, inversas e de cavalgamento. O limite da fase transicional se dá no início do Albiano (110-112 Ma), com o progressivo afogamento da bacia (Modica & Brush, 2004).

A fase drifte apresenta deposição em ambientes francamente marinhos, e as unidades basais encontram-se em contato com os evaporitos (Moreira *et al.*, 2007). A deposição do Albiano ao Cenomaniano é representada por sucessões siliciclásticas que registram o início da deposição em uma margem passiva. O início do Turoniano registra uma fase de afogamento e formação de importantes intervalos radioativos (Fig. 3; Contreras, 2010). No final do Turoniano, o soerguimento da Serra do Mar na região continental e a consequente denudação deste relevo dá início a uma extensa fase regressiva chamada progradação Juréia (Fig. 3; Macedo, 1989), que persiste ao longo do Neocretáceo, Paleoceno e Eoceno (Mohriak & Magalhães, 1993). No início do Paleoceno foi formada uma discordância regional que corresponde a uma fase reorganização do sistema de drenagens do rio Paraíba do Sul, aumentando o influxo clástico no norte da bacia (Modica & Brush, 2004). Ao mesmo tempo, a região sul da bacia passou a ser faminta em sedimentos clásticos.

O intervalo eoceno no norte da Bacia de Santos, objetivo deste projeto, corresponde a um pico do aporte sedimentar na bacia em função de um evento de aquecimento global (Eocene Thermal Maximum; Lourens *et al.*, 2005) que ocasionou um aumento da pluviosidade nas áreas-fonte (Zalán & Oliveira, 2005). Assim, o intervalo é marcado por ciclos de progradação deltaica e eventos de geração de turbiditos e depósitos de transporte em massa, principalmente no Eoceno Médio a Superior (Mohriak & Magalhães, 1993; Ribeiro, 2007). No Eoceno Superior o rio Paraíba do Sul foi capturado ao norte e começou a desaguar na Bacia de Campos (Karner & Driscoll, 1999), ocasionando diminuição do influxo sedimentar e da geração de depósitos turbidíticos na Bacia de Santos. Este período também coincidiu com um evento de resfriamento global na transição Eoceno Oligoceno (Sahy *et al.*, 2015), havendo diminuição na pluviosidade nas áreas-fonte e reconfiguração da circulação de correntes termo-halinas na bacia

(Duarte & Viana, 2007). Em seção sísmica, Assine *et al.* (2008) delimitam o topo do intervalo eoceno por uma superfície transgressiva (Fig. 3; 30-35 Ma). A partir do início do Oligoceno a bacia se tornou faminta em sedimentos, predominando o retrabalhamento sedimentar por correntes de fundo (Duarte & Viana, 2007). Em relação ao potencial econômico dos depósitos turbidíticos do norte da bacia, Pereira & Macedo (1990) ressaltam o potencial para acumulações de petróleo em turbiditos em águas profundas dos intervalos Neocretáceo e Terciário. Segundo Chang *et al.* (2008), a porosidade destes depósitos passa de 15%. Entretanto, Morais Júnior & Toledo (1993) afirmam que não há *plays* economicamente atrativos nos intervalos terciários.

2. RESULTADOS E DISCUSSÕES

2.1 Seismic expression of depositional elements associated with a strongly progradational shelf margin: northern Santos Basin, southeastern Brazil

2.1.1 ABSTRACT

Seismic facies analysis and seismic geomorphology are important tools for the understanding of environmental conditions during deposition and architecture of buried depositional elements and erosive features. This paper aims to investigate the character and genesis of such elements and features formed during the Eocene in north Santos Basin, in a context of high sediment supply and mainly negative base-level fluctuations. The main geometry is of prograding clinoforms with thin to truncated topsets and descendant shelf-margin trajectories. The identified facies include shelf-margin deltas, tagential slope-accretion clinoforms, sigmoidal slope-accretion clinoforms, complex sigmoidal-oblique clinoforms, topset reflectors, mass-transport deposits and turbidites. These facies were encompassed in five facies associations that represent periods of relatively constant environmental conditions. Association 1 is composed by shelf-margin deltas, tangential slope-accretion clinoforms and extensive sand-rich turbidites. Turbidites are composed by submarine channels ending in frontal splays with a sand-rich composition. A progressive increase on the angles of clinoforms within this association have been identified, culminating in high-relief sigmoidal clinoforms with smaller turbidites of facies association 2. Association 3 is composed by subparallel to divergent topset reflectors, interpreted as continental to shelfal deposits deposited during base-level rises. These are always truncated in the distal domain by slump scars, formed as a consequence of sediment overload in the shelf margin during periods of aggradation. Associations 4 and 5 are composed by high-relief sigmoidal/complex sigmoidal-oblique clinoforms, mass-transport deposits and turbidites. Clinoform angles are strongly influenced by the steep topography associated with the slump scars, and a progressive lowering of dip angles is registered, as the system approach to equilibrium profile. The steep physiography was also favorable for canyon incision, and these erosive features played an important role for turbidite deposition. Mass-transport deposits, formed after slope collapse, are composed by mud-rich diamictites with sand interbeds, and show strong internal deformation.

Keywords: seismic facies, seismic geomorphology, deep-marine deposition

2.1.2 INTRODUCTION

The Eocene interval in northern Santos Basin, Brazilian offshore, comprises a complex of high-relief progradational clinoforms (Moreira et al., 2001; Henriksen et al. 2011; Dixon, 2013) associated with shelf-margin accretion developed under high sediment supply and low accommodation. Because of these characteristics, depositional elements from outer shelf to basinal settings are well preserved, including slope clinoforms, submarine channels and lobes, slump scars and mass-transport deposits (e.g. Moreira and Carminatti, 2004). The succession is well imaged by 2D and 3D seismic surveys from oil exploration, providing the opportunity of investigating the depositional architecture by applying concepts and methods of seismic facies analysis and seismic geomorphology.

Seismic facies analysis and seismic geomorphology (e.g. Posamentier and Kolla, 2003) are important tools for seismic stratigraphy and hydrocarbon exploration, allowing a detailed visualization of internal and external architecture of depositional elements in subsurface, and have been specially applied to infer sedimentary processes operating in deep-marine environments (e.g. Benan and Cauquil, 2000; Prather and Steele, 2000). Despite the indirect character of seismic data and inherent difficulties associated to limited data resolution (see Shanmugam, 2000 for a critical review), reliable genetic interpretations for buried deep-marine deposits have been done based on high-quality seismic data (e.g. Gee *et al.*, 2007; Back *et al.*, 2011; Jiang *et al.*, 2012; Sylvester *et al.*, 2012).

In the present paper we apply the methodology of seismic facies analysis and seismic geomorphology to the Eocene interval of northern Santos Basin in order to characterize the depositional architecture of a strongly progradational shelf-margin. Emphasis is on depositional and erosive features developed in the outer shelf, slope and basin with the aim of determining the spatial and genetic relationships among different sediment dispersal systems.

2.1.3 REGIONAL SETTING

The Santos Basin is located in the southeastern Brazilian margin and is limited in the north by the Cabo Frio high and in the south by the Florianópolis high (Fig. A1).

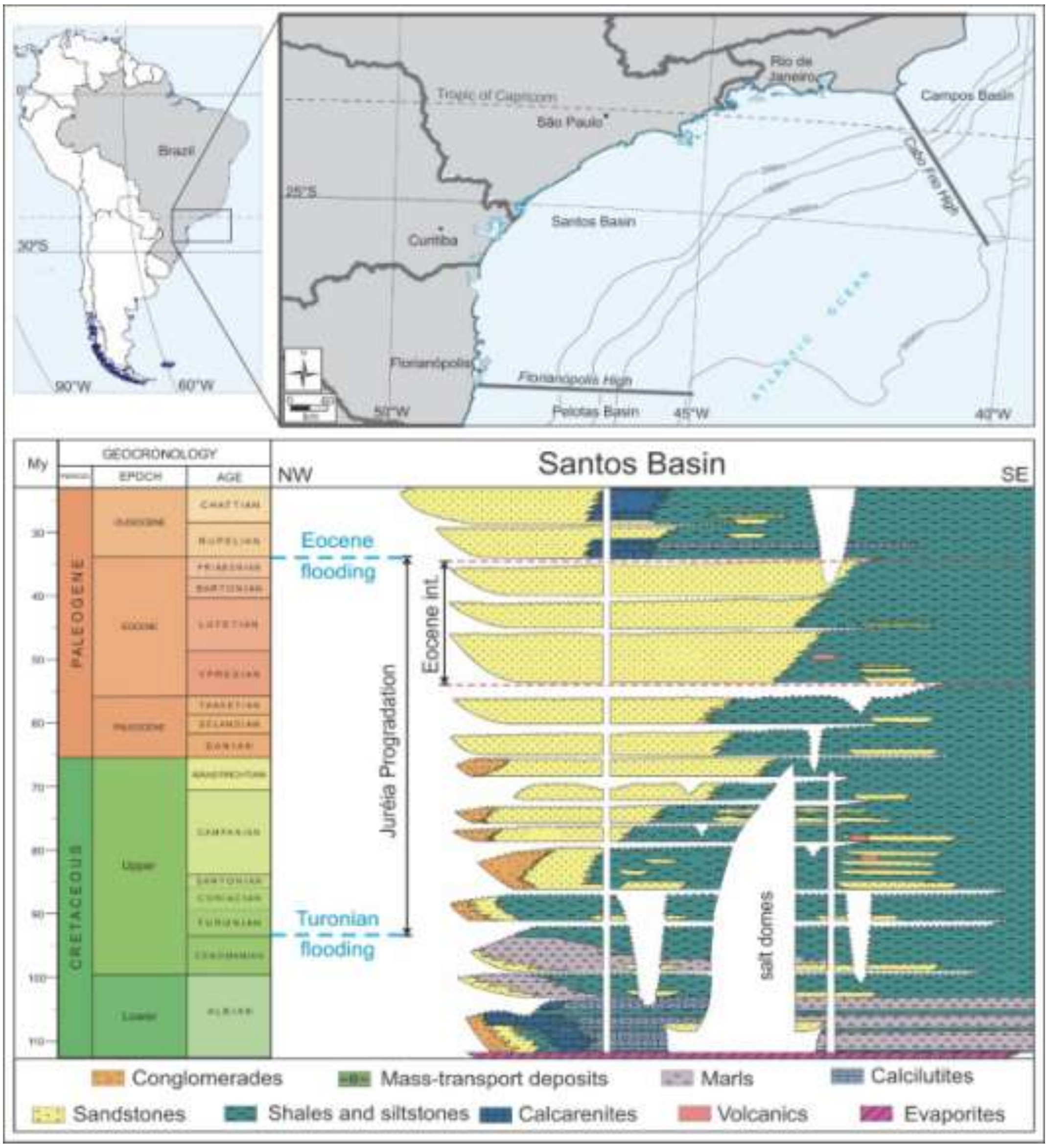

Figure A1: Location map of the Santos Basin in the southeastern Brazilian margin, and stratigraphic chart of the passive-margin interval adapted from Moreira *et al.* (2007). Juréia progradations and the Eocene intervals are indicated.

Basin evolution is related to the break-up of Gondwana and opening of the South Atlantic Ocean, including an Early Cretaceous rift and a Late Cretaceous to modern divergent margin (Moreira *et al.*, 2007). Remarkable was the development of a late Aptian evaporitic phase during which very thick halite deposits accumulated in a restricted marine environment. Subsequent displacement of salt played an important role creating depocenters and structural highs for post-salt deposition.

After a maximum marine flood in the Turonian, isostatic adjustments on the continental margin resulted in the Serra do Mar uplift. Denudation of this mountain range increased sediment supply to the basin and started an extensive regressive phase (Juréia progradation; Macedo, 1989), that persisted through the Eocene (Mohriak and Magalhães, 1993; Fig. A1). Sediment load associated with progradation contributed to the offshore movement of salt and for the generation of important structures in the basin (Sombra *et al.*, 1990; Assine *et al.*, 2008; Badalini *et al.*, 2010).

The Eocene interval, object of the present study, comprise the uppermost section of the Juréia progradation. In addition to uplifting and denudation, this period was the stage for a dramatic climate warming (Eocene Thermal Maximum; Lourens *et al.*, 2005) that increased rainfall and contributed to intensify the sediment supply (Zalán and Oliveira, 2005). In northern Santos Basin, the high sediment input during the Eocene was controlled by the Paraíba do Sul paleodrainage system (Modica and Brush, 2004; Ribeiro, 2007). Due to this combination of climatic and tectonic controls, high-relief shelf-margin clinoforms with thin to truncated topsets are the most common depositional geometry of the Eocene. In slope-to-basin areas, expressive muddy and sandy deposits associated with sediment gravity flows have formed and can be identified in different stratigraphic levels within the clinoform packages (d'Ávila *et al.*, 2008).

The end of the Eocene records another important climate change, when a global cooling altered the rainfall regime (Sahy *et al.*, 2015). In addition, tectonic adjustments in the Serra do Mar range caused a reorganization of the drainage system, leading the Paraíba do Sul river to migrate to the north and start to deliver its load to the Campos Basin (Karner and Driscoll, 1999). As a result, a dramatic reduction in sedimentation rate took place in northern Santos Basin, leading to transgression and reworking by bottom currents (Duarte and Viana, 2007).

2.1.4 DATASET AND METHODS

The study area is located in northern Santos Basin, approximately 150 km offshore from the city of Rio de Janeiro (Fig. A2). Database was provided by the Brazilian National Agency of Petroleum, Natural Gas and Biofuels (BDEP-ANP) and consist of 20 2D seismic lines with approximately 2300 km² of total coverage, including data from surveys 0228 SANTOS 11A, 0231 Santos 18A, 0247 CABO FRIO 3A, 0261 VB99 2D BMS, and R0003 0259 2D SPP 2Q 1999, approximately 50 km² of a 3D seismic volume (survey 0276 BS500), and composite logs of ten exploratory wells (Fig A2).

Seismic facies analysis consists in the visual determination of three-dimensionally-recognizable reflection patterns, represented by their amplitude-, geometry- and continuity-related characteristics, and by general trends of reflector terminations (e.g. Veeken and Van Moerkerken, 2013). According to Posamentier *et al.* (2007), seismic geomorphology consists in the interpretation of ancient geomorphic features in the subsurface using 3D seismic data. The interpretation of these geomorphic features, along with the recognition of the environmental setting of the analyzed interval (Hadler-Jacobsen *et al.*, 2007), allows the determination of the paleogeomorphological evolution through time (Prather *et al.*, 2012). In this study, seismic facies analysis and seismic geomorphology were complemented by the analysis of shelf-margin trajectories (e.g. Steel and Olsen, 2002; Henriksen *et al.*, 2011) in order to determine base-level fluctuations during the deposition of each of the seismic facies recognized.

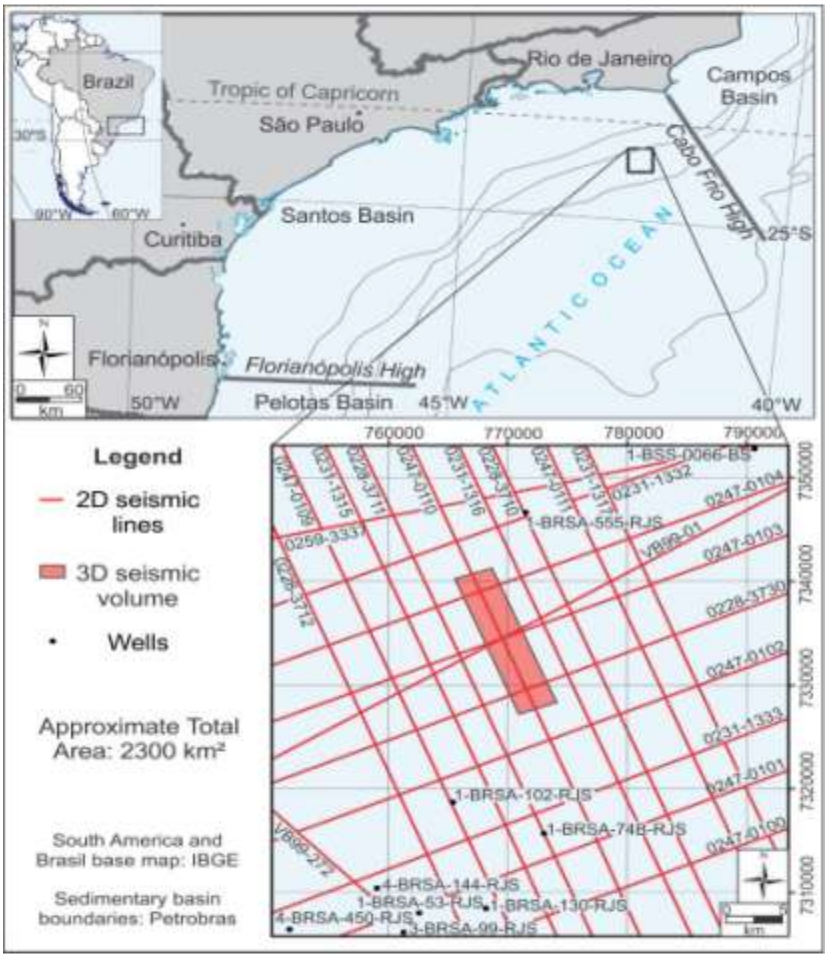

Figure A2: Location of the study area in north Santos Basin, and dataset location.

2.1.5 SEISMIC FACIES

The Eocene interval in the study area ranges in thickness from approximately 230 m in proximal (shelf) and distal (basin) areas, to approximately 590 m at the slope-accretion prisms. The basal boundary of the interval is a downlap surface with predominantly low seismic amplitudes that limits the top of the Paleocene interval (Fig. A3). The upper boundary (Eocene-Oligocene limit) is a truncation surface with predominantly high seismic amplitudes at the study area (Fig. A3).

Seven main seismic facies were recognized (Fig. A4), including prograding clinoforms, topset deposits, and slope-toe to basin deposits. Clinoform classification took into account their geometry, using a classification system based on Berg (1982; Fig. A5).

This system considers reflection patterns for fluvial- and wave-dominated deltas, in geometries such as oblique (tangential), complex oblique, sigmoid, complex oblique sigmoid, oblique (parallel), and shingled. It is important to consider that clinoforms in seismic data are depositional forms with dimensions varying from few hundreds of meters to several kilometers (slope-accretion clinoforms; Steel and Olsen, 2002; Johannessen and Steel, 2005).

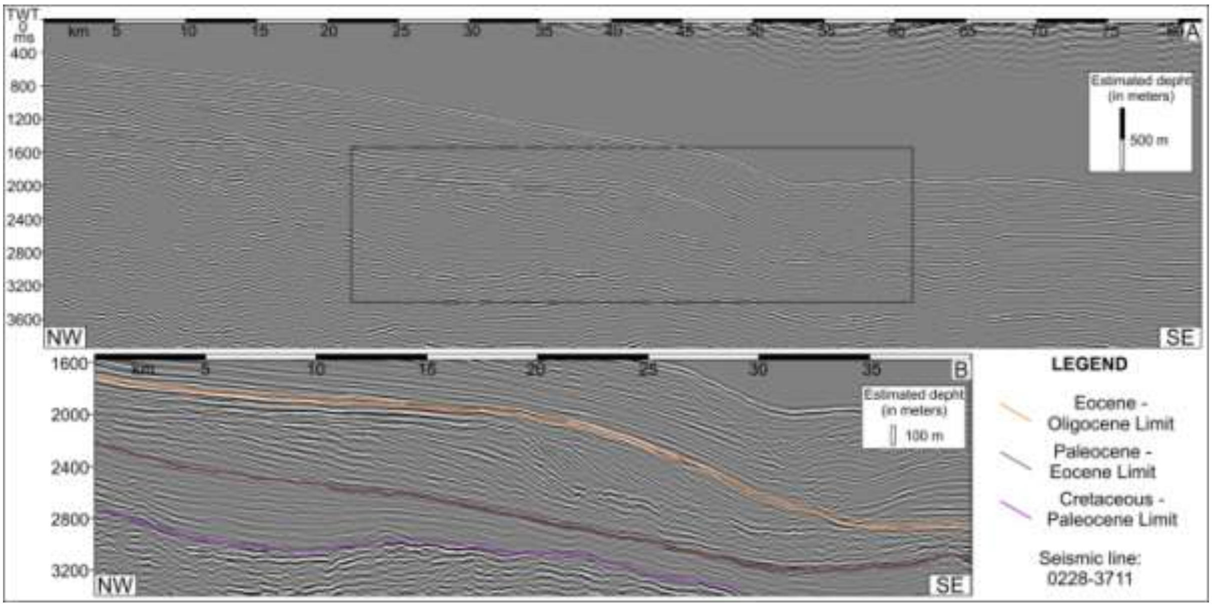

Figure A3: 2-D, dip-oriented seismic line with interpretations of the main stratigraphic surfaces associated to the studied interval: the Cretaceous-Paleocene boundary, the Paleocene-Eocene boundary, and the Eocene-Oligocene boundary.

Slope-accretion clinoforms are composed of topset, foreset and bottomset domains. The topset corresponds to the continental to shelfal domain, extending to the shelf margin and encompassing reflectors that dip in very low angles towards the basin (Safronova *et al.*, 2014). An inflexion marks the shelf break, when gradients become steeper in slope areas (foreset domain). At the slope toe, a new gradient change marks the decrease in dip angles, in the transition between slope to basin, and beginning of the bottomset domain. Within these domains, depositional elements and erosive features were interpreted based on morphological characteristics identified in seismic sections, and on modern examples described in the literature, following the orientations by Stow and Mayall (2000) for sub-surface studies.

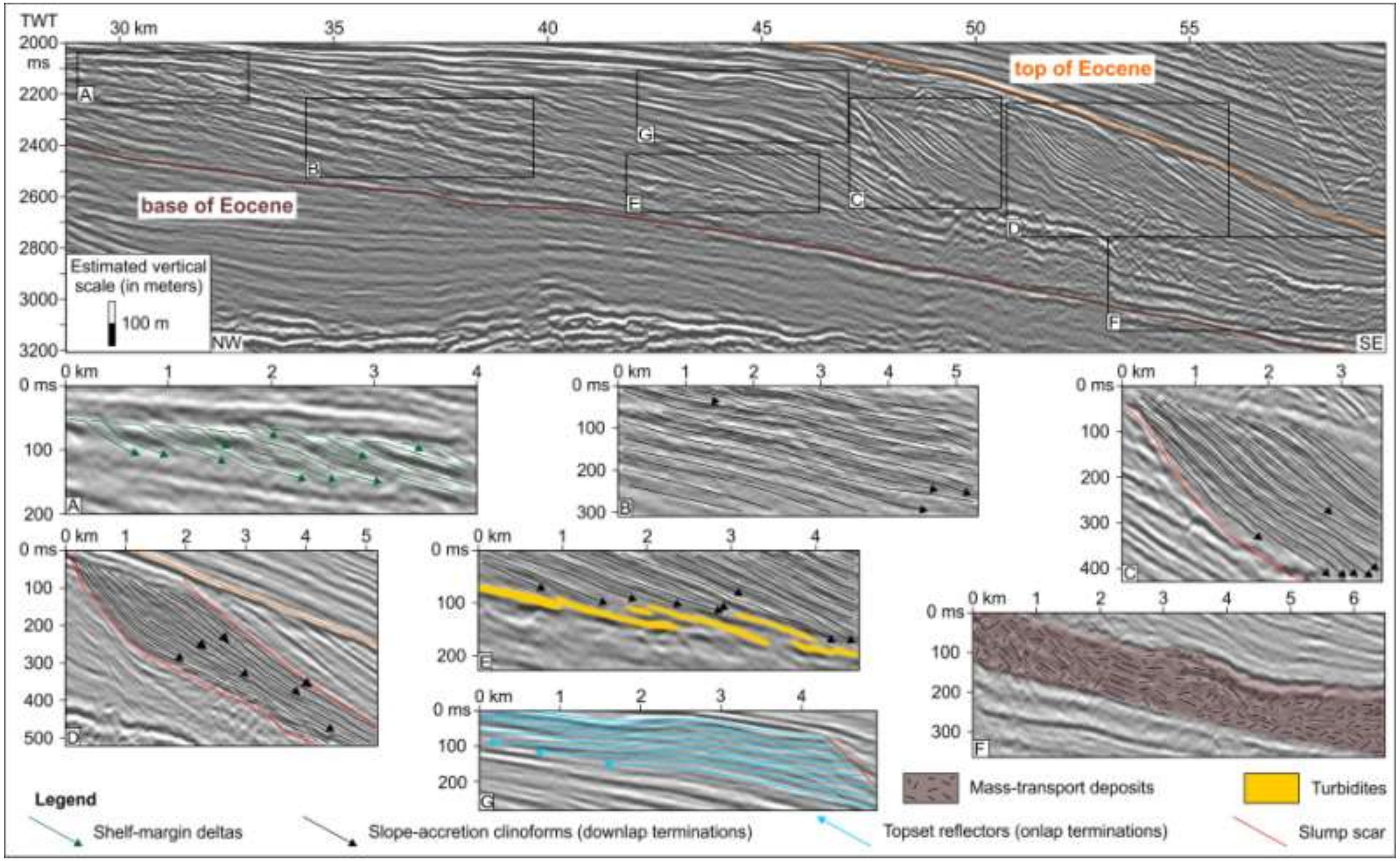

Figure A4: Interpretation of the main seismic facies on the Eocene interval in north Santos Basin. (A) corresponds to shelf-margin deltas, while (B), (C) and (D) are correspondent to tangential (oblique) clinoforms, sigmoid clinoforms and complex sigmoid oblique clinoforms, respectively. In the bottomset domain are identified sand-rich turbidites (E) and mass-transport deposits (F). Facies (G) is interpreted as continental to shelfal deposits in the topset domain.

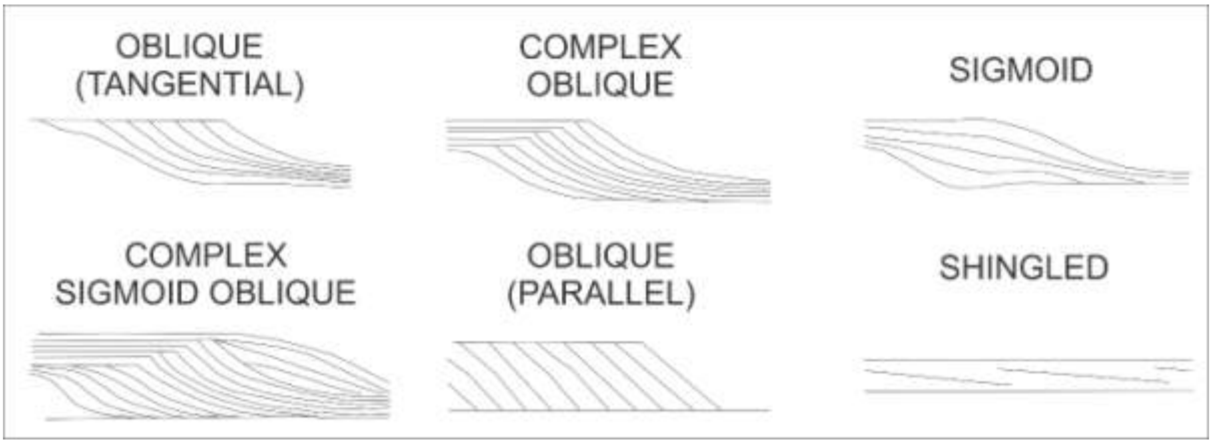

Figure A5: Classification of clinoforms based on geometry patterns, as suggested by Berg (1982).

2.1.5.1 Shelf-margin deltas (facies A)

This facies is composed of small-sized oblique (tangential) clinoforms, with maximum relief reaching 200 ms TWT (approx. 115 m) and maximum longitudinal extension of 3 km (Fig. A6). Seismic amplitudes are moderate to high, and in many cases a transition of high acoustic impedance contrasts on topsets to low contrasts on foresets and bottomsets is observed (Fig. A6). Topsets are generally truncated, with flat to descending trajectories of the clinoform rollover (Fig. A6). Foreset angles vary from 4° to 5°.

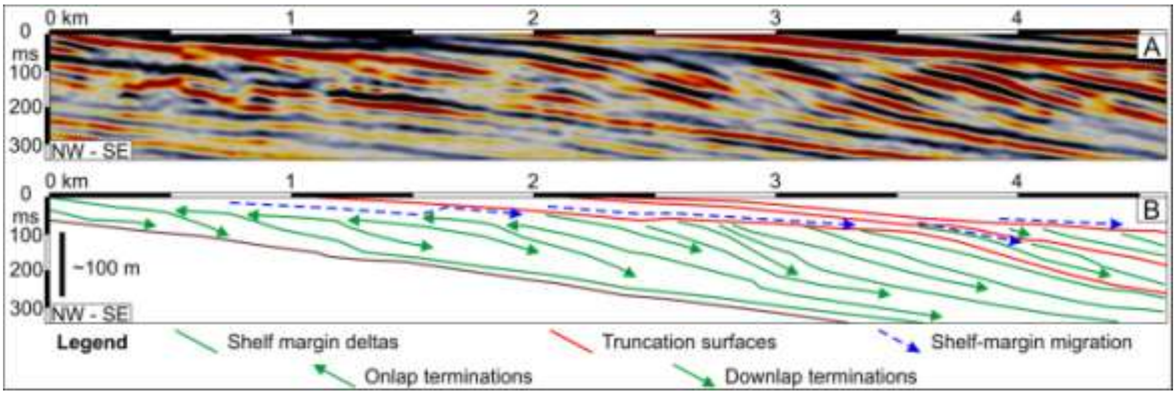

Figure A6: Interpretation of shelf-margin deltas (B) in the 3D seismic volume (A). Shelf-margin trajectories are mainly descending, and topsets are generally truncated.

This facies is interpreted as shelf-margin deltas (e.g. Porębski and Steel, 2003; Moreira and Carminatti, 2004; Patruno *et al.*, 2015) formed when deltaic systems advanced beyond the original shelf edge. Shelf-margin trajectories, long-term progradation and thin to truncated topsets indicate that the progradation was influenced by high sediment supply in periods of stationary to falling base level. Acoustic impedance contrast variations indicate a transition from sandy proximal deposits to muddy distal deposits which, in many cases, drape onto high-relief oblique clinoforms.

2.1.5.2 Oblique (tangential) shelf-margin clinoforms (facies B)

This facies is composed of high-relief oblique (tangential) clinoforms with relatively low angles (up to 2°), longitudinal extension reaching 15 km, and maximum relief of 650 ms TWT (approx. 380 m; Fig. A7 A and B). A gentle increase in slope dip angles is observed from the oldest to the youngest clinothemes, from approximately 1° to up to 2° (Fig. A7 A). Topsets are generally truncated, and trajectory of clinoforms rollover is slightly (when topsets are preserved) to strongly descending (when topsets are truncated; Fig. A7 B). Seismic amplitudes are generally high in topset areas, but a transition to low amplitudes in bottomset areas can also be identified. In some cases, seismic amplitude peaks are observed in the foresets. Frequency of the reflections vary from low to moderate.

In many cases, these high-relief clinoforms are contiguous to the shelf-margin deltas, being interpreted as low-angle shelf-margin clinoforms (e.g. Porębski and Steel, 2003; Johannessen and Steel, 2005; Patruno *et al.*, 2015). Descending trajectories and truncated topsets indicate that their genesis is related to periods of relative sea-level fall. Variations of seismic amplitudes are associated to the transition from proximal sandy deposits to distal muddy deposits, while amplitude peaks in foreset areas suggest the occurrence of intra-slope (shingled) sand-rich turbidites (e.g. Johannessen and Steel, 2005). Despite the lack of well control and/or 3-D seismic data to reinforce the interpretation of such accumulations, sand concentration on slope areas are generally associated to channel and/or canyon filling (e.g. Carvajal and Steel, 2006). The gradual increase in foreset dip with time may be related to a progressively increase on sediment supply, as a consequence of relative sea level fall and erosion in the shelfal domain (Zecchin & Catuneanu, 2013).

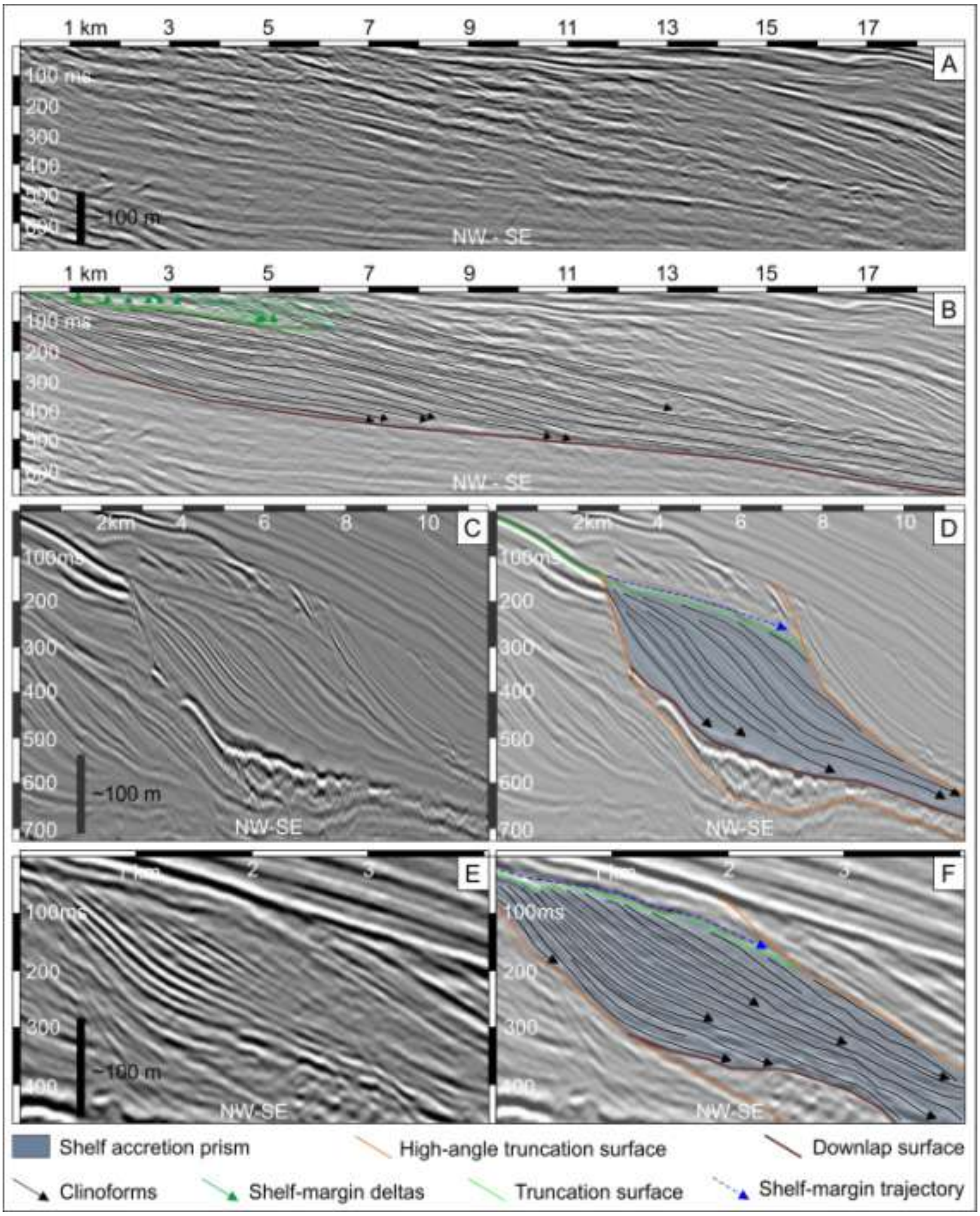

Figure A7: In (A), oblique (tangential) clinoforms with relatively low dip angles, interpreted in (B). Note that some of these clinoforms are contiguous to shelf-margin deltas. In (C), sigmoid high-angle clinoforms, interpreted in (D). In (E), sigmoid-shaped and oblique (tangential)-shaped clinoforms composing a complex pattern, interpreted in (F). All clinoforms are associated to descending trajectories.

2.1.5.3 Sigmoidal slope clinoforms (facies C)

This is the most characteristic facies in the study area, and is composed of high-relief (up to 700 ms TWT; approx. 410 m) sigmoidal clinoforms, with maximum longitudinal extension of 15 km (Fig. A7 C and D). Dip angles slightly decreases from the older to the youngest clinothemes (from 9° to 7°). Seismic amplitudes are high on foreset areas and low to moderate on the bottomsets, and frequency of the reflections is moderate to high. Topsets are truncated, and shelf-margin trajectories are descending (Fig. A7 D).

Sigmoidal clinoforms are interpreted as slope-accretion clinoforms (e.g. Porębski and Steel, 2003; Johannessen and Steel, 2005; Patruno *et al.*, 2015), deposited during base-level falls. The external geometry of the clinoform sets is of high-relief shelf-margin-accretion prisms, limited on the top by subaerial unconformities (Fig. A7 D). The accretion prisms were formed from steep physiographies, in most cases associated to high-angle truncation surfaces interpreted as large-scale slump scars (Fig. A7 D). Variations on clinoform dip angles are interpreted as a consequence of the progressive approach to equilibrium profile from an initial steep gradient promoted by slope failure.

2.1.5.4 Complex sigmoidal-oblique clinoforms (facies D)

This facies is an association of high-relief clinoforms with oblique or sigmoidal geometries, composing a complex facies. Maximum extension reaches 15 km, and maximum relief is up to 700 ms TWT (approx. 410 m; Fig. A7 E and F). Seismic amplitudes are moderate to high, and frequency of the reflectors is mainly high. Topsets are truncated, and shelf-margin trajectories are descending (Fig. A7 F). In addition to the geometric variations within the clinoform sets, internal variations on dip angles are also identified, with a general tendency of slope decrease from the oldest to the youngest clinotheme (from 9º to 6°).

The clinoforms prograded from high-angle truncation surfaces interpreted as slump scars (Fig. A7 F) that conditioned the steep clinoform configuration. Approximation to the submarine equilibrium profile resulted in the reduction of clinoform angles and variations on geometries. Truncated topsets and descending shelf-margin trajectories indicate that deposition occurred during periods of forced regression. This facies is interpreted as shelf-margin clinoforms (e.g. Porębski and Steel, 2003; Johannessen and Steel, 2005; Patruno *et al.*, 2015), composing shelf-accretion prisms limited on the top by a subaerial unconformity.

2.1.5.5 Sand-rich turbidites (facies E)

The turbidite facies is composed of reflectors with high acoustic impedance contrasts and low-frequency reflectors, with maximum thickness reaching 40 ms TWT (approx. 25 m). Longitudinal extension is variable, ranging from 1,5 to 15 km. This facies is common on the bottomsets of slope-accretion clinoforms, being interpreted as turbidites with variable dimensions, and with a sand-rich composition (Fig. A8; e.g. Posamentier and Erskine, 1991; Moreira & Carminatti, 2004; Johannessen and Steel, 2005).

In 3-D seismic data, it is possible to observe that this facies configures channels and frontal splays (Fig. A9). Submarine channels width vary from 100 to 150 m, generally with low to moderate sinuosity and, more locally, with high sinuosity (Fig. A9 A and B).

Moreira and Carminatti (2004), using a larger 3-D seismic volume than the used in the present paper and recognized a meandering pattern for submarine channels that compose the turbidite systems. Therefore, the mainly straight geometry observed in the study area may be a local characteristic.

In the terminal portions of the submarine channels, asymmetric-fan-shaped frontal splays were identified (Fig. A9). Lateral extension of the frontal splays varies from few hundreds of meters to thousands of meters. Negative acoustic impedance peaks and well information indicate a sandy composition for these deposits (Figs. A8 and A9).

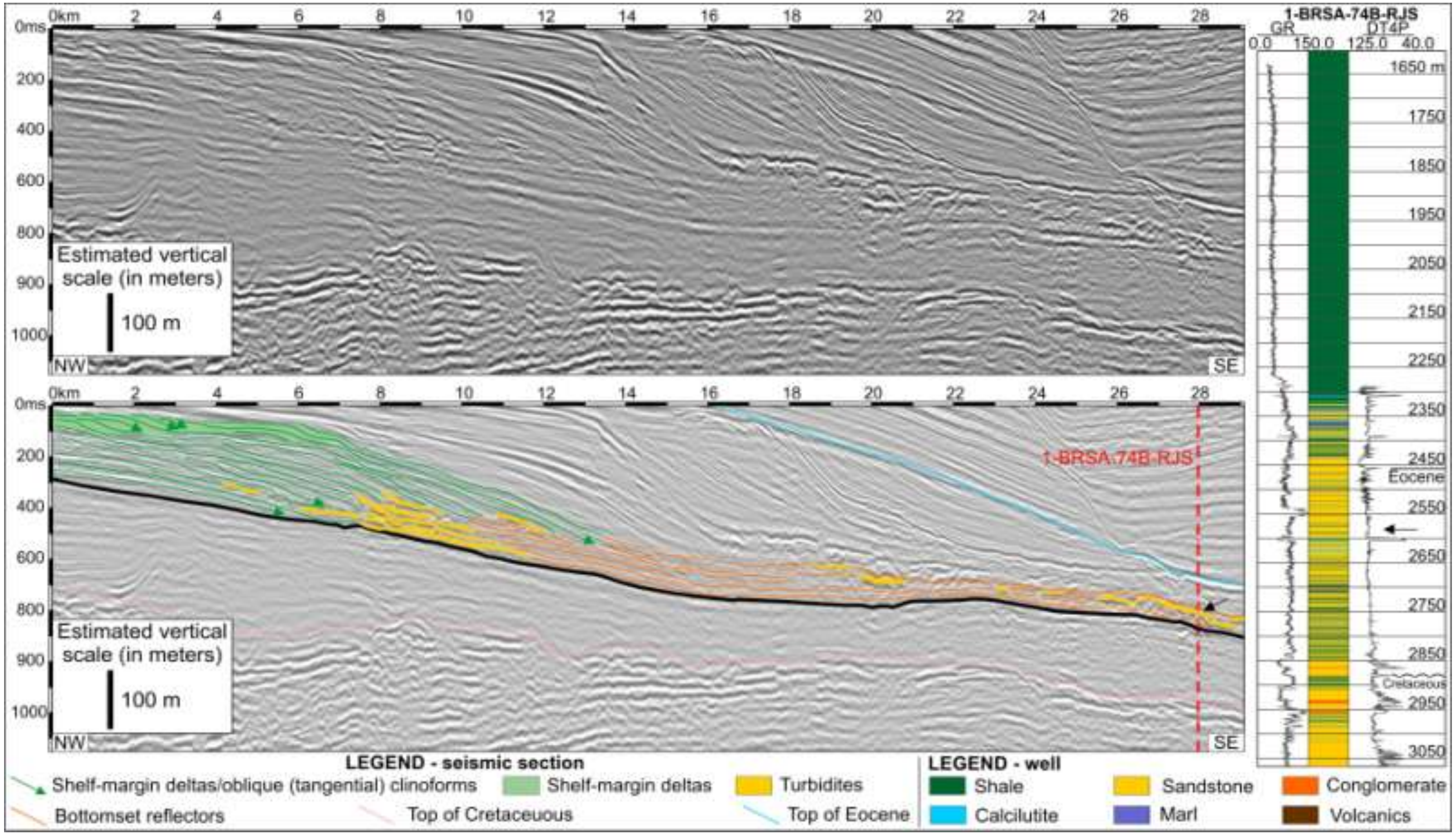

Figure A8: Submarine fans and sandy turbidites interpreted in 2D seismic section (in yellow), in the bottomset domain (orange reflectors) of slope-accretion clinoforms (green reflectors). Note the association between turbidites and shelf-margin deltas (green reflectors in the topset domain). In the right, the projection of the well 1-BRSA-74B-RJS shows the sand-rich composition of the turbidites. The black arrow points to a sand-rich turbidite with large dimensions, used for correlation between well and seismic data.

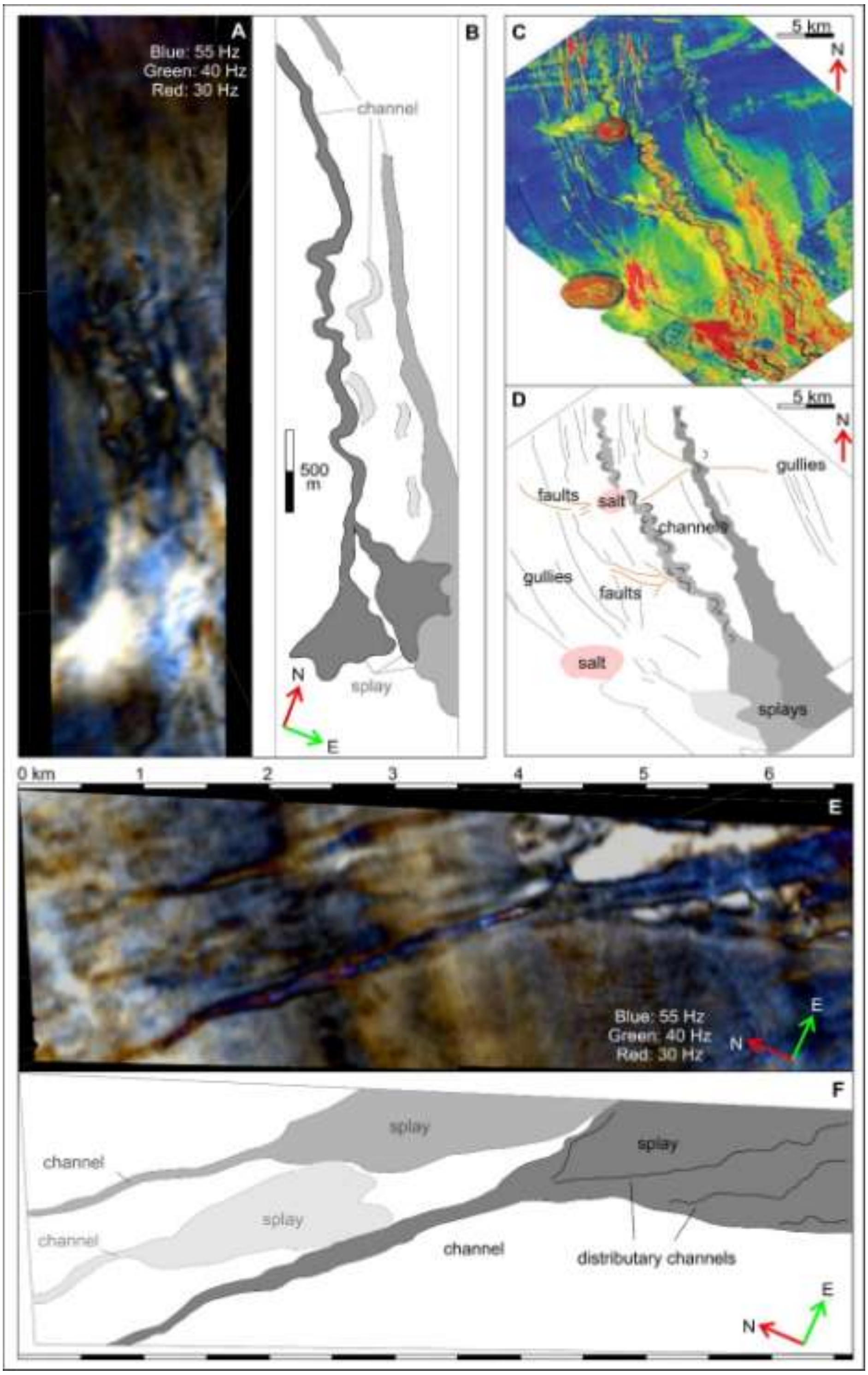

Figure A9: Systems of submarine channels and frontal splays that compose turbidites from the high-amplitude facies at the bottomset of clinoforms, visualized in (A) and (E) in a spectral decomposition. These systems are interpreted in (B) and (F). In (C) and (D), systems of submarine channels and fans as the identified by Sylvester *et al.* (2012) at the Pleistocene of the Gulf of Mexico. They have geometries similar to the channels and frontal splay systems identified in the present paper.

Sediment-feeding of these splays seem to be related to submarine canyon incision on slope areas. Canyons reach up to 35 ms TWT deep (approx. 20 m), and have a mainly straight morphology. These erosive forms acted as preferential points to clastic sediment influx to the basin (Stow and Mayall, 2000). Canyon-fill deposits display a divergent seismic configuration according to the classification by Mitchum *et al.* (1977).

2.1.5.6 Mass-transport deposits (facies F)

The mass-transport deposits have a predominantly chaotic reflector pattern, with low to moderate seismic amplitudes and high frequencies. The external form of the deposits, in strike and dip sections, is of mound-shaped bodies at the slope toe, with few to tens of kilometers of longitudinal extension (maximum of 30 km; Fig. A10). The chaotic pattern is interpreted as mass-transport deposits (e.g. Posamentier and Kolla, 2003; Martinez *et al.*, 2005; Alfaro and Holz, 2014).

In well data, the chaotic facies is described as of gravelly mudstones (diamictites) or mudstones with sand interbeds. Internally, this facies is strongly affected by sin-sedimentary deformation, more typically reverse faults pointing to a compressive regime (Fig. A10; e.g. Posamentier and Kolla, 2003; Posamentier and Martinsen, 2011). Other compressive structures, such as open folds (Fig. A10) are observed both in 2D seismic lines and in the 3D seismic volume, being comparable to examples reported in the literature (e.g. Martinez *et al.*, 2005; Moscardelli *et al.*, 2006; Alfaro and Holz, 2014).

Isopach maps for the two largest MTDs show a maximum thickness of 135 ms TWT (approx. 80 m) and a longitudinal extension 30 km for MTD 1 (Fig. A11). Thickness variation in MTD 1 is subtle, but larger thicknesses are concentrated in its northwestern portion. This pattern is also onserved in the smaller deposit (MTD 2), but in this case the chaotic facies is restricted to the central to NW part of the deposit and not observed in the SE domain. The third MTD, associated to a smaller slump scar, was not mapped, as it is observed only in few strike sections.

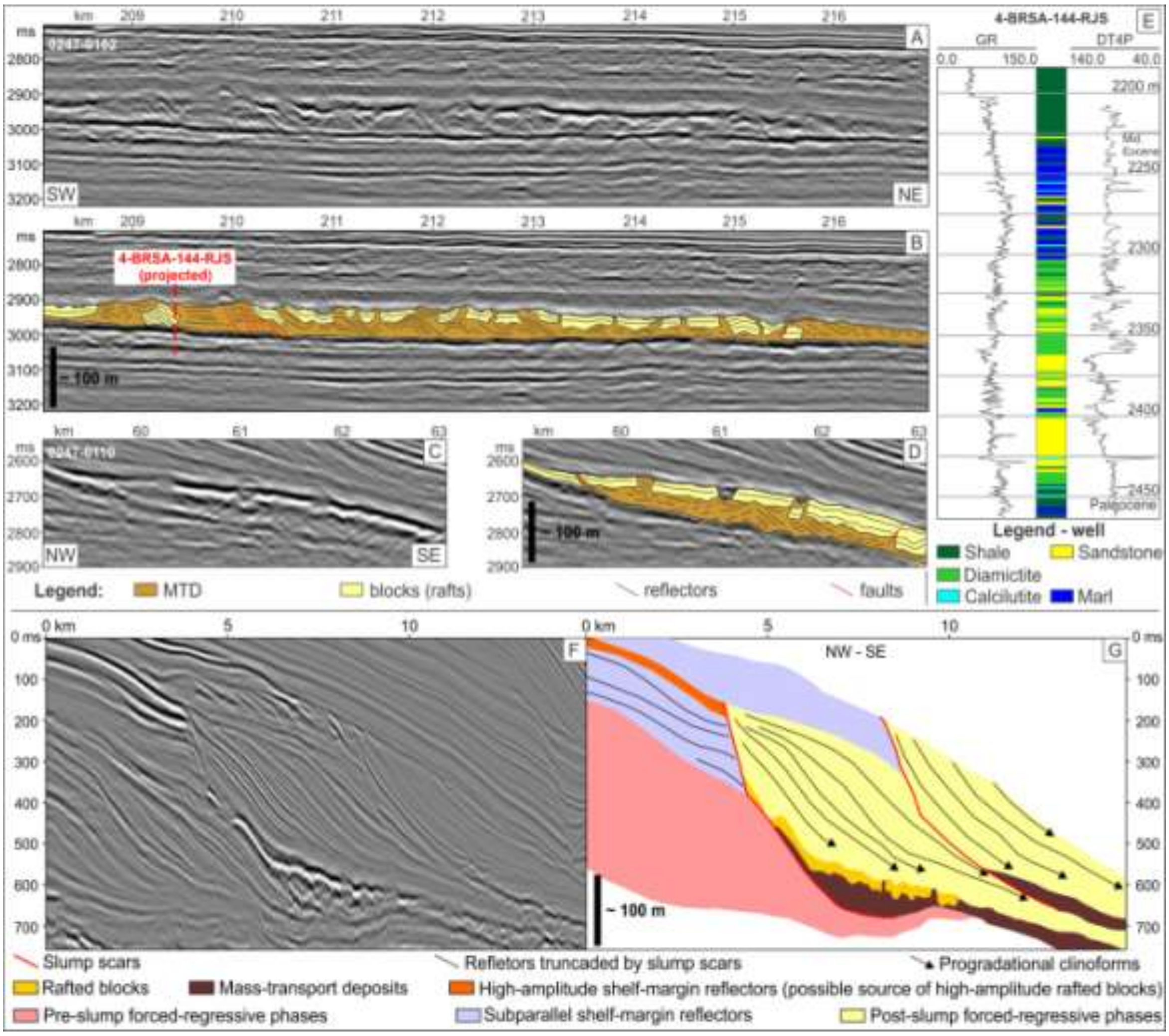

Figure A10: Mass-transport deposits in strike (A and B) and dip sections (C and D). MTDs show a mainly chaotic pattern, but some parts with folded, arched or subparallel reflectors are observed, as consequence of the internal variations on deformation intensity. Faults are also identified, many times contiguous to the basal detachment surfaces of the slumps. In the lower part of the figure, interpretation of blocks from topset areas transported in a rafting process over the muddy mass movement. In pink, slope-accretion clinoform sets older than the first slump, undifferentiated. In purple, topset deposits truncated by the slump scars. In clear yellow and green, high-angle slope-accretion clinoform sets developed from the slump scars.

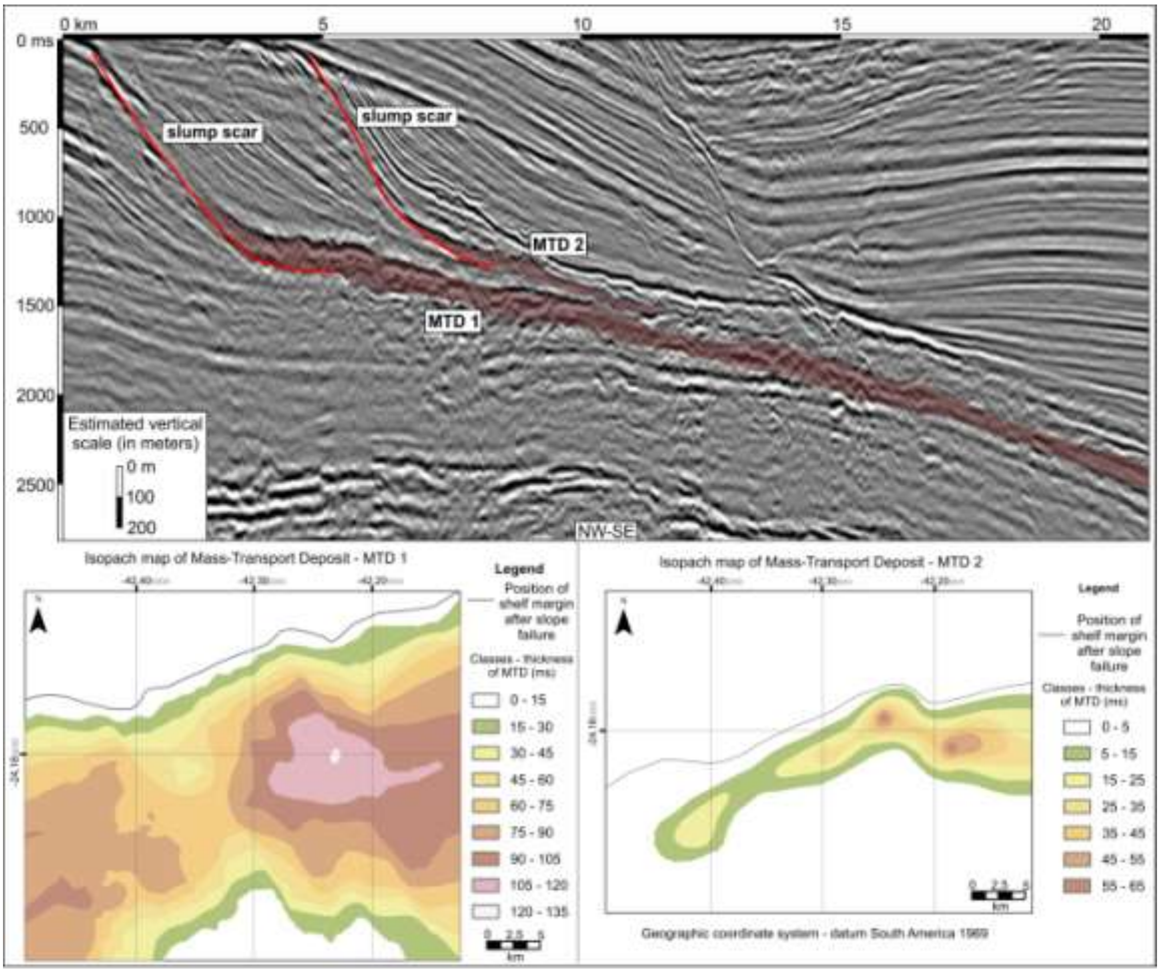

Figure A11: Isopachs maps for the two main MTDs in the study area.

The MTDs are associated to three major slump scars and the generation of these deposits is interpreted as related to the catastrophic collapse of the slope (Figs. A10 and A12). Relief of the slump scars vary from 420 to 550 ms (245 – 320 m, approximately), while their longitudinal extension vary from 3,0 to 3,7 km, resulting in a steep topography with angles exceeding 10°. In the upper slope the scars are truncated by unconformities, and basinward they are contiguous to the basal detachment surfaces of the MTDs (Fig. A12). Reflectors with more lateral and longitudinal continuity and higher amplitudes are also associated with the chaotic facies (Fig. A10). These are interpreted as low-deformed sand-rich slipped blocks, transported as rafts within the mass flow (Fig. A10; e.g. Gamboa *et al.*, 2012; Alfaro and Holz, 2014). The rafted blocks are concentrated in the upper part of the MTDs, but they also occur in the middle part or directly on the basal detachment surfaces.

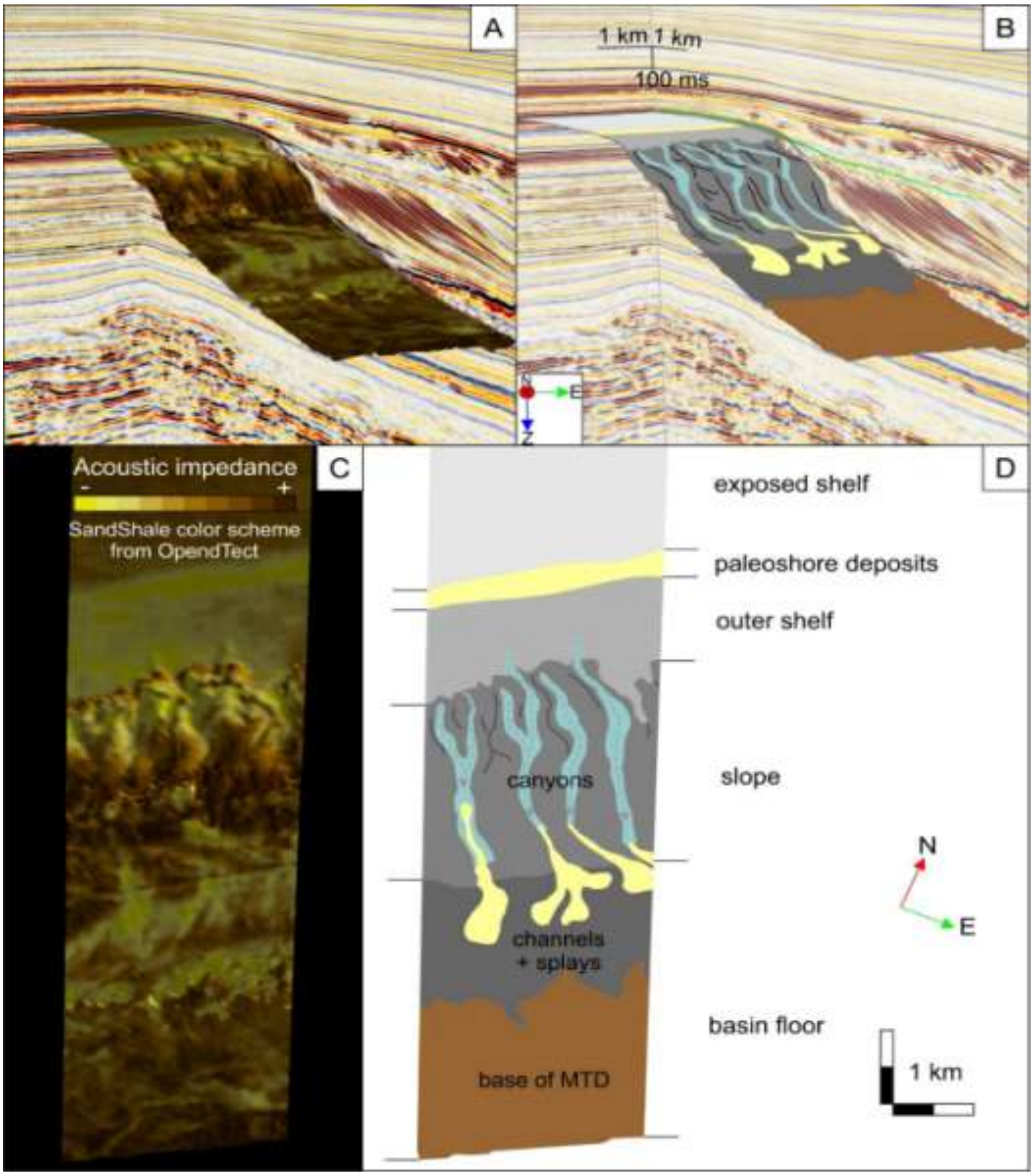

Figure A12: Slump scar that generated a muddy MTD (A), interpreted in B. Note the development of canyons on the steep physiography that resulted from the slump, which acted as preferential points to sediment influx and development of channels and submarine frontal splays. From the scar, sigmoid slope-accretion clinoforms prograded, downlapping over the MTD. In C, a plan-view of the scar, interpreted in D.

2.1.5.7 Continental to shelfal deposits (facies G)

This facies is composed of reflectors with subparallel to divergent pattern, with moderate to high amplitudes and high frequency (Fig. A13). Onlap terminations of the reflectors migrate toward the continent, while basinward they are truncated by the slump scars (Fig. A13). The maximum thickness of these topset deposits is about 300 ms TWT (approx. 175 m), recording extensive periods of aggradation on the shelf. They are probably constituted of non-marine (coastal plain) to outer shelf deposits, formed in periods of positive accommodation in the shelf related to rising base-level and high sedimentation rates (normal-regressions).

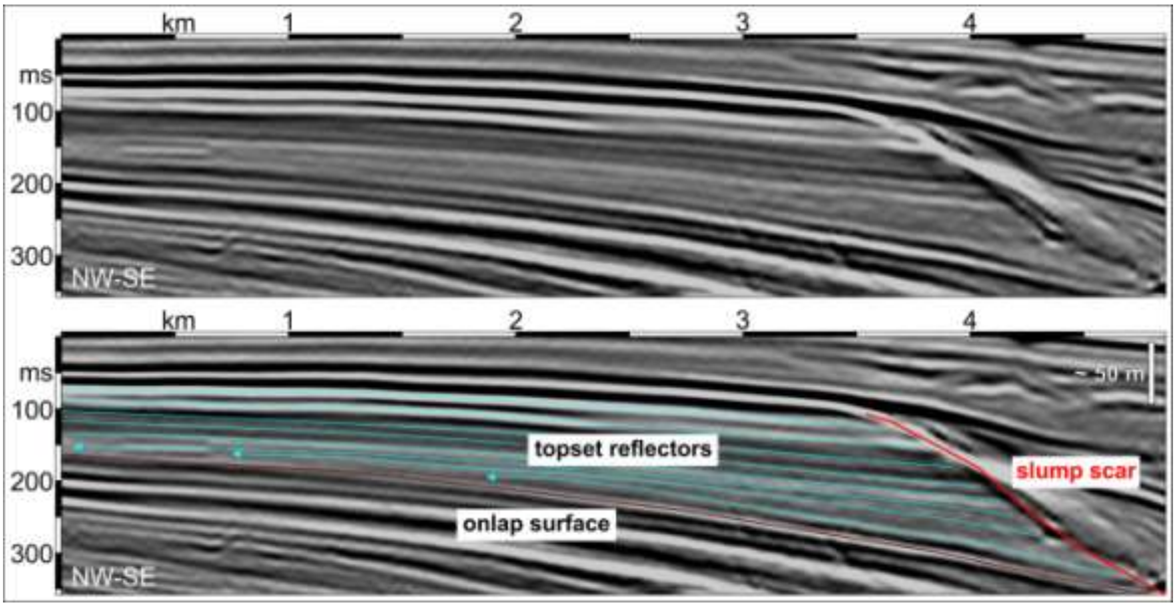

Figure A13: Topset reflectors interpreted in blue, registering migration of the onlap towards the continent. Reflectors are truncated by a slump scar at the distal areas, traced in red.

2.1.5.8 Seismic facies associations

Seismic facies were grouped in genetic associations (Fig. A14) that reflects the environmental conditions during deposition. Association 1 is composed of shelf-margin deltas, low-angle slope-accretion clinoforms and sand-rich turbidites, representing periods of high sediment supply and stationary to falling base level. In the younger part of the association shelf-margin deltas are rarer, and low-angle slope-accretion clinoforms with truncated topsets and turbidites are predominant. This configuration is coherent to a period of falling sea-level, when shelf-margin deltas were eroded. Despite the relative low angle of the clinoforms, a gradually steeper slope is built from the older part of the association to the younger. Gradients considerably increases in association 2, which is composed of high-angle, sigmoidal slope-accretion clinoforms with truncated topsets, and sand-rich turbidites.

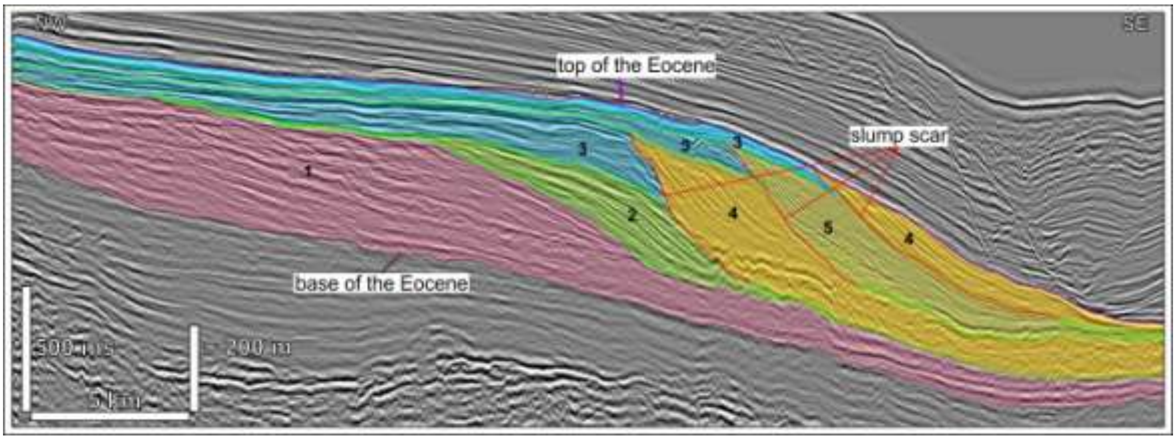

Figure A14: Genetically related seismic facies associations. Each facies association represent a depositional interval when conditions of sediment supply and relative sea-level were constant. Association 1 is composed by shelf-margin deltas, tangential (oblique) clinoforms and sad-rich turbidites; association 2 is composed by sigmoidal clinoforms and sand-rich turbidites; association 3 is composed by continental to shelfal deposits; association 4 is composed by MTDs, sigmoidal clinoforms and sand-rich turbidites; and association 5 is composed by MTDs, complex sigmoidal-oblique clinoforms and sand-rich turbidites.

Association 3 records a period of relative sea-level rise, when aggrading deposits associated to a normal regression were deposited in the shelf. The aggradational phase culminates in the slope catastrophic collapse and consequent MTD generation. Association 4 is composed of MTDs, high-angle (sigmoidal) slope-accretion clinoforms and sand-rich turbidites. A new set of reflectors composing association 3 is formed, composed by subparallel topset reflectors deposited during a base level rise. Slope gravitational collapse marks the onset of a falling stage, and association 5 is composed of MTD, high relief complex-pattern slope-accretion clinoforms and sandy turbidites. Subparallel reflectors compose another set of facies association 3, formed during the last base-level rise registered at the interval in the study area. A clinoform set of association 4 represents the final depositional stage from the Eocene in north Santos Basin, when a new base-level fall originated MTD, high-angle slope-accretion clinoforms and sand-rich turbidites.

2.1.6 DISCUSSION

The studied interval is dominated by prograding clinoforms with few aggradation (figs A4, A7 and A14), indicating conditions of forced regressions and high sediment supply (e.g. Zecchin and Catuneanu, 2013). In this context, seismic facies associations with their related depositional elements and erosive features represent tridimensional depositional intervals characterized by specific paleoenvironmental conditions and associated base-level behavior (Fig. A14).

High sediment supply and forced regressions are favorable for the development of shelf-margin deltas (Mellere *et al.*, 2002). However, in the studied interval, seismically detectable shelf-margin deltas are concentrated in the first two seismic facies associations, being sparse in the others (Figs. A4, A6 and A14). This characteristic is possibly a consequence of erosion of the deltas during extensive periods of exposure of the shelf margin, associated to base-level falls (Mellere *et al.*, 2002). In these periods, the knick-points of canyons developed on slope areas may migrate landward and become connected to shelf-incised fluvial systems, preventing the generation of shelf-margin deltas (Kolla and Perlmutter, 1993). Such connection was suggested by Moreira and Carminatti (2004) in their analysis of canyons developed during the Eocene in northern Santos Basin.

Oblique (tangential) slope-accretion clinoforms and sand-rich turbidites occur in association with the shelf-margin deltas. The increase on dip angles from older to youngest clinothemes (Fig. A7 B) in association 1 suggests an increase in sediment supply and sediment caliper as a result of base level fall and erosion on the shelf (e.g. Zecchin and Catuneanu, 2013; Safronova *et al.*, 2014). While in the first parts of association 1 lower-angle clinothemes (maximum slope angle of approximately 1°) are associated to flat to mildly descending shelf-margin trajectories, steeper clinoforms in the last stages of the association (maximum slope angle reaching 2°) are related to strongly descending trajectories (Figs. A7 and A14). Consequently, shelf-margin deltas are abundant in the older stages of association 1, and rarer in the younger that were formed during a more expressive phase of base level fall (Fig. A14). Slope angle increase in these depositional intervals is a consequence of extensive forced regressions that caused the migration of the sediment input points to areas closer to the shelf margin and upper slope (Catuneanu, 2006; Catuneanu *et al.*, 2009).

Although sand transport to the deep-sea is favored by forced regressions (e.g. Muto and Steel, 2002; Helland-Hansen and Hampson, 2009), occurrence and volume of turbidites are not exclusively controlled by base-level falls. Turbidites were identified in all seismic facies associations formed during base-level falls, but are more frequently observed on the bottomset of clinoforms from association 1, where well-developed shelf-margin deltas occur (Figs. A4 and A8). Based on similar observations, Moreira and Carminatti (2004) divided the Eocene deep-water deposits in north Santos Basin in a sand-rich domain – corresponding to association 1 in the present paper – and a mud-rich domain – equivalent to associations 4 and 5 (Fig. A14). Sand-rich turbidites are also identified in facies associations corresponding to the mud-rich domain of Moreira and Carminatti (2004), but MTDs associated with submarine slumps in these associations probably prevented the formation of well-developed submarine fans, by creating an irregular topography over the sea-floor with barriers to the propagation of the turbiditic flow (e.g. Machado *et al.*, 2004). Only in more distal parts of the basin, well-developed turbidites with high-amplitude reflectors and extensions up to 10 km are observed, subsequent to MTD emplacement.

Recurrence of submarine slumps truncating reflectors from associations 2 to 5 and the low thickness of bottomset deposits make hard to correlate these distal submarine fans to a specific depositional interval or base-level trend. However, considering the high sediment supply in relation to the mainly falling base-level trend, it seems coherent to consider that the more distal submarine fans were fed by turbidity current during both rising and falling of relative sea level (e.g. Mutti and Normark, 1991; Burgess and Hovius, 1998; Shanmugam, 2002; Dixon et al., 2012; Safronova et al., 2014; de Gasperi and Catuneanu, 2014; Fig. 14). Therefore, the primary control on turbidite deposition was the sediment supply (e.g. Burgess and Hovius, 1998; Dixon et al., 2012; Safronova et al., 2014), although the influence of falling to low relative sea level was crucial to the development of shelf-margin deltas that were the main feeders for deep-water sands (e.g. Mellere *et al.*, 2002; Johannessen and Steel, 2005; Dixon *et al.*, 2013). The architectural pattern of the turbidite systems (channels ending in frontal splays) is well known and well documented in the classic literature on deep-water systems (e.g. Mutti and Normark, 1991; Posamentier and Erskine, 1991; Shanmugam, 2000; Sylvester et al., 2012; de Gasperi and Catuneanu, 2014). The mainly straight geometry of the submarine channels identified in the study area (Fig. A9) differs from the meandering pattern identified by Moreira and Carminatti (2004). However, in the Pleistocene of the Gulf of Mexico, Sylvester *et al.* (2012) identified sinuous channels confined (entrenched) within straight features (Fig. A9 C and D). This is a result of confinement between levees that prevent a larger-scale lateral migration of the channel system. Thus, the straight character of channels observed in the present study may imply that intra-channel features are smaller than the seismic resolution.

Slope-accretion clinoforms show important geometric changes, that are consequence of variations on depositional conditions (e.g. Saller and Dharmasamadhi, 2012; Patruno et al., 2015; Fig. A7). As discussed above, an increase in the dip angles of oblique (tangential) clinoforms is observed within association 1 (Figs. A7 and A14). This increase culminated in high-relief sigmoid clinoforms with truncated topsets in facies association 2 (Fig. A14). Progradation of these clinoforms resulted in the construction of a steep gradient (approximately 6°) that probably influenced the depositional morphology of the reflectors of association 3. This association records an aggradational phase on the shelf following a relative sea-level rise, but the reflectors are truncated basinward by a slump scar (Fig. A13). The slump scar created a steep submarine physiography (exceeding 10°) that influenced the geometry of the subsequent slope-accretion clinoforms (Fig. A12). Therefore, a slope-accretion prism composed of high-relief sigmoidal clinoforms (higher than in association 2) is part of association 4 (Fig. A7 B and C).

Decrease in slope angle with time in association 4 records a progressive approach to the equilibrium profile, compensating the initial steep slope (e.g. Friedrichs and Wright, 2004). Considering the depositional conditions during the interval, post-slump physiography and maintenance of high sediment supply during forced regressions controlled the geometry and high angle of the clinoforms formed just after slope failure (e.g. Zecchin and Catuneanu, 2013; Safronova et al., 2014). These conditions repeated during deposition of the subsequent associations (3 to 5), with new aggradation phases preceding slumps in associations 4 and 5, and high-relief prograding clinoforms in other stages of association 3 (Fig. A14). In association 5, the angle of the clinoforms decreases from approximately 9° to 6°, originating a complex pattern where initially sigmoidal geometries gradually evolve to oblique (tangential) clinoforms within the same slope-accretion prism. The steep submarine bathymetry resulted from slope failure favored the incision of straight canyons (e.g. Clausen *et al.*, 2012; Fig. A12). These features represent preferential conduits for sediment transfer to deeper waters, and their development affected the deposition of turbidites.

The successive occurrence of submarine slumps during the interval also caused the deposition of large MTDs at the slope toe. All slumps occurred immediately after an aggradational phase composed of topset reflectors, which are the most probable source of the MTDs. Despite the relative scarcity of normal-regressive, aggradational strata in the succession, their deposition was important for MTD generation in accumulating sediment at the shelf margin. In the case of the larger MTD, the volume of displaced shelf deposits was sufficiently large to originate a deposit with up to 30 km of lateral extent and an average thickness of about 70 ms TWT (Figs. A4 and A14). The smaller-sized MTDs are also proportional to the thickness of the precursor topset deposits (association 3), which are significantly thinner than those of the first stage of association 3 (Fig. A14). The emplacement of MTDs over sand-rich turbidites has relevance for oil exploration, as potential reservoirs (turbidites) are capped by potential seals (muddy MTDs). The sandy turbidites of the Eocene were previously recognized as good reservoirs (Moreira and Carminatti, 2004; Chang *et al.*, 2008), and oil shows associated to these deposits were detected in some wells. However, Moreira and Carminatti (2004) do not consider the MTDs as good seals due to the presence of compressive structures such as thrust faults that reduce sealing capacity (e.g. Bull et al., 2009; Posamentier and Martinsen, 2011; Alves et al., 2014; Fig. A10). Therefore, three-dimensional mapping of these deformational structures, combined with petrophysical data of the diamictites, may help in the determination of the quality of these deposits as top seals.

2.1.7 CONCLUSIONS

Seismic facies analysis combined with seismic geomorphology and analysis of shelf-margin trajectory allowed a better understanding of the environmental conditions that operated during the evolution of the Eocene shelf-margin in northern Santos Basin:

- the geometry of strongly prograding clinoforms with thin to truncated topsets and flat to descending shelf-margin trajectories is the most common in the interval, indicating conditions of high sediment supply and base level falls;
- variations of geometry and dimensions of the clinoforms were a response of equilibrium profile to conditions of sediment supply, base level fluctuations and pre-depositional submarine topography;

- moments of base-level rise and maintenance of high sediment supply caused sediment storage at the outer shelf, which was essential to subsequent slope failure;
- mud-rich MTDs with chaotic internal pattern and deformation by compressive structures are associated to slump scars;
- the geometry of high-relief clinoforms was conditioned by high sediment supply and steep physiographies associated to slumps. A progressive decrease on slope gradient during progradation records approach to the submarine equilibrium profile;
- shelf-margin deltas were efficient for the transport of sand to the deep-marine environment, as the largest volumes of sand-rich turbidites are associated to this seismic facies;
- turbidite systems included channels and frontal splays. In many cases, these features are amalgamated;
- the steep physiography associated to slump scars was favorable for canyon incisions. These canyons were important for sediment-feeding of deep-marine turbiditic splays;
- turbidites have a good potential as reservoir rocks, but the compressive structures in the MTDs decrease their potential as sealing rocks.

2.1.8 ACKNOWLEDGEMENTS

The authors thank Universidade Federal do Paraná (UFPR) and Laboratório de Análise de Bacias (LABAP) for infrastructure and institutional support. F.B. acknowledges the scholarship provided by the Programa Interdisciplinar em Engenharia de Petróleo e Gás Natural of UFPR (PRH-24). F.F.V. thanks the Conselho Nacional de Desenvolvimento Científico e Tecnológico (CNPq) for financial support (grants:

461628/2014-7). Seismic and well data were provided by the Agência Nacional do Petróleo, Gás Natural e Biocombustíveis (BDEP-ANP).

2.1.9 REFERENCES

Alfaro, E. & Holz, M. 2014. Seismic geomorphological analysis of deepwater gravity-driven deposits on a slope system of the southern Colombian Caribbean margin. Mar. and Petr. Geol., **57,** 294-311.

Alves, T.M., Kurtev, K., Moore, G.F., Strasser, M. 2014. Assessing the internal character, reservoir potential, and seal competence of mass-transport deposits using seismic texture: a geophysical and petrophysical approach. AAPG Bull., **98**(4), 793-824.

Assine, M.L., Corrêa, F.S. & Chang, H.K. 2008. Migração de depocentros na Bacia de Santos: importância na exploração de hidrocarbonetos. Rev. Bras. de Geoc., **38**(2), 111-127.

Back, S, van Gent, H., Reuning, L., Grötsch, J., Niederau, J., Kukla, P. 2011. 3D seismic geomorphology and sedimentology of the Chalk Group, southern Danish North Sea. J. of the Geol. Soc., **168**, 393-405.

Badalini, G., Browner, F., Bourque, R., Blight, R., de Bruin, G. 2010. Seismic-sequence stratigraphic analysis of regional 2D lines in the Santos Basin, offshore Brazil. Search and Disc. Article, **40538,** *online publ*.

Benan, A.O.A.C. & Cauquil, E. 2000. Seabed morphologies and recent turbidite architectural elements as interpreted from 3D seismic data – some implications for exploration and production of the deep offshore. *Deep-water sedimentation: technological challenges for the next millennium – 31st International Geological Congress*. Rio de Janeiro, BR, 111-112.

Berg, O.R. 1982. Seismic detection and evaluation of delta and turbidite sequences: their application to exploration for the subtle trap. AAPG Bull., **66**(9), 1271-1288.

Bull, S., Cartwright, J. & Huuse, M. 2009. A review of kinematic indicators from mass-transport complexes using 3D seismic data. *Mar. and Petr. Geol.*, **26**:1132-1151.

Burgess, P.M. & Hovius, N. 1998. Rates of delta progradation during highstands: consequences for timing of deposition in deep-marine systems. J. of the Geol. Soc., **155**, 217-222.

Carvajal, C.R. & Steel, R.J. 2006. Thick turbidite successions from supply-dominated shelves during sea-level highstand. Geology, **34**(8), 665-668.

Catuneanu, O. 2006. *Principles of Sequence Stratigraphy*. Elsevier, Amsterdam, ND, 375p.

Catuneanu, O., Abreu, V., Bhattacharya, J.P., Blum, M.D., Dalrymple, R.W., Eriksson, P.G., Fielding, C.R., Fisher, W.L., Galloway, W.E., Gibling, M.R., Giles, K.A., Holbrook, J.M., Jordan, R., Kendall, C.G.St.C., Macurda, B., Martinsen, O.J., Miall, A.D., Neal, J.E., Nummedal, D., Pomar, L., Posamentier, H.W., Pratt, B.R., Sarg, J.F., Shanley, K.W., Steel, R.J., Strasser, A., Tucker, M.E., Winker, C. 2009. Towards the standardization of sequence stratigraphy. Earth-Science Rev., **92**, 1-33.

Chang, H.K., Assine, M.L., Corrêa, F.S., Tinen, J.S., Vidal, A.C., Koike, L. 2008. Sistemas petrolíferos e modelos de acumulação de hidrocarbonetos na Bacia de Santos. Rev. Bras. de Geoc., **38**(2), 29-46.

Clausen, O.R., Śliwińska, K.K. & Gołędowski, B. 2012. Oligocene climate changes controlling forced regression in the eastern North Sea. Mar. and Petr. Geol., **29**, 1-14.

D'Ávila, R.S.F., Arienti, L.M., Aragão, M.A.N.F., Vesely, F.F., Santos, S.F., Voelcker, H.E., Viana, A.R., Kowsmann, R.O., Moreira, J.L.P., Coura, A.P.P., Paim, P.S.G., Matos, R.S., Machado, L.C.R. 2008. Ambientes de águas profundas. *In*: *Ambientes de sedimentação siliciclástica do Brasil*. 2008. Org. by A.J.C.L.P. Silva, M.A.N.F. Aragão & A.J.C. Magalhães. Beca, 244-300.

de Gasperi, A. & Catuneanu, O. 2014. Sequence stratigraphy of the Eocene turbidite reservoirs in Albacora field, Campos Basin, offshore Brazil. AAPG Bull., **98**(2), 279-313.

Dias, J.L. 2008. Estratigrafia e sedimentação dos evaporitos neo-aptianos na margem leste brasileira. *In*: *Sal: geologia e tectônica*. 2008. Org. by W.U. Mohriak, P. Szatman & S.M.C. Anjos. Beca, São Paulo, BR, 220-229.

Dixon, J.F., Steel, R.J. & Olariu, C. 2012. Shelf-edge delta regime as a predictor of deep-water deposition. J. of Sed. Res., **82,** 681-687.

Dixon, J.F., Steel, R.J. & Olariu, C. 2013. A model for cutting and healing of deltaic mouth bars at the shelf edge: mechanism for basin-margin accretion. J. of Sed. Res., **83**, *online publ*.

Duarte, C.S.L. & Viana, A.R. 2007. Santos drift system: stratigraphic organization and implications for late Cenozoic palaeocirculation in the Santos Basin, SW Atlantic Ocean. *In*: *Economic and Palaeocenographic Significance of Contourite Deposits*. 2007. Ed. by A.R. Viana & M. Rebesco. Geological Soc. Special Publ., **276**:171-198.

Friedrichs, C.T. & Wright, L.D. 2004. Gravity-driven sediment transport on the continental shelf: implications for equilibrium profiles near river mouths. Coastal Engin., **51**, 795-811.

Gamboa, D., Alves, T. & Cartwright, J. 2012. Seismic-scale rafted and remnant blocks over salt ridges in the Espirito Santo Basin, Brazil. *In*: *Submarine mass movements* *and their consequences*. 2012. Ed. by Y. Yamada, K. Kawamura, K. Ikehara, Y. Ogawa, R. Urgeles, D. Mosher, J. Chaytor, M. Strasser. Springer, London, UK, 629-638.

Garcia, S.F.de M., Letouzey, J., Rudkiewicz, J.-L., Danderfer Filho, A., de Lamotte, D. F. 2012. Structural modeling based on sequential restoration of gravitational salt deformation in the Santos Basin. Mar. and Petr. Geol., **35**, 337-353.

Gee, M.J.R., Gawthorpe, R.L., Bakke, K., Friedmann, S.J. 2007. Seismic geomorphology and evolution of submarine channels from the Angolan continental margin. J. of Sed. Res., **77**, 433-446.

Hadler-Jacobsen, F., Gardner, M.H. & Borer, J.M. 2007. Seismic stratigraphic and geomorphic analysis of deep-marine deposition along the West African continental margin. *In: Seismic geomorphology: applications to hydrocarbon exploration and production*. 2007. Ed. by J.A. Davies, H.W. Posamentier, L.J. Wood, J.A. Cartwright. Geol. Soc. Spec. Publ., London, UK, 47-84.

Helland-Hansen, W. & Hampson, G. J. 2009. Trajectory analysis: concepts and applications. Basin Res., **21**, 454-483.

Henriksen, S., Helland-Hansen, W. & Bullimore, S. 2011. Relationships between shelf-edge trajectories and sediment dispersal along depositional dip and strike: a different approach to sequence stratigraphy. Basin Res., **23**, 3-21.

Jiang, S., Weimer, P., Henriksen, S., Hammon III, W.S. 2012. 3D seismic stratigraphy and evolution of Upper Pleistocene deepwater depositional systems, Alaminos Canyon, northwestern Gulf of Mexico. SEPM Spec Publ., **99**, 309-327.

Johannessen, E.P. & Steel, R.J. 2005. Shelf-margin clinoforms and prediction of deepwater sands. Basin Res., **17,** 521-550.

Karner, G.D. & Driscoll, N.W. 1999. Tectonic and stratigraphic development of the West African and eastern Brazilian Margins: insights from quantitative basin modeling. *In*: *The oil and gas habitats of the South Atlantic*. 1999. Ed. by N.R. Cameron, R.H. Bate & V.S. Clure. Geol. Soc. Spec. Publ., London, **153**, 11-40.

Kolla, V. & Perlmutter, M. A. 1993. Timing of turbidite sedimentation on the Mississippi Fan. AAPG Bull., **77,** 1129-1141.

Lourens, L.J., Sluijs, A., Kroon, D., Zachos, J.C., Thomas, E., Röhl, U., Bowles, J., Raffi, I. 2005. Astronomical pacing of late Palaeocene to early Eocene global warming events. Nature Let., **435**, 1083-1087.

Macedo, J.M. 1989. Evolução tectônica da Bacia de Santos e áreas continentais adjacentes. Bol. de Geoc. da Petrobras, **3**, 159-173.

Machado, L.C.R., Kowsmann, R.O., de Almeida Jr., W., Murakami, C.Y., Schreiner, S., Miller, D.J., Piauilino, P.O.V. 2004. Geometria da porção proximal do sistema deposicional turbidítico moderno da Formação Carapebus, Bacia de Campos; modelo para heterogeneidades de reservatório. Bol. de Geoc. da Petrobras, **12**(2), 287-315.

Martinez, J.F., Cartwright, J. & Hall, B. 2005. 3D seismic interpretation of slump complexes: examples from the continental margin of Israel. Basin Res., **17,** 83-108.

Mellere, D., Plink-Björklund, P. & Steel, R. J. 2002. Anatomy of shelf deltas at the edge of a prograding Eocene shelf margin, Spitsbergen. Sedimentology, **49,** 1181-1206.

Mitchum, R.M., Vail, P.R. & Thompson, S. 1977. Seismic stratigraphy and global changes in sea level, part 2: the depositional sequence as a basic unit for stratigraphic analysis. *In: Seismic stratigraphy: application to hydrocarbon exploration*. 1977. Ed. by C.E. Payton. AAPG Memoir 26, AAPG, Tulsa, USA, 53-62.

Modica, C.J. & Brush, E. R. 2004. Postrift sequence stratigraphy, paleogeography, and fill history of the deep-water Santos Basin, offshore southeast Brazil. AAPG Bull., **88**(7), 923-945.

Mohriak, W.U. & Magalhães, J. M. 1993. Estratigrafia e evolução estrutural da área norte da Bacia de Santos. *Atas do III Simp. de Geol. do Sudeste*, **1,** 19-26.

Moreira, J.L.P. & Carminatti, M. 2004. Sistemas deposicionais de talude e de bacia no Eoceno da Bacia de Santos. Bol. de Geoc. da Petrobras, **12**(1), 73-87.

Moscardelli, L., Wood, L. & Mann, P. 2006. Mass-transport complexes and associated processes in the offshore area of Trinidad and Venezuela. AAPG Bull., **90**(7), 1059-1088.

Muto, T. & Steel, R.J. 2002. In defense of shelf-edge delta development during falling and lowstand of relative sea level. The J. of Geol., **110**, 421-436.

Mutti, E. & Normark, W. R. 1991. An integrated approach to the study of turbidite systems. *In: Seismic facies and sedimentary processes of submarine fans and turbidite systems*. 1991. Ed. by P. Weimer & M.H. Link. Springer, 75-106.

Patruno, S., Hampson, G.J. & Jackson, C.A.-L. 2015. Quantitative characterization of deltaic and subaqueous clinoforms. Earth-Sci. Rev., **142**, 79-119.

Porębski, S.J. & Steel, R.J. 2003. Shelf-margin deltas: their stratigraphic significance and relation to deepwater sands. Earth-Science Rev., **62,** 283-326.

Posamentier, H.W., Davies, J.A., Cartwright, J.A., Wood, L.J. 2007. Seismic geomorphology – an overview. *In: Seismic geomorphology: applications to hydrocarbon exploration and production*. 2007. Ed. by J.A. Davies, H.W. Posamentier, L.J. Wood, J.A. Cartwright. Geol. Soc. Spec. Publ., London, UK, 1-14.

Posamentier, H.W. & Erskine, R. D. 1991. Seismic expression and recognition criteria of ancient submarine fans. *In*: *Seismic facies and sedimentary processes of submarine fans and turbidite systems*. 1991. Ed. by P. Weimer & M.H. Link. Springer, 197-222.

Posamentier, H.W. & Kolla, V. 2003. Seismic geomorphology and stratigraphy of depositional elements in deep-water settings. J. of Sed. Res., **73**(3), 367-388.

Posamentier, H.W. & Martinsen, O. J. 2011. The character and genesis of submarine mass-transport deposits: insights from outcrop and 3D seismic data. SEPM Spec. Publ., **96**, 7-38.

Prather, B.E., Deptuck, M.E., Mohrig, D., Van Hoom, B., Wynn, R.B. 2012. Application of the principles of seismic geomorphology to continental-slope and base-of-slope systems: case studies from seafloor and near-seafloor analogues. SEPM Spec. Publ., **99**, 5-9.

Prather, B.E. & Steele, D.R. 2000. Methodologies for uncertainty assessment of deep-water facies and basins. *Deep-water sedimentation: technological challenges for the next millennium – 31st International Geological Congress*. Rio de Janeiro, BR, 85-92.

Ribeiro, M.C.S. 2007. *Termocronologia e história denudacional da Serra do Mar e implicações no controle deposicional da Bacia de Santos*. Tese de Doutoramento, Rio Claro, Instit. de Geoc. e Ciên. Exat. da Univ. Estad. Paul., 227p.

Safronova, P.A., Henriksen, S., Andreassen, K., Laberg, J.S., Vorren, T. O. 2014. Evolution of shelf-margin clinoforms and deep-water fans during the middle Eocene in the Sørvestsnaget Basin, southwest Barents Sea. AAPG Bull., **98**(3), 515-544.

Sahy, D., Condon, D.J., Terry Jr., D.O., Fischer, A.U., Kuiper, K.F. 2015. Synchronizing terrestrial and marine records of environmental change across the Eocene-Oligocene transition. Earth and Plan. Sci. Lett., **427**, 171-182.

Saller, A., Dharmasamadhi, I.N.W. 2012. Controls on the development of valleys, canyons, and unconfined channel-levee complexes on the Pleistocene slope of East Kalimantan, Indonesia. Mar. and Petr. Geol., **29**, 15-34.

Shanmugam, G. 2000. 50 yars of the turbidite paradigm (1950s – 1990s): deep-water processes and facies models – a critical perspective. Mar. and Petr. Geol., **17**, 285-342.

Shanmugam, G. 2002. Ten turbidite myths. Earth-Science Rev., **58**, 311-341.

Sombra, C.L., Arienti, L.M., Pereira, M.J., Macedo, J.M. 1990. Parâmetros controladores da porosidade e da permeabilidade nos reservatórios clásticos profundos do campo de Merluza, Bacia de Santos, Brasil. Bol. de Geoc. da Petrobras, **4**(4), 451-466.

Steel, R.J. & Olsen, T. 2002. Clinoforms, clinoform trajectories and deepwater sands. *In*: *Sequence stratigraphic models for exploration and production: evolving models and application histories*. 2002. Ed. by J. M. Armentrout & N.C. Rosen. GCS-SEPM Spec. Publ., 367-381.

Stow, D.A.V. & Mayall, M. 2000. Deep-water sedimentary systems: new models for the 21st century. Mar. and Petr. Geol., **17**, 125-135.

Sylvester, Z., Deptuck, M.E., Prather, B.E., Pirmez, C., O'Byrne, C. 2012. Seismic stratigraphy of a shelf-edge delta and linked submarine channels in the northeastern Gulf of Mexico. SEPM Spec. Publ., **99,** 31-59.

Veeken, P.C.H. & van Moerkerken, B. 2013. *Seismic stratigraphy and depositional facies models*. EAGE, Houten, ND.

Williams, B.G. & Hubbard, R.J. 1984. Seismic framework and depositional sequences in the Santos Basin. Mar. and Petr. Geol., **1**, 90-104.

Zalán, P.V. & Oliveira, J. A. B. 2005. Origem e evolução estrutural do Sistema de Riftes Cenozóicos do Sudeste do Brasil. Bol. de Geoc. da Petrobras, **13**(2), 269-300.

Zecchin, M. & Catuneanu, O. 2013. High-resolution sequence stratigraphy of clastic shelves I: units and bounding surfaces. Mar. and Petr. Geol., **39,** 1-25.

2.2 Base-level and sediment-supply controls on shelf-margin growth and deep water depositional systems: Eocene clinoforms from northern Santos Basin, offshore Brazil

Article submitted for Marine and Petroleum Geology in October 29th, 2015.

2.2.1 ABSTRACT

In order to assess the effects of base-level change and sediment supply on the stratigraphic architecture of a shelf margin, a seismic stratigraphic investigation was carried out in the Eocene interval of northern Santos Basin, offshore Brazil. The studied succession configures a complex of prograding shelf-margin clinoforms formed in a passive margin during an epoch of overall low relative sea level and high sediment supply. The clinoform complex encompasses five seismic facies and their respective depositional settings: shelf-margin deltas, oblique shelf-margin clinoforms, sigmoidal shelf-margin clinoforms, continental to shelfal deposits and mass-transport deposits. These are stratigraphically arranged as seven depositional sequences recording a total displacement of the shelf-margin of about 30 km. Two main types of sequences can be recognized, the first one (type A) being dominated by oblique shelf-margin clinoforms and shelf-margin deltas in which shelf-edge trajectories were essentially flat to descending and thick sandy turbidites were deposited on the foreset to bottomset zone. Sequences of this type are represented by forced regressive units deposited during extensive periods of relative sea level fall. Type B comprises a lower part represented by lowstand, aggradational shelfal deposits and an upper part composed of mass-transport deposits and sigmoidal clinoforms with descending shelf-margin trajectory. A steep slump scar deeply cut the shelfal strata and constitutes the boundary between the two intervals observed in these sequences. Sequence stratigraphic interpretation coupled with trajectory analysis reveals that sandy turbidites are more common and more voluminous within falling-stage systems tract in which shelf-margin deltas are well developed (type A sequences and forced-regressive units of type B sequences). Slope failure and mass-transport deposits, by the other hand, occurred exclusively in type B sequences during the onset of sea-level fall and their volume are directly related to the thickness of the shelfal sediments formed during the pre-failure normal regressions.

Keywords: sequence stratigraphy, trajectory analysis, turbidites, mass-transport deposits, lowstand systems tract, falling-stage systems tract

2.2.2 INTRODUCTION

Sequence stratigraphic models predict that the deposition of coarse-grained clastic sediment in deep marine environments occurs preferentially during base-level fall and/or lowstand, when accommodation space is reduced and fluvio-deltaic systems become able to deliver its sediment load to the outer shelf and slope (e.g. Vail et al., 1977; Posamentier and Vail, 1988; Walker, 1990; Posamentier and Allen, 1999; Catuneanu, 2002). These moments would be favorable for the generation of sandy submarine fans (turbidites), which constitute the main exploratory targets in continental margins (e.g. Mutti et al., 2007). Other authors, however, argue that sediment supply is the main control on shelf-margin accretion (e.g. Carvajal and Steel, 2006; Monteverde et al., 2008; Carvajal et al., 2009; Dixon et al., 2013), and demonstrate the deposition of thick turbidite successions even during high and/or ascending relative sea level.

The timing of slope failure and mass-flow generation in deep water is also under discussion (e.g. Moscardelli et al., 2006; Posamentier and Martinsen, 2011). These processes generate thick and extensive mass-transport deposits (MTDs), which occur in close association with turbidites and play an important role as seal or reservoir in deep water petroleum systems (e.g. Moscardelli and Wood, 2008; Gamberi et al., 2011; Posamentier and Martinsen, 2011; Alves et al., 2014). Although slope instability generally results from a combination of local and regional factors (e.g. Alves and Cartwright, 2010; Olafiranye et al., 2013; Gong et al., 2014), the association between MTDs and base-level falls is widely admitted in sequence-stratigraphic models (e.g. Posamentier and Kolla, 2003; Catuneanu et al., 2011). As a consequence, the identification of MTDs in the stratigraphic record may be an important guide for the reconstruction of relative sea-level fluctuations, when combined with sequence-stratigraphic analysis.

Erecting a genetic stratigraphic framework and its relationship to base-level fluctuations and sediment supply to the basin is thus necessary for determining the timing of turbidite and MTD generation. In seismic stratigraphy, classic systems tracts and sequence schemes (e.g. Vail et al., 1977; Galloway, 1989; Embry and Johannessen,

1992) have been complemented by model-independent approaches (Catuneanu and Zecchin, 2013), such as the analysis of shelf-edge and delta-front trajectories (e.g. Johannessen and Steel, 2005; Henriksen et al., 2009; Steel et al., 2010; Dixon et al., 2012), and architectural styles of shelf-margin clinoforms (e.g. Driscoll and Karner, 1999; Petter et al., 2011; Gong et al., 2015).

In northern Santos Basin, offshore Brazil, the Eocene interval is composed of shelf-margin clinoform complexes formed during a phase of general low accommodation and high sediment supply. The stratigraphic architecture is mainly characterized by prograding clinoform sets with thin or truncated topsets, where progradation were higher than aggradation, and thick MTDs and turbidites were formed at the slope toe. The scope of this paper is to characterize this succession in order to evaluate the role of relative sea level fluctuations and sediment supply on stratal geometries and stratigraphic stacking patterns, as well as on the timing of deposition of turbidites and mass-transport deposits in deep waters.

2.2.3 GEOLOGICAL SETTING

The Santos Basin is located in the southeastern sector of the Brazilian continental margin, and is bounded in the north by the Cabo Frio high and in the south by the Florianópolis high (Fig. B1). The geologic evolution of this basin is associated with the breakup of Gondwana and opening of the South Atlantic Ocean, during which three major tectonic phases are recognized – a Barremian to Early Aptian rift phase, an Aptian to Early Albian evaporitic sag phase, and an Albian to present divergent margin (Moreira et al., 2007). The main chronostratigraphic horizons recognized in the basin (according to Contreras et al., 2010) are shown in the regional dip-oriented seismic section of figure B2.

Following a Turonian maximum marine flooding, the basin experienced a long-term regressive phase (~60 My), known as the Jureia progradation (Macedo, 1989). This regressive episode was driven by a significant increase in sediment supply associated with uplifting and denudation on the Serra do Mar range. As a result, extensive deltaic progradations and associated deep-water depositional systems (Fig. B1) took place during the Upper Cretaceous, Paleocene and Eocene (Mohriak and Magalhães, 1993). Sediment load associated with these high supply periods has contributed to trigger salt movements towards the offshore, and to the generation of important sin-sedimentary regional faults (e.g. Cabo Frio fault zone), structural highs and mini-basins (Assine et al., 2008; Badalini et al., 2010).

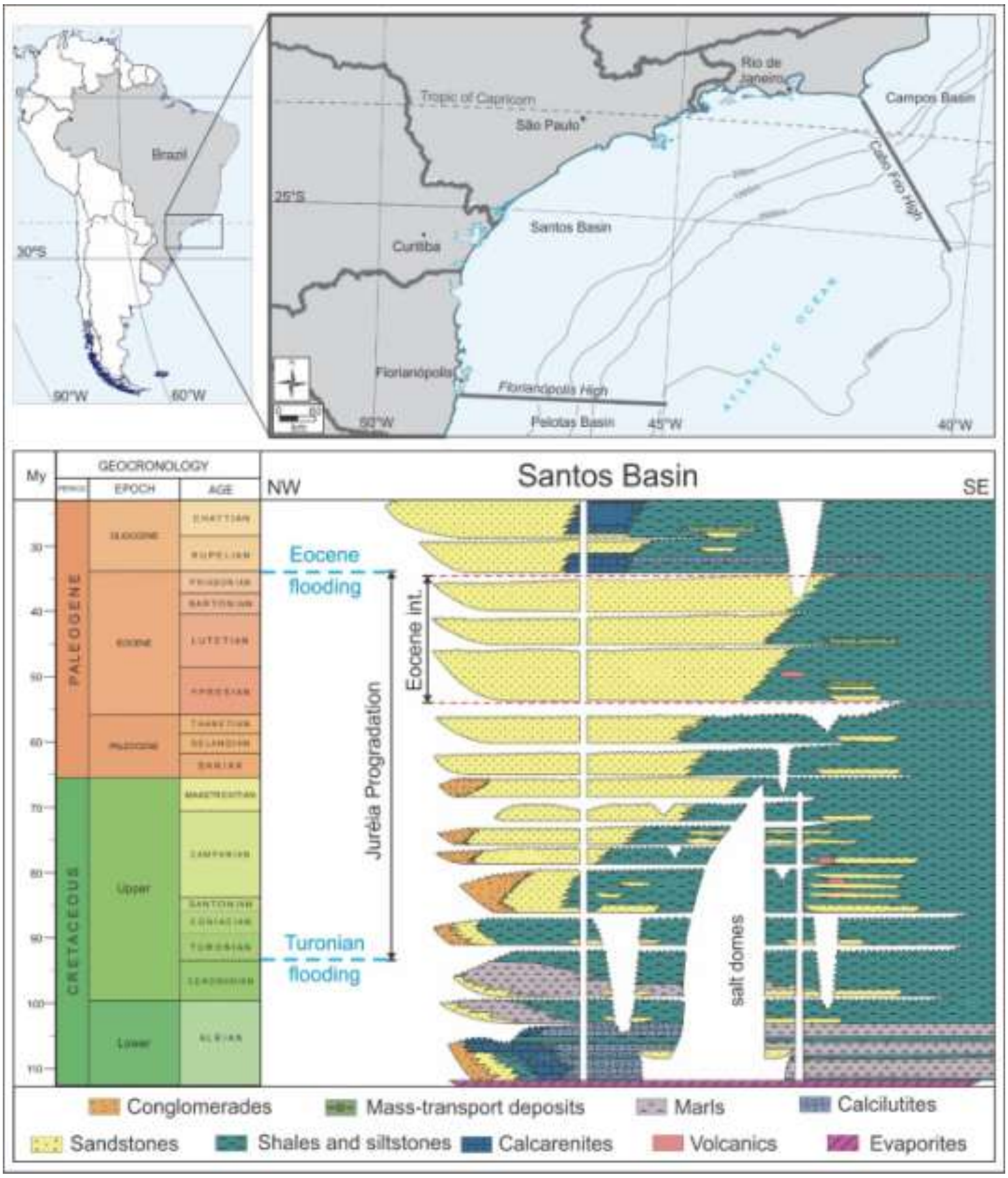

Figure B1: Location map of Santos Basin in offshore Brazil, and stratigraphic chart for its post-rift succession (modified from Moreira et al., 2007). Note the location of the Eocene interval at the uppermost part of the Juréia progradation.

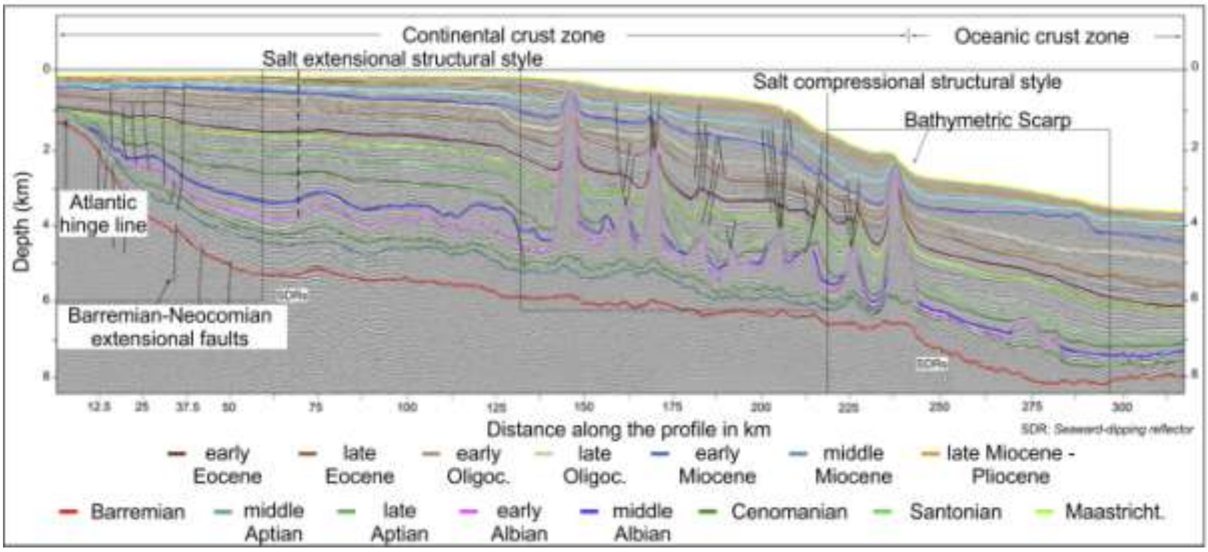

Figure B2: Regional dip-oriented seismic section from the Santos Basin, showing geological framework and the main chronostratgraphic horizons according to Contreras et al. (2010).

The Eocene corresponds to the latest phase of the Juréia progradation, in which the high sediment supply is related to the paleodrainage of the Paraíba do Sul river system (Ribeiro, 2007), and can be attributed to exhumation of the uplifted Serra do Mar coupled with intense rainfall associated to the Eocene Thermal Maximum (Lourens et al., 2005; Zalán and Oliveira, 2005). The Eocene-Oligocene boundary records an important environmental change in Santos Basin, with the beginning of a global cooling period (Duarte and Viana, 2007; Sahy et al., 2015) and the shift of the Paraíba do Sul river, which at this time started to deliver its load to the Campos Basin (Karner and Driscoll, 1999). As a result of this dramatic decrease in sediment supply, a major transgression occurred in the Santos Basin, leading to sediment starvation and reworking by bottom currents (Duarte and Viana, 2007).

In the study area, the Eocene succession displays high relief shelf-margin clinoforms (Mohriak and Magalhães, 1993). At the slope-basin area, expressive gravity-driven sandy and muddy deposits have been recognized (e.g. d’Ávila et al., 2008), but there is no agreement amongst previous authors about the timing of these deposits during the stratigraphic evolution of the interval (e.g. Modica and Brush, 2004; Moreira and Carminatti, 2004; Assine et al., 2008; Dixon, 2013).

2.2.4 DATABASE AND METHODS

The study area is located in northern Santos Basin, approximately 150 km offshore from the city of Rio de Janeiro (Fig. B3). Database consists of 20 2D seismic lines and logs from four wells (Fig. B3) provided by the Brazilian National Agency of Petroleum, Natural Gas and Biofuels (ANP), covering an area of approximately 2300 km². Seismic data are from different surveys performed since the 1990's, including 0228 SANTOS 11A, 0231 Santos 18A, 0247 CABO FRIO 3A, 0261 VB99 2D BMS, and R0003 0259 2D SPP 2Q 1999.

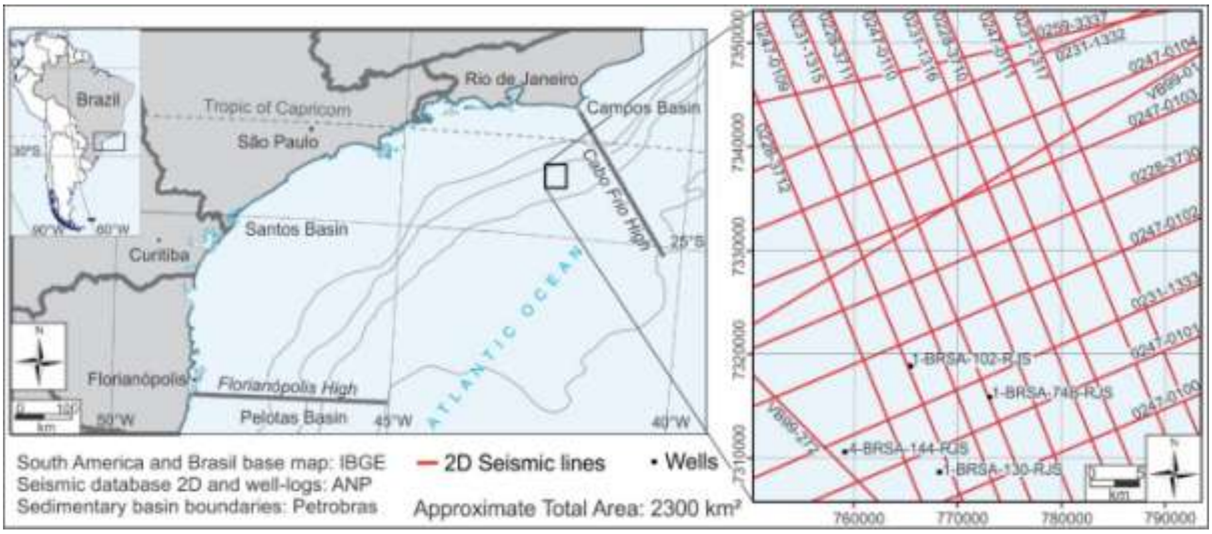

Figure B3: Location map of the study area in northern Santos Basin, and dataset used in the present paper.

The stratigraphic succession was investigated through seismic facies analysis, seismic sequence stratigraphy and shelf-edge trajectory analysis, according to the methodology described, for instance, in Catuneanu et al. (2011). Seismic interpretation started with the determination of reflectors termination patterns and the definition of key surfaces (downlap, onlap and truncation surfaces).

Seismic facies analysis helped in sequence boundary determination and systems tracts definition and interpretation (e.g. Monteverde et al., 2008). The identification of seismic facies was based on the tridimensional reconnaissance of the configuration of reflectors considering their geometry, lateral continuity, seismic amplitude and frequency

(Veeken and van Moerkerken, 2013). Well logs were tied to seismic sections and used as a support to the seismic facies interpretations. When available, time-to-depth conversion tables were used to detect thicknesses.

For sequence-stratigraphic analysis, it was applied the concept of depositional sequence, i.e. a unit bounded by subaerial unconformities or its correlative conformities developed during maximum falls of relative sea level (Catuneanu, 2006). Interpretations of depositional trends and relative sea level changes were based on chronostratigraphic charts (Wheeler diagrams) from dip-oriented seismic sections and on shelf-edge trajectories (e.g. Steel and Olsen, 2002; Henriksen et al., 2011). The naming of sequences identified is based on an adaptation of the nomenclature proposed by Moreira et al. (2007) for the Santos Basin.

The term turbidite is used here in a broad sense (e.g. Mutti, 1992) to define sandy-gravelly deposits formed by turbidity currents and other types of cohesionless gravity flows. In the studied seismic sections they appear as sheet-like high-amplitude reflections at the foresets or bottomsets of shelf-margin clinoforms. Mud-rich, chaotic deposits related to slumps and debris flows are not included in this category and for this the generic term mass-transport deposit (MTD) was employed.

2.2.5 SEISMIC FACIES: DESCRIPTION AND INTERPRETATION

In the studied area, the Eocene interval ranges in thickness from about 230 m in proximal (shelf) and distal (basin) areas, to about 590 m at the slope-accretion prisms. The predominant seismic expression is of moderated- to high-angle prograding clinoforms (Fig. B4 A, B and C). Within this clinoform complex, five main seismic facies have been recognized, whose naming was based on the terminology used by Berg (1982) for clinoform geometric classification.

2.2.5.1 Facies A – shelf-margin deltas

This facies consists of prograding clinoforms with maximum relief of 200 ms (TWT; approx. 115 m), and maximum longitudinal extension of 3 km (Fig. B4). Trajectory of clinoform rollover varies from flat to gently descending. When preserved, topsets have high seismic amplitudes, which decrease towards the bottomsets. This variation suggests a transition from sandy proximal deposits to muddy distal deposits.

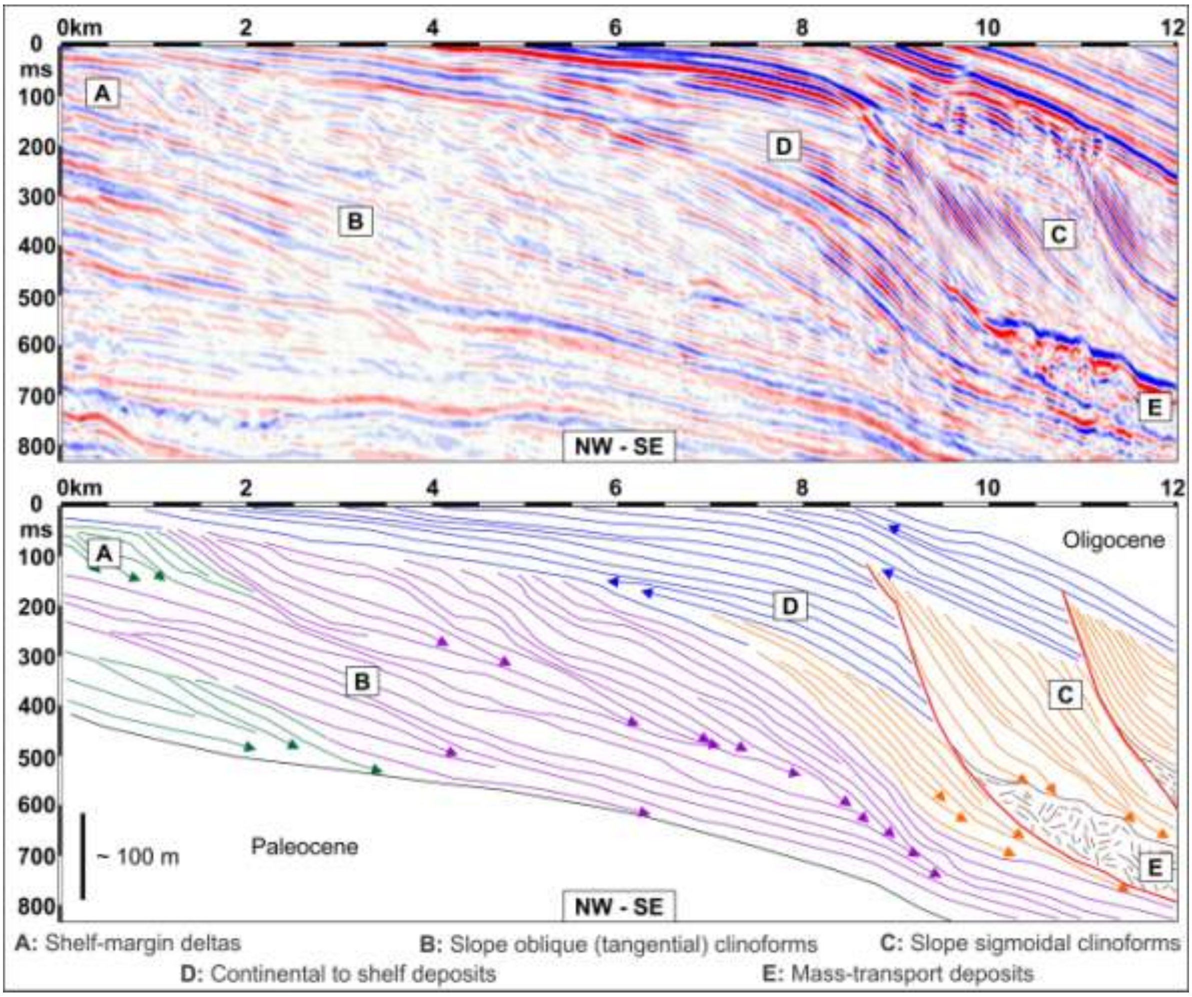

Figure B4: Dip-oriented seismic section showing the main seismic facies identified in the Eocene succession. Facies A corresponds to shelf-margin deltas; facies B corresponds to tangential (oblique) shelf-margin clinoforms, facies C corresponds to sigmoidal shelf-margin clinoforms; and facies D corresponds to continental to shelfal deposits.

In their more distal reaches, the bottomsets of facies A drape onto the foresets of high-relief oblique clinoforms (facies B). Based on the characteristics presented above, this facies can be interpreted as shelf-margin deltas (e.g. Porębski and Steel, 2003; Moreira and Carminatti, 2004; Patruno et al., 2015) developed due to the advance of deltaic systems beyond the original shelf edge. Flat to descending trajectories, longdistance progradation and thin to truncated topsets suggest the dominance of forced regressions (e.g. Posamentier and Allen, 1999).

2.2.5.2 Facies B - oblique (tangential) shelf-margin clinoforms

Facies composed of large-sized clinoforms with relief from 250 ms to 750 ms (TWT, approx 145 to 430 m), and longitudinal extension up to 10 km. Foresets dip at relatively low angles (1° to 2°; Fig. B4 B), and a gentle increase in slope angles is recorded from the oldest to the youngest clinotheme. Topsets are generally truncated, and the trajectory of clinoform rollovers is mainly descending. Seismic amplitudes are high in topset reflectors, but generally decrease towards the foresets. High-amplitude reflectors are common at the bottomsets (Fig. B5), extending longitudinally from 0,5 to 5 km and displaying a characteristic sheet-like geometry with a convex-upward (mound-shaped) longitudinal profile.

This facies is interpreted as shelf-margin clinoforms (e.g. Porębski and Steel, 2003; Patruno et al., 2015), formed as a result of sediment accretion on the slope face during periods of predominance of forced regressions. The gradual increase in foreset dip with time may be related to a progressively increase on sediment supply, as a consequence of relative sea level fall and erosion in the shelfal domain (Zecchin and Catuneanu, 2013), combined with continuous subsidence.

Localized high-amplitude reflectors in some foresets suggest the occurrence of intra-slope (shingled) sand-rich turbidites (e.g. Johannessen and Steel, 2005). High-amplitude reflectors at the bottomsets suggest the occurrence of sandy submarine fans (Posamentier and Erskine, 1991; Johannessen and Steel, 2005), which were interpreted as high-density turbidites by Moreira and Carminatti (2004).

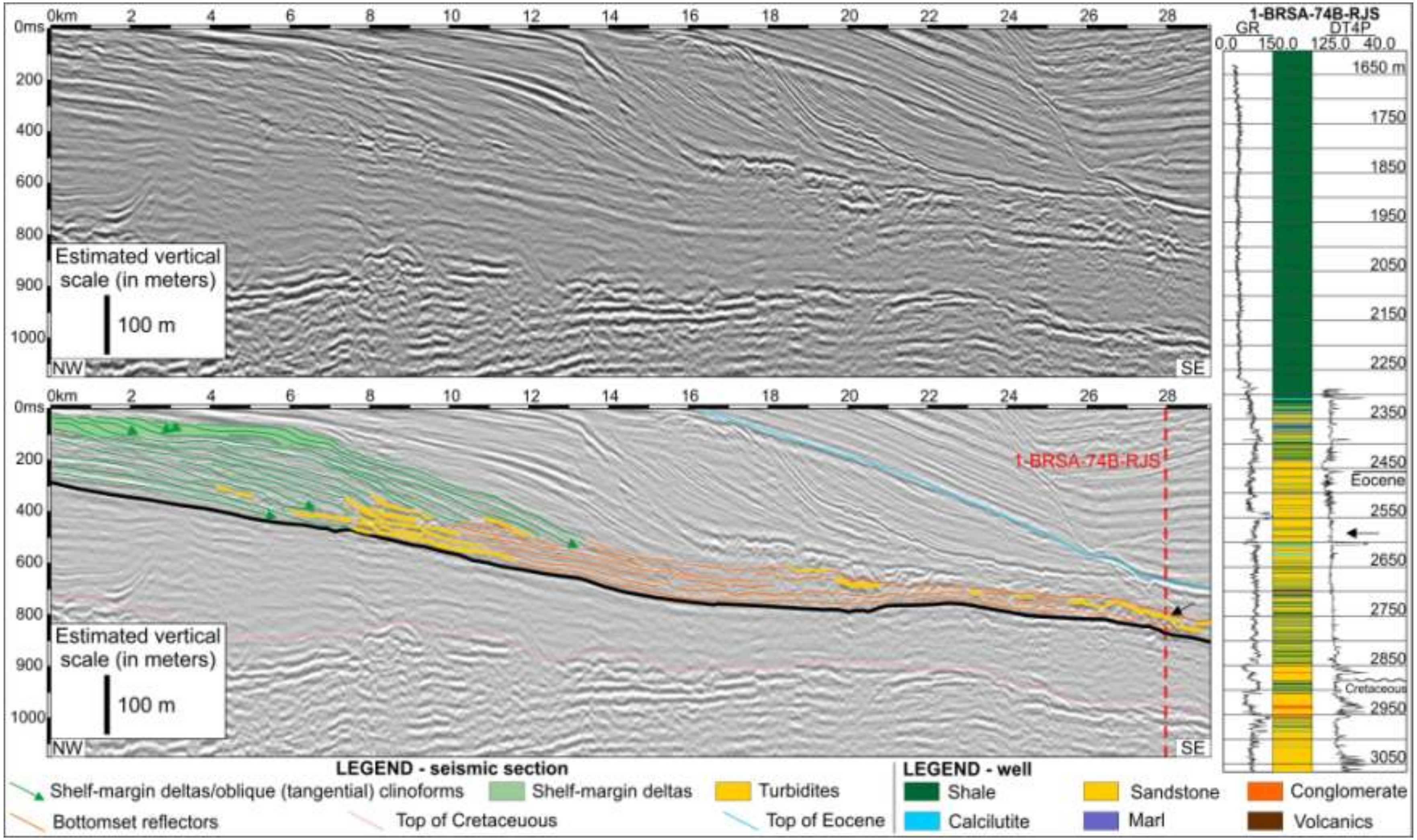

Figure B5: Dip-oriented seismic section and tied well log highlighting sand-rich, bottomset deposits associated with shelf margin deltas and oblique (tangential) clinoforms.

2.2.5.3 Facies C – sigmoidal shelf-margin clinoforms

This facies consists of high-relief (up to 700 ms TWT, approx. 410 m) and high-angle sets of clinoforms (6° - 9°) with a characteristic sigmoidal profile and a longitudinal extension of up to 15 km (Fig. B4 C). These clinoforms start prograding onto a very irregular surface that truncate previous reflectors. From the oldest to the youngest clinotheme within each clinoform set, it is observed a gradual decrease in slope angle. Topsets are generally truncated, and trajectories of clinoform rollovers are mainly descending. Seismic amplitudes vary from moderate to high in the foreset domain, and generally low to moderate in the bottomset domain. However, laterally discontinuous, high-amplitude reflectors may occur at the bottomsets, allowing the inference of lenticular sand-rich units (e.g. Posamentier and Erskine, 1991), which longitudinal extension varies from 2 to 10 km. These clinoforms are interpreted as a result of slope accretion (e.g. Porębski and Steel, 2003; Patruno et al., 2015), associated with forced regressions. The irregular surfaces on which clinoforms developed are interpreted as large-scale slump scars. These scars clearly controlled the steepness and geometry of the clinoforms, as the maximum angles of the scars exceed 10°. Reduction in clinoform steepness with time indicated a progressive approach to slope equilibrium profile.

2.2.5.4 Facies D - continental to shelfal deposits

Facies composed of low-angle, high to moderate amplitude sets of reflectors with subparallel to divergent pattern (Fig. B4 D). Reflectors terminate in onlap towards the continent and are truncated basinward by slump scars (Fig. B6). Based on these characteristics, this facies can be interpreted as a result of shelfal aggradation, and is probably constituted of continental (coastal plain) to outer shelf deposits. The aggradational pattern is indicative of positive accommodation in the shelf due to a general rise in base level. Time-equivalent clinoforms are not preserved due to the subsequent truncation by catastrophic failure of the shelf-margin.

2.2.5.5 Facies E - mass-transport deposits (MTDs)

This facies has a chaotic seismic configuration and define low to moderate amplitude mound-shaped sedimentary bodies located at the slope toe and terminating in onlap against the slump scars (Figs. B4 E, B6 and B7).

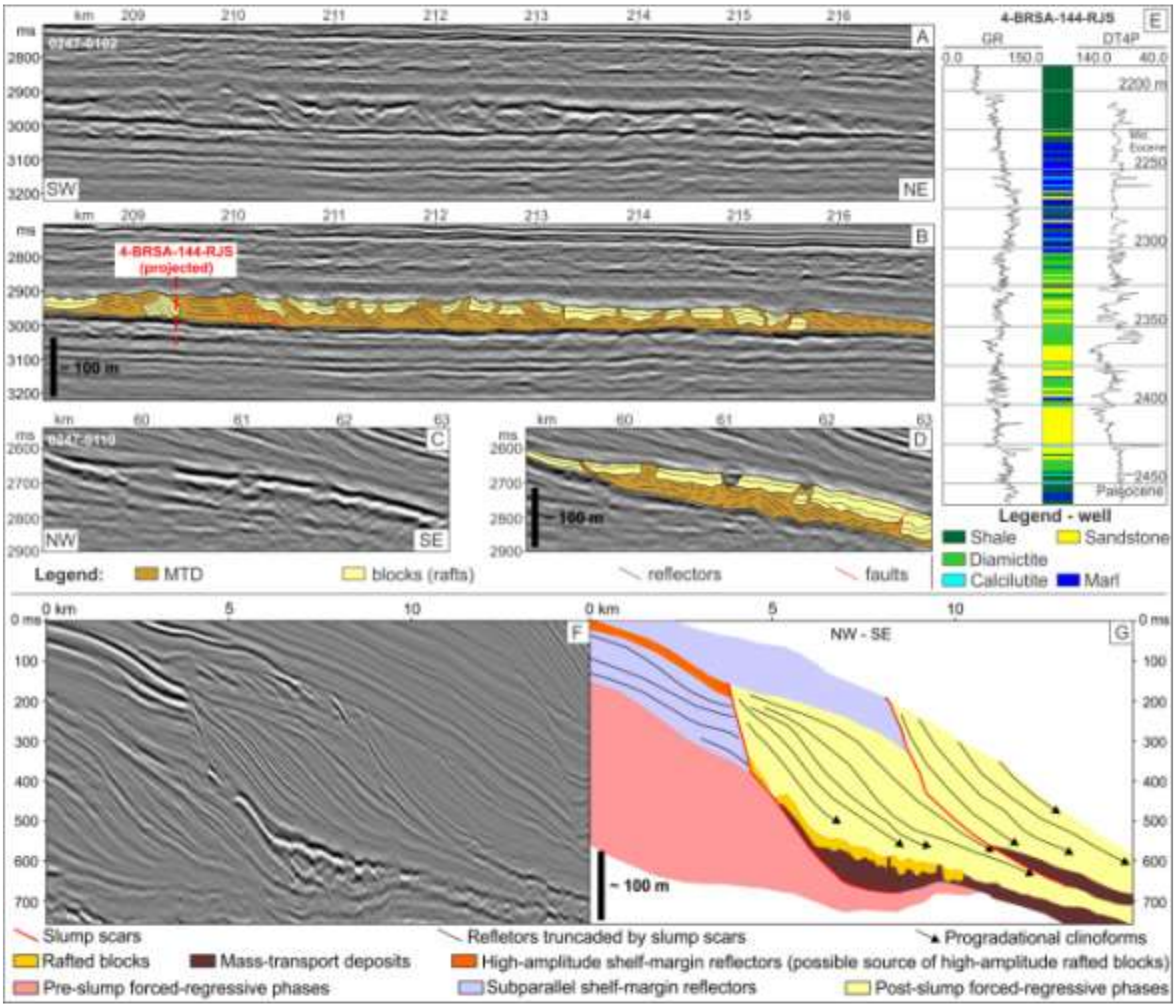

Figure B6: Mass-transport deposits interpreted in strike (A and B) and dip sections (C and D), tied to well log. The discontinuous, high-amplitude reflectors on top of the chaotic facies show signs of deformation and are interpreted as sandy rafted blocks. In the lower part of the figure, interpretation of rafted blocks from the shelf, transported above the muddy mass and deposited in deep-marine settings over the MTD at the slope toe.

Isopach maps for the two main bodies observed in the studied succession (MTD 1 and MTD 2) are shown in figure B7. MTD 1 is significantly larger, with a maximum thickness of 135 ms (TWT, approx. 80 m), downdip maximum extension of up to 30 km, and strike-parallel extension of 55 km (Fig. B7). Discontinuous, high-amplitude reflectors often occur on the upper part of the chaotic facies in the larger body (Fig. B6). The upper part of the chaotic deposits configures a downlap surface for sigmoidal clinoforms of facies C (Figs. B6 and B8). In well data, these facies are composed of gravelly mudstones (diamictites) or mudstones.

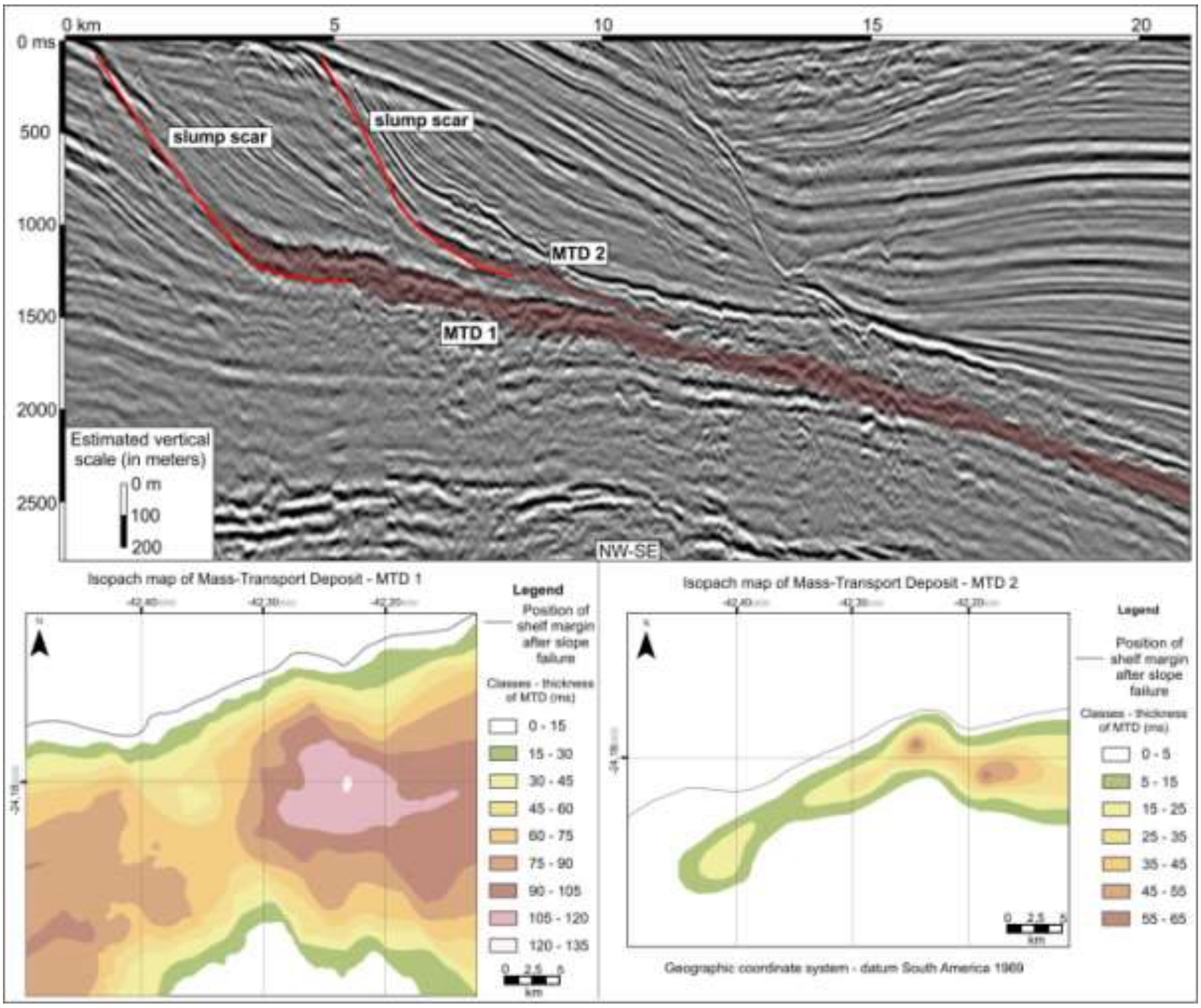

Figure B7: Seismic interpretation and isopach maps (in TWT) of the two main MTDs identified in the study area (MTD1 and MTD2).

Chaotic, low amplitude seismic facies located at the slope toe have been widely interpreted as MTDs (e.g. Posamentier and Kolla, 2003; Martinez et al., 2005; Alfaro and Holz, 2014). The chaotic character and their close association with scars point an origin related to catastrophic mass failures on the outer shelf and slope. The high amplitude reflectors on top of the MTDs are interpreted as poorly deformed rafted blocks carried downslope by the mass flows, similar to those identified, for instance, on the Colombian continental margin by Alfaro and Holz (2014).

2.2.6 SEQUENCE STRATIGRAPHY

Seven depositional sequences were identified, whose boundaries are onlap surfaces (subaerial unconformities) that pass basinward to downlap surfaces (correlative conformities; Fig. B8). Based on the stratigraphic chart of the Santos Basin (Moreira et al., 2007), the temporal amplitude of each sequence is of approximately 3 My, but they incorporate higher-frequency sequences not detailed in this paper. Sequences are stacked in a prominent progradational fashion, reflecting high progradation/aggradation ratios during the Eocene, and can be grouped in two different types.

Type A sequences (E31, E32, E41 and E42) are composed of shelf-margin deltas and oblique to sigmoidal slope clinoforms with poorly preserved topsets and general forced-regressive stacking pattern. Distinction among these four sequences was based on downlap surfaces that separate clinoform sets and are interpreted as changes in the rate of base level fall or short periods (below seismic resolution) of base level rise. Type B sequences (E51, E52 and E60) have a different architecture due to the presence of thick aggradational topset reflectors and higher relief (sigmoidal) slope clinoforms, in such a way that sequence boundaries are more clear and highlighted by preserved onlap terminations. A brief description of the seven sequences is presented below.

2.2.6.1 Sequence E31

The lower boundary of sequence E31 corresponds to the Paleocene – Eocene limit (SB0), which is a downlap surface with low to moderate seismic amplitudes due to low acoustic impedance contrasts between Paleocene and Eocene strata. This sequence represents the first depositional stage of the Eocene recorded in the study area, and is composed of shelf-margin deltas (facies A) and oblique shelf-margin clinoforms (facies B) developed on an initially low-angle, ramp-like morphology.

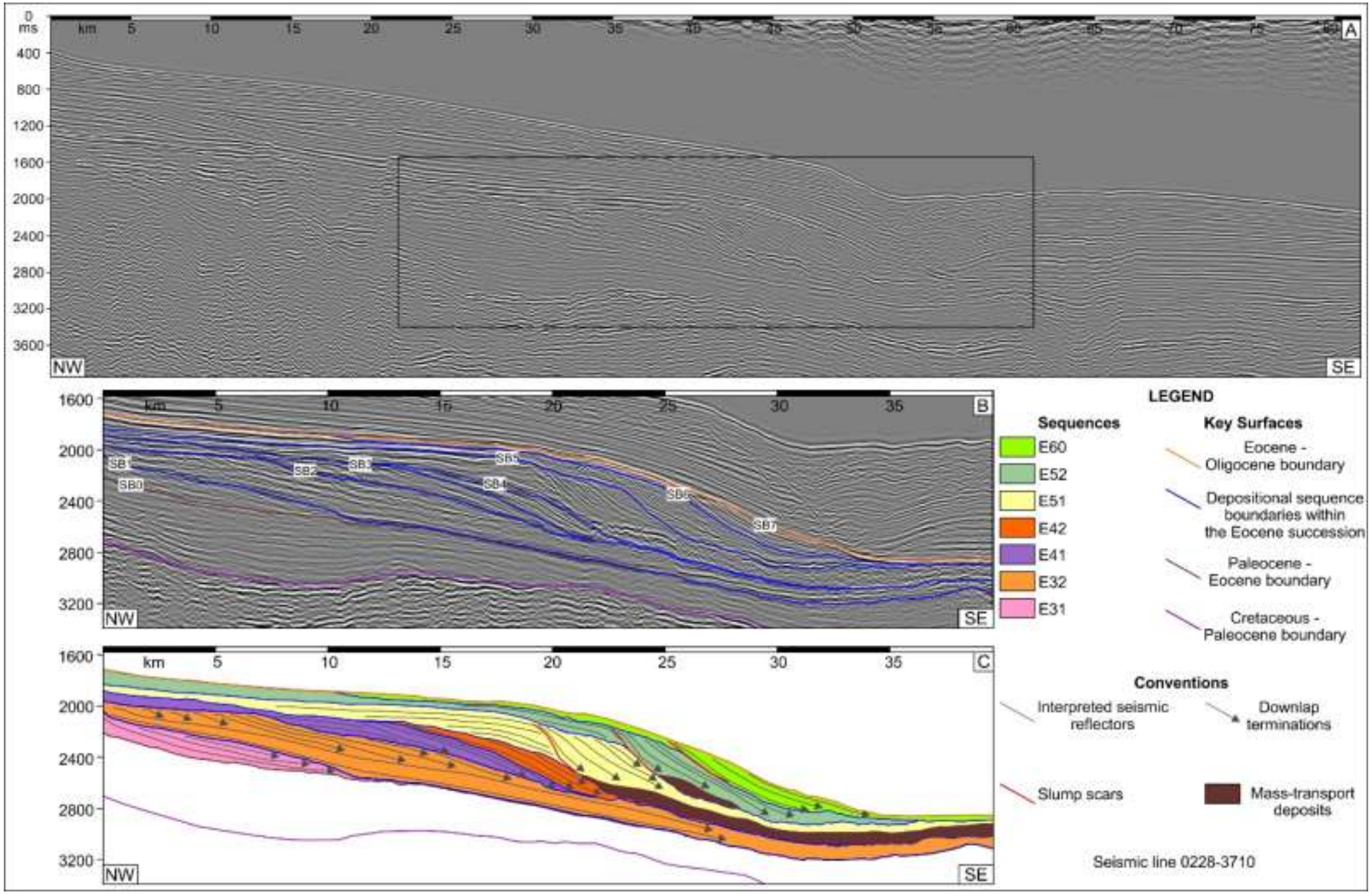

Figure B8: Seismic line representative of the Eocene interval on northern Santos Basin (A), with an interpretation of the sequence boundaries (B) and sequences, slump scars and mass-transport deposits (C).

Thick sand-rich deposits are also observed in some of the seismic sections within this sequence, forming packages of high-amplitude reflectors with a maximum thickness of 100 ms (TWT, approx. 60 m). Shelf-edge trajectories vary from flat to descending, and truncated topsets are common (Fig. B9), which would indicate deposition mainly during relative sea level fall. The total basinward displacement of the shelf edge during sequence E31 was approximately 8 km (Fig. B10).

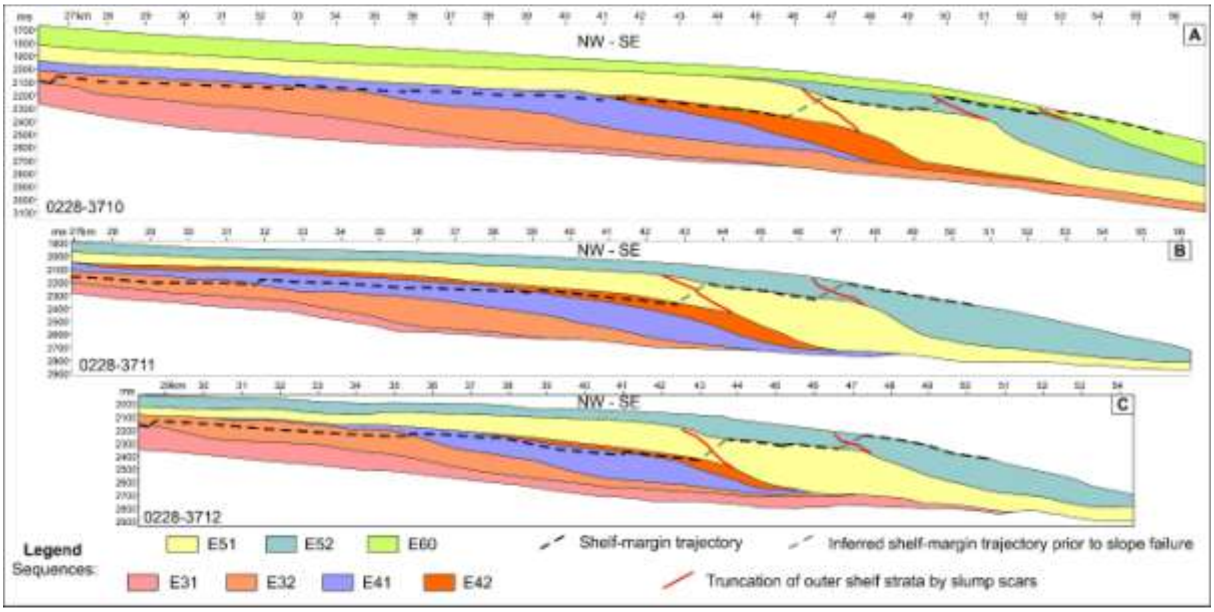

Figure B9: Depositional sequences and shelf-margin trajectories during the Eocene interval as observed in the northwestern (A), central (B) and southeastern (C) sectors of the study area.

2.2.6.2 Sequence E32

The lower boundary of sequence E32 is the surface SB1, a well-defined horizon separating higher amplitude reflectors above from lower amplitude reflectors below. Like in sequence E31, E32 is composed of shelf-margin deltas and oblique shelf-margin clinoforms, showing shelf-edge trajectories with flat to descending pattern and with a total basinward displacement of 13 km (Figs. B9, B10). Sequence E32 also records distal high-amplitude reflectors associated with the development of thick sand-rich turbidite deposits (Fig. B5 and Fig. B8) which a total thickness of 140 ms (TWT; approx. 80 m).

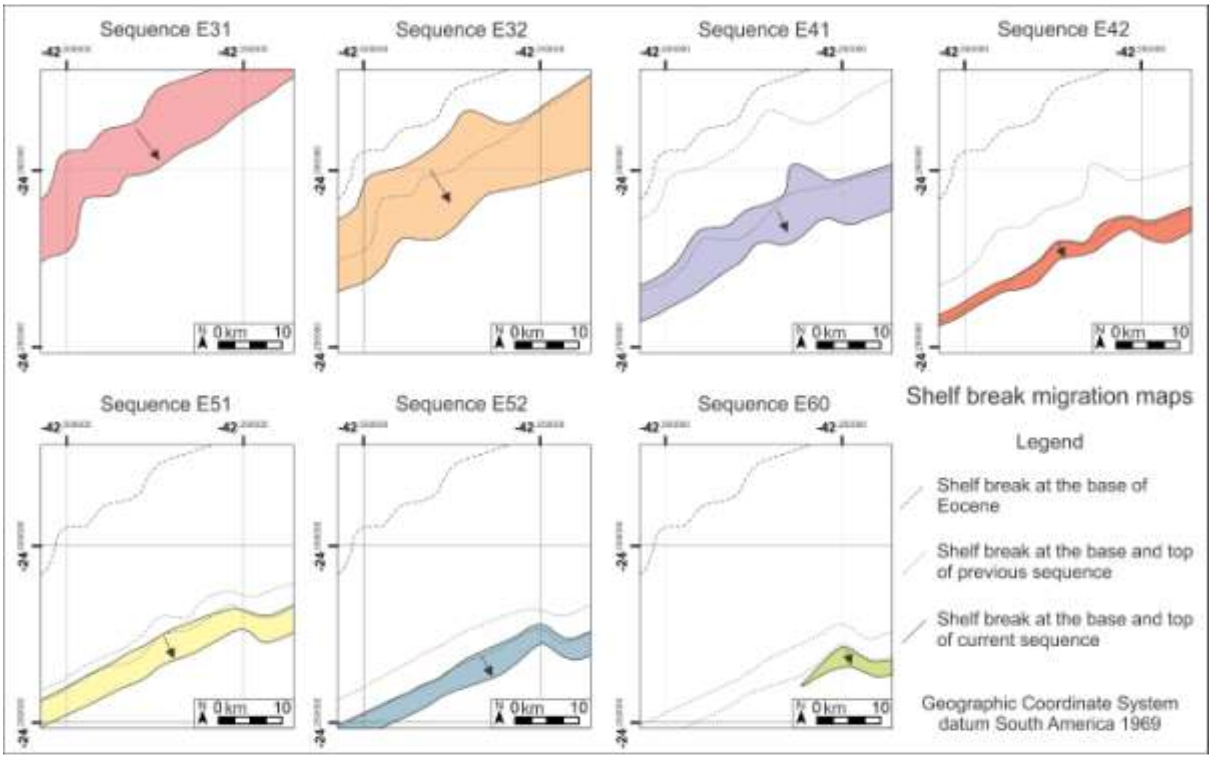

Figure B10: Maps representing the migration of the shelf-margin in different time intervals recorded by the seven depositional sequences identified.

2.2.6.3 Sequence E41

The lower boundary of sequence E41 (SB2) is a prominent downlap surface. In this sequence, shelf-margin deltas are less common, and oblique shelf-margin clinoforms are slightly steeper than in the previous sequences. Shelf-edge trajectories are flat to descending (Fig. B9), indicating deposition during forced regression, and have a maximum basinward displacement of 11 km (Fig. B10).

2.2.6.4 Sequence E42

This sequence has as lower boundary a downlap surface (SB3) above which there is a significant increase in clinoform dip angles (Fig. B8). Shelf-margin deltas are absent or poorly developed and the entire sequence is composed of sigmoidal slope clinoforms (facies C) with truncated topsets and flat to descending trajectories (fig. B9). Progradation distances are smaller than in the previous sequences, reaching a maximum displacement of 3 km (Fig. B10).

2.2.6.5 Sequence E51

The base of sequence E51 is a truncation surface (SB4) onto which aggradational topset reflectors terminate in downlap. These continental to shelfal deposits (facies D) have a maximum thickness of 300 ms TWT (approx. 175 m), and record the first important phase in the Eocene in which accommodation was created in the continental shelf. These topset reflectors are truncated by a pronounced slump scar (Figs. B8 and B9), in such a way that coeval slope clinoforms are not preserved. However, it is possible to infer that the shelf-margin during the deposition of the first half of E51 (prior to slump scar development) had an ascending trajectory, because no evidences of landward trajectories are observed and because reflectors have a divergent pattern basinward (Figs. B9 and B11). The second half of sequence E51 (subsequent to slump-scar development) is composed of high-relief, sigmoidal clinoforms (facies C) and MTDs (MTD 1; facies E). The clinoforms advanced up to 6 km basinward and followed a descending shelf-margin trajectory indicative of forced regression (Figs. B9 and B10). Based on the geometric relationships among the different seismic facies that constitute this sequence, it can be interpreted that the development of the slump scar and its associated MTD corresponds to the onset of base-level fall.

2.2.6.6 Sequence E52

This sequence rests onto SB5, a sequence boundary that truncates underlying reflectors and act as an onlap surface for subsequent strata. Sequence E52 has the same seismic configuration of E51, showing an early aggradational phase composed of continental to shelfal deposits with a total thickness of about 115 ms TWT (approx. 65 m), a slump scar and genetically related MTD (MTD2) and a late phase of slope accretion in the form of forced-regressive, high-relief, sigmoidal clinoforms recording a basinward displacement of about 6 km (Fig. B10). Shelf-edge trajectory prior to slump scar development cannot be directly observed but was inferred to be essentially ascending as in sequence E51 (Fig. B9). Subsequent to slump-scar development, shelf-edge trajectory turns to descending (Fig. B9), meaning that the onset of base-level fall in this sequence is also reflected in large-scale slope failure and MTD formation.

2.2.6.7 Sequence E60

Sequence E60 sits on surface SB6, which is easily recognized because of truncation of underlying clinoforms and a prominent increase in seismic amplitude. The lower part of this sequence is a relatively thin package of aggradational topset reflectors corresponding to continental to shelfal deposits, truncated at the foreset area by a slump scar (Fig. B8). Shelf-margin trajectory was inferred to be progradational and ascending (Fig. B9), indicating a period of sea-level rise and normal regression (Fig. B11). From the slump scar, high relief sigmoidal slope clinoforms developed, with a total progradation of about 6 km (Fig. B10), and descending shelf-margin trajectory (Fig. B9), indicating deposition during a relative sea-level fall. Sequence E60 represents the last progradational phase of the Eocene and is only identified in the southwestern part of the study area (Fig. B10). Its absence to the northeast is due to erosion related to a widespread transgressive episode that marks the top of the Juréia progradation. This surface (SB7) is easily recognizable because of high seismic amplitudes, truncation of underlying reflectors, and changes on general configuration of reflectors (Fig. B8). Therefore, SB7 differs from other sequence boundaries for recording a transgressive surface of erosion that reworked the subaerial unconformity on top of sequence E60.

2.2.6.8 Synthesis of the interpreted stratigraphic evolution

Based on seismic facies and sequence analysis, it is possible to conclude that the Eocene interval as a whole was deposited during a net regressive period with the predominance of forced regressions, punctuated by normal regressions. This high progradation/aggradation ratio is indicative of a phase of reduced accommodation space in the shelf area due to lowstand to falling sea level.

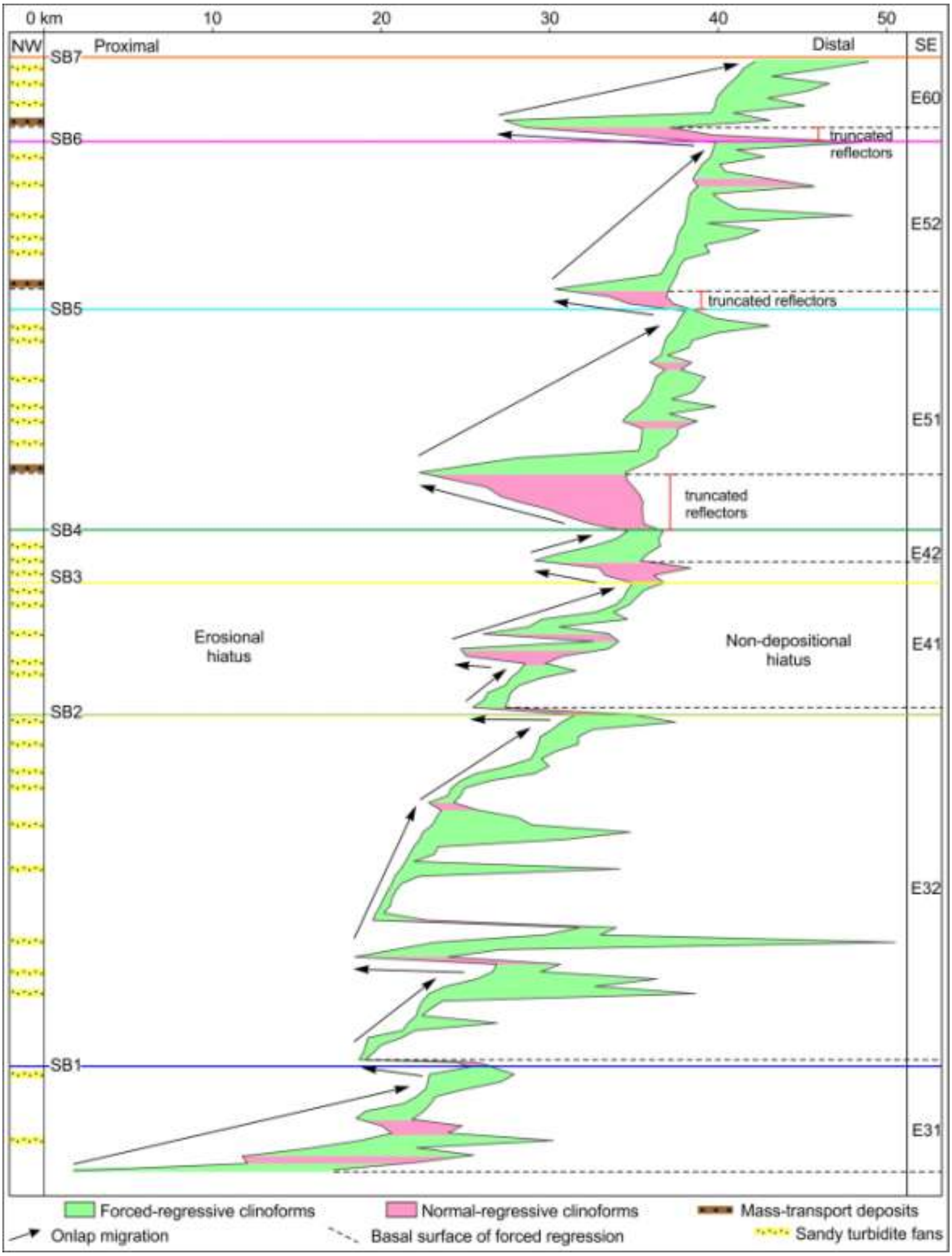

Figure B11: Chronostratigraphic chart (Wheeler diagram) based on detailed seismic mapping on section 0228-3710, located in the northwestern part of the study area. Position of sandy turbidites and MTDs as well as boundaries of depositional sequences are shown in the columns at left and right respectively.

Shelf margin displacement was higher during the deposition of type A sequences (Fig. B10), a phase during which shelf-margin deltas and oblique slope clinoforms prograded with a flat to descending trajectory controlled by a general trend of sea-level fall (Fig. B9) and high sediment supply. Chiefly in sequences E31 and E32, in which shelf-margin deltas are well developed, the thickest and most extensive sand-rich turbidites have been formed (Figs. B5 and B8). Shelf-margin migration distances, as shown in Figure B10, were relatively constant along strike, without evidences of point sources of sediment input. This suggests that despite the high sediment supply shelf-margin migration during the Eocene was strongly influenced by relative sea-level. In type B sequences, periods of relative sea-level rise interrupted the forced-regressive trend, leading to increasing accommodation in the shelf and the deposition of thick aggradational packages. A maintenance of high sediment supply resulted in normal-regressive clinoform sets with relatively shorter shelf break displacements (Fig. B10).

The analysis of shelf-margin trajectories (Fig. B9) and stratal relationships indicates that in all sequences sediment supply outpaced accommodation, even during rises in relative sea-level. This implies in a general arrangement in which transgressive episodes are not recorded, or are below seismic resolution and/or associated with higher order cyclicity. Therefore, the sequences are composed only of falling-stage and lowstand systems tracts, and only surfaces associated with the onset of sea-level fall (basal surface of forced regression) and maximum sea-level fall (depositional sequence boundary) can be observed (Fig. B12).

2.2.7 DISCUSSION

The Eocene of northern Santos Basin is a study case that allows to assess the effects of sediment supply and base level change on the stratigraphic architecture of a continental margin, and as controls on sediment transfer to deep-water settings. In the studied interval as a whole, forced-regressions dominated the depositional trend and, during periods of sea-level rise, sedimentation rates outpaced accommodation leading to normal regressions. As a consequence, only depositional units attributed to falling-stage and lowstand systems tracts can be recognized (Fig. B12). This framework differs from the classic models where four systems tracts are expected and falling-stage deposits are positioned between highstand and lowstand systems tracts (Plint and Nummedal, 2000), demonstrating the importance of a model-independent sequence stratigraphic analysis (e.g. Houseknecht et al., 2009; Catuneanu et al., 2011; Zecchin and Catuneanu, 2013).

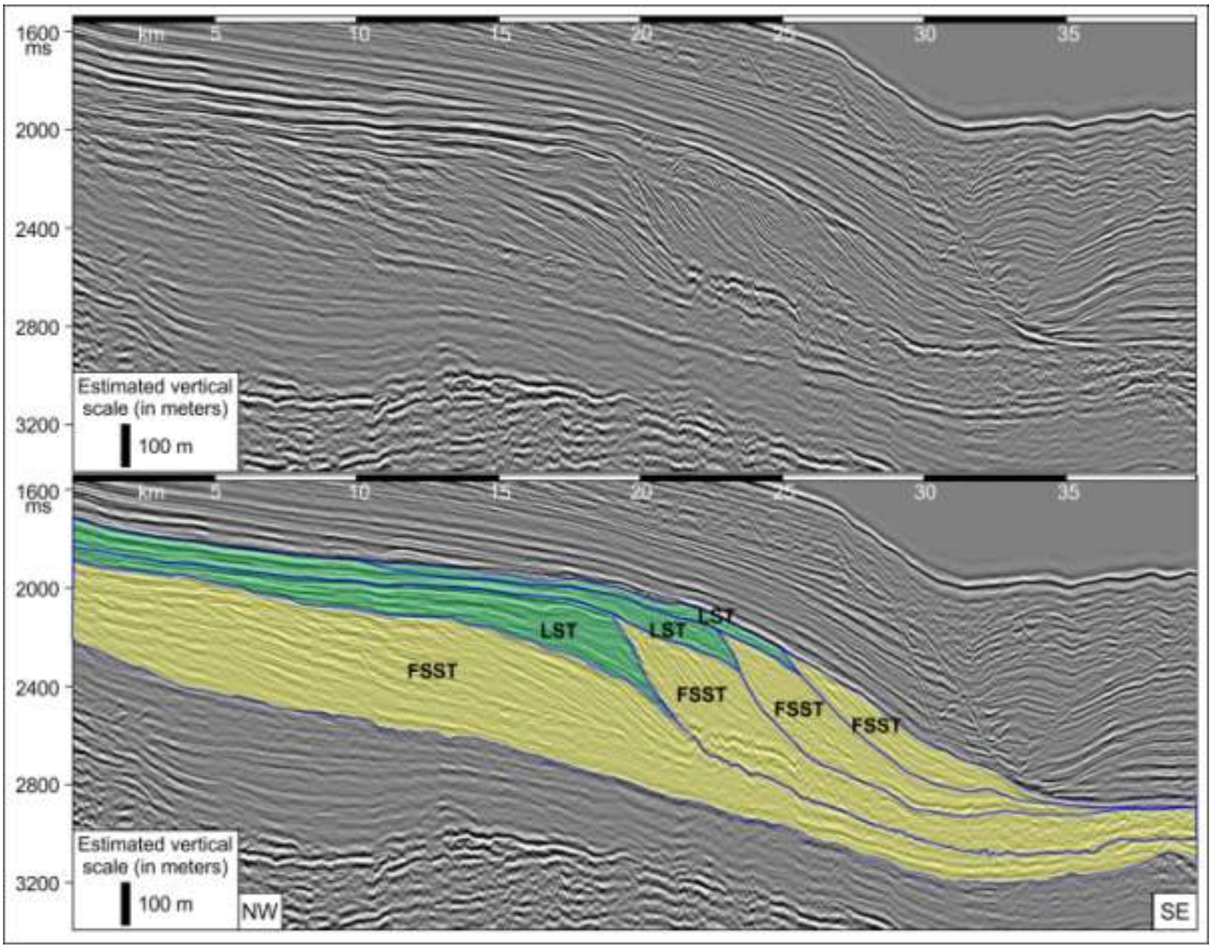

Figure B12: Interpreted, dip-oriented seismic section highlighting the alternation of falling-stage (FSST) and lowstand (LST) systems tracts and the absence of recognizable highstand and transgressive deposits.

The results of the present study demonstrate that the architectural style of the Eocene shelf-margin resulted from a combination of sediment supply and relative sea level fluctuations, and that these controls cannot be considered individually to determine the timing of deep-water systems (e.g. Schlager, 1993). Our results corroborate the conclusions of previous workers (e.g. Vail et al., 1977; Posamentier and Vail, 1988; Walker, 1990; Posamentier and Allen, 1999; Posamentier and Morris, 2000; Catuneanu, 2002; Catuneanu 2006; Catuneanu et al., 2009) that consider the influence of sea level change in deep-marine sedimentation, thus validating the predictive character of classic sequence stratigraphic schemes. Although the importance of sediment supply on deep-water deposition is indubitable (e.g. Plink-Björklund and Steel, 2002; Carvajal and Steel, 2006; Carvajal et al., 2009), our study case shows that the most voluminous sediment accumulation on the slope and basin occurred during base level fall (Fig. B11).

High-amplitude reflectors at the bottomset of shelf-margin clinoforms, which were attributed to sand-rich turbidites, occur in the whole Eocene interval and are placed in both falling-stage and lowstand systems tracts (Fig. B11). This suggests a minor influence of relative sea level fluctuations on turbidite deposition, and a more important role of sediment supply as suggested by Carvajal and Steel (2006). Muto and Steel (2002) and Helland-Hansen and Hampson (2009) argue that clastic sedimentary transport to deep-marine environments under high-supply conditions is favored during descending shelf-margin trajectories. In the other hand, other authors identify deposition of coarse-grained clastic sediments in deep-marine environments through shelf-margin deltas even during sea-level highstands (e.g. Burgess and Hovius, 1998; Carvajal and Steel, 2006; Dixon et al., 2012; Safronova et al., 2014). In the studied succession thicker submarine sands occur in sequences E31 and E32, which were formed entirely during a forced-regressive depositional trend (fig. B5). The deposition of sandy turbidites in these sequences was also strongly favored by shelf-margin deltas that supplied sand directly to the slope, indicating that the positioning of a sediment input-point close to the shelf-margin is determinant for the deposition of high volumes of sand in the deep water (e.g. Porebski and Steel, 2003), a condition more easily achieved during falling sea levels and lowstands.

The development of large MTDs in slope settings has been attributed to base level falls and high sediment supply (e.g. Catuneanu, 2006; Moscardelli and Wood, 2008;

Posamentier and Martinsen, 2011). Indeed, in the studied succession base level changes played a role as a controlling factor on slope instability and MTD generation, along with slope angle and sediment storage in the shelf. According to the classification of Moscardelli and Wood (2008), MTDs from the Eocene in Santos Basin are classified as shelf-attached, with generation associated to relative sea level fluctuations and high sediment supply.

Starting in sequence E31, progradation of shelf-margin clinoforms under high sediment supply and low shelf accommodation built a depositional surface gradually steeper by accumulating sediment exclusively on the slope face until the deposition of sequence E42. Subsequently, base level rise during early sequence E51 caused aggradation and sediment storage in the entire shelf. With the onset of base-level fall, a massive failure occurred at the shelf margin, mobilizing part of the outer shelf and slope sediment downslope and forming chaotic MTDs (Fig. B13). The same succession of events (derived from an equivalent history of base-level change) occurred two more times in sequences E52 and E60, resulting in two other events of mass failure. This indicates that base-level falls following periods of base-level rise acted as the main trigger for slope failure, as chronostratigraphically depicted in the Wheeler diagram of Fig. B11. In addition, the sizes of the two main MTDs (fig. B7) are proportional to the thicknesses of the pre-failure aggradational successions formed during base level rise. These observations explain why MTDs are not observed in type A sequences (E31 to E42) where a change from rising to falling base level has never occurred.

Slope failure and mud-rich mass-flow deposits during early forced regressions are predicted in sequence stratigraphic models (e.g. Catuneanu, 2006). Lowering of storm wave base due to relative sea level fall causes instability on the outer shelf, where distal fine-grained sediments are predominant (Catuneanu, 2006; Catuneanu et al., 2011; Posamentier and Martinsen, 2011). Large MTDs in the studied succession are thus positioned in the early falling-stage systems tract. This conclusion diverges from previous workers dealing with the Eocene of northern Santos Basin (Moreira et al., 2001; Moreira and Carminatti, 2004; Henriksen et al. 2011; Dixon, 2013), who considered that slope collapse were coeval to aggradation on the shelf during a sea-level highstand. Aggradation in the outer shelf during relative sea level rise was, in fact, a determinant factor for slope instability, but the onset of base level fall acted as the trigger for slope failure. Additionally, the assumption that MTD generation is time-equivalent to shelfal aggradation is unlikely once shelf strata are clearly truncated by slump scars.

Seismic correlation of MTDs can thus be a key for the recognition of a basal surface of forced regression (BSFR; Hunt and Tucker, 1992), particularly in shelf-margin settings characterized by high-relief slopes that are susceptible to large scale mass transport (Fig. B13). According to Catuneanu (2002), the BSFR is the depositional surface at the onset of forced regression, a chronostratigraphic horizon hard to recognize in the stratigraphic record because of the absence of an evident physical expression. In the study area, this surface has a hybrid character, corresponding to a slump scar in the slope and a decollement surface at the sole of MTDs. At the shelf margin, this surface is truncated by a subaerial unconformity generated concomitantly to the slope clinoforms of the late falling-stage systems tract (Fig. B13 C and D).

2.2.8 CONCLUSIONS

From the examination of Eocene shelf-margin clinoforms from northern Santos Basin, which are spectacularly imaged by 2D seismic data, a number of general conclusions can be drawn regarding the controlling factors on shelf-margin growth and deep-water sedimentation:

1. The Eocene interval in northern Santos Basin was deposited during high sediment supply and predominance of base level fall. As a result, the overall stratigraphic architecture is of prograding shelf-margin clinoforms with few preserved topsets, shelf-margin deltas, sandy turbidites at the bottomsets, and huge mass-transport deposits.

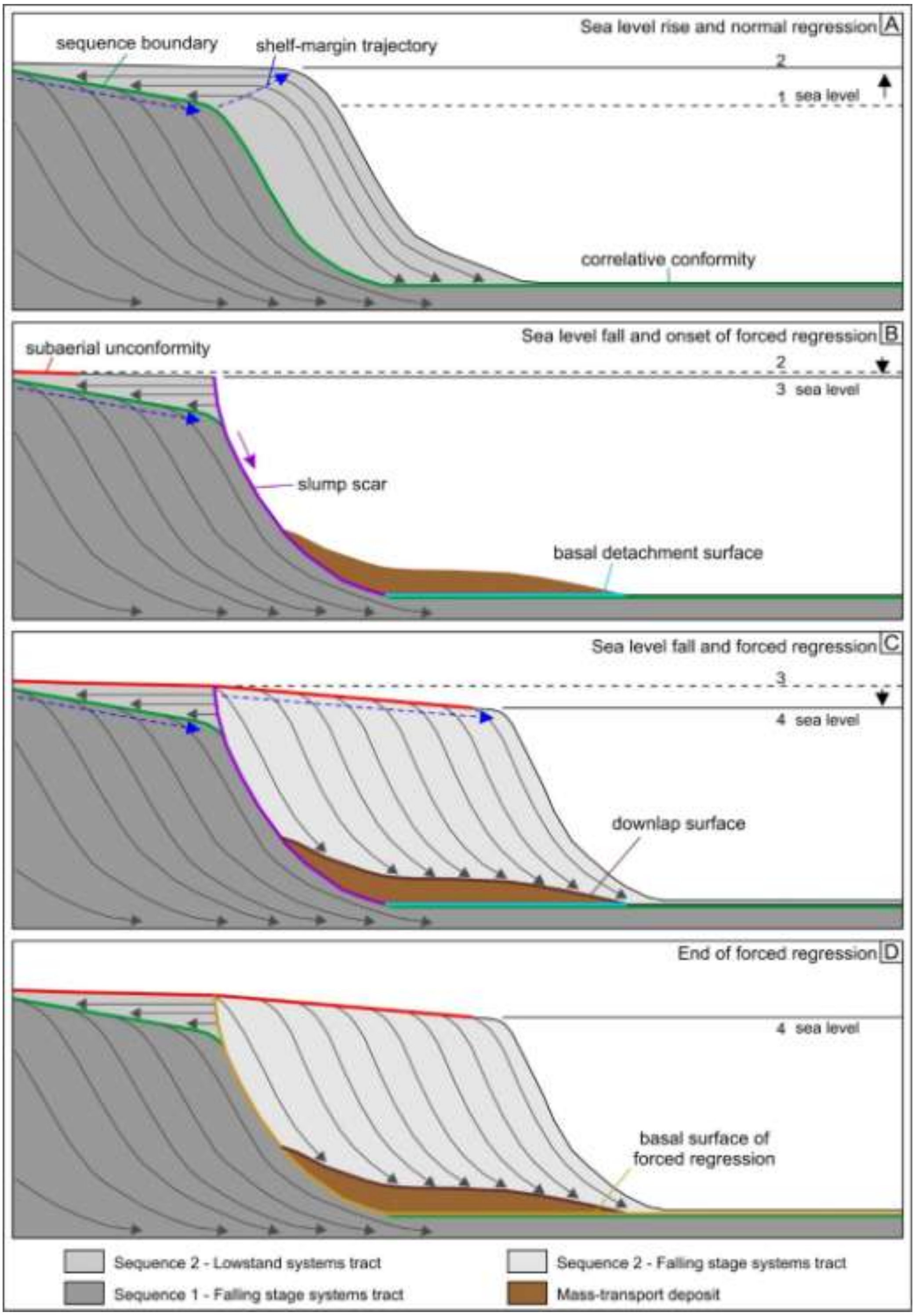

Figure B13: Conceptual model for slope instability, MTD development and key surfaces in a scenario of high sediment supply and alternating normal and forced regressions. A) Rising relative sea level and high sedimentation rates favoring topset aggradation and sediment storage in the outer shelf (LST). B) Onset of base level fall triggering slope failure and MTD generation (early FSST). C) Forced-regressive shelf-margin clinoforms terminating in downlap onto MTD (late FSST). D) Final configuration showing key surfaces and general stratigraphic architecture.

2. The stratigraphic succession includes seven depositional sequences with about 3 My of time-span each and composed of falling-stage and lowstand systems tracts. The total basinward migration of the shelf-margin was of 35 km. Rates of progradation were mainly constant along depositional strike, suggesting a primary control of relative sea level on shelf-margin growth.

3. Deposition of sandy turbidites took place on both falling-stage and lowstand systems tracts. However, sand transference to deep water was in larger volume and more frequent during forced regressions, facilitated by the presence of shelf-margin deltas.

4. Slope failure and MTD generation are associated with falling-stage systems tracts. The onset of base-level fall following a period of base-level rise and shelf aggradation was the main cause for shelf-margin collapse. As thicker is the pre-failure shelfal succession the bigger is the volume of the resulted MTD unit. The basal detachment surface of the MTDs and the contiguous slump scar are equivalent to the basal surface of forced regression of the sequence stratigraphic model.

2.2.9 ACKNOWLEDGEMENTS

The authors thank Universidade Federal do Paraná (UFPR) and Laboratório de Análise de Bacias (LABAP) for infrastructure and institutional support. The Programa Interdisciplinar em Engenharia de Petróleo e Gás Natural (PRH-24) and Coordenação de Aperfeiçoamento de Pessoal de Nível Superior (CAPES) are acknowledged for providing scholarship to F.B. and M.H.P.E. respectively. F.F.V. thanks the Conselho Nacional de Desenvolvimento Científico e Tecnológico (CNPq) for financial support (grants: 461628/2014-7). Seismic and well data were provided by the Agência Nacional do Petróleo, Gás Natural e Biocombustíveis (BDEP-ANP).

2.2.10 REFERENCES

Alfaro, E. and Holz, M. 2014. Seismic geomorphological analysis of deepwater gravity-driven deposits on a slope system of the southern Colombian Caribbean margin. Mar. and Petr. Geol., **57**, 294-311.

Alves, T.M. and Cartwright, J.A. 2010. The effect of mass-transport deposits on the younger slope geomorphology, offshore Brazil. Mar. and Petr. Geol., **27**, 2027-2036.

Alves, T.M., Kurtev, K., Moore, G.F., Strasser, M. 2014. Assessing the internal character, reservoir potential, and seal competence of mass-transport deposits using seismic texture: a geophysical and petrophysical approach. AAPG Bull., **98**(4), 793-824.

Assine, M.L., Corrêa, F.S. and Chang, H.K. 2008. Migração de depocentros na Bacia de Santos: importância na exploração de hidrocarbonetos. Rev. Bras. de Geoc., **38**(2), 111-127.

Badalini, G., Browner, F., Bourque, R., Blight, R., de Bruin, G. 2010. Seismic-sequence stratigraphic analysis of regional 2D lines in the Santos Basin, offshore Brazil. Search and Disc. Article, **40538**, online publ.

Berg, O.R. 1982. Seismic detection and evaluation of delta and turbidite sequences: their application to exploration for the subtle trap. AAPG Bull., **66**(9), 1271-1288.

Burgess, P.M. and Hovius, N. 1998. Rates of delta progradation during highstands: consequences for timing of deposition in deep-marine systems. J. of the Geol. Soc., **155**, 217-222.

Carvajal, C.R. and Steel, R.J. 2006. Thick turbidite successions from supply-dominated shelves during sea-level highstand. Geology, **34**(8), 665-668.

Carvajal, C.R., Steel, R.J. and Petter, A. 2009. Sediment supply: the main driver of shelf-margin growth. Earth-Science Rev., **96**, 221-248.

Catuneanu, O. 2002. Sequence stratigraphy of clastic systems: concepts, merits, and pitfalls. J. of African Earth Scienc., **35**, 1-43.

Catuneanu, O. 2006. Principles of Sequence Stratigraphy. Elsevier, Amsterdam, 375p.

Catuneanu, O., Abreu, V., Bhattacharya, J.P., Blum, M.D., Dalrymple, R.W., Eriksson, P.G., Fielding, C.R., Fisher, W.L., Galloway, W.E., Gibling, M.R., Giles, K.A., Holbrook, J.M., Jordan, R., Kendall, C.G.St.C., Macurda, B., Martinsen, O.J., Miall, A.D., Neal, J.E., Nummedal, D., Pomar, L., Posamentier, H.W., Pratt, B.R., Sarg, J.F., Shanley, K.W., Steel, R.J., Strasser, A., Tucker, M.E., Winker, C. 2009. Towards the standardization of sequence stratigraphy. Earth-Science Rev., **92**, 1-33.

Catuneanu, O., Galloway, W.E., Kendall, C.G.St.C., Miall, A.D., Posamentier, H.W., Strasser, A., Tucker, M.E. 2011. Sequence stratigraphy: methodology and nomenclature. Newsletters on Strat., **44/3**, 173-245.

Catuneanu, O. and Zecchin, M. 2013. High-resolution sequence stratigraphy of clastic shelves II: controls on sequence development. Mar. and Petr. Geol., **39**, 26-38.

Contreras, J., Zühlke, R., Bowman, S., Bechstädt, T. 2010. Seismic stratigraphy and subsidence analysis of the southern Brazilian margin (Campos, Santos and Pelotas basins). Mar. and Petr. Geol., **27**, 1952-1980.

D'Ávila, R.S.F., Arienti, L.M., Aragão, MAN.F., Vesely, F.F., Santos, S.F., Voelcker, H.E., Viana, A.R., Kowsmann, R.O., Moreira, J.L.P., Coura, A.P.P., Paim, P.S.G., Matos, R.S., Machado, L.C.R. 2008. Ambientes de águas profundas. In: Ambientes de sedimentação siliciclástica do Brasil (Org. by A.J.C.L.P. Silva, MAN.F. Aragão and A.J.C. Magalhães), Beca, 244-300.

Dixon, J.F. 2013. Shelf-edge deltas: stratigraphic complexity and relationship to deep-water deposition. Dr. Scient. thesis, University of Texas.

Dixon, J.F., Steel, R.J. and Olariu, C. 2012. Shelf-edge delta regime as a predictor of deep-water deposition. J. of Sed. Res., **82**, 681-687.

Dixon, J.F., Steel, R.J. and Olariu, C. 2013. A model for cutting and healing of deltaic mouth bars at the shelf edge: mechanism for basin-margin accretion. J. of Sed. Res., **83**, online publ.

Driscoll, N.W. and Karner, G.D. 1999. Three-dimensional quantitative modeling of clinoform development. Mar. Geol., **154**, 383-398.

Duarte, C.S.L. and Viana, A.R. 2007. Santos drift system: stratigraphic organization and implications for late Cenozoic palaeocirculation in the Santos Basin, SW Atlantic Ocean. In: Economic and Palaeocenographic Significance of Contourite Deposits (Ed. by A.R. Viana and M. Rebesco), Geological Soc. Special Publ., **276**, 171-198.

Embry, A.F. and Johannessen, E.P. 1992. T-R sequence stratigraphy, facies analysis and reservoir distribution in the uppermost Triassic – Lower Jurassic succession, western Sverdrup Basin, Arctic Canada. In: Arctic geology and petroleum potential (Ed. by T.O. Vorren, E. Bergsager, Ø.A. Dahl-Stamnes, E. Holter, B. Johansen, E. Lie, T.B. Lund), NPF Special Publ., **2**, 121-146.

Galloway, W.E. 1989. Genetic stratigraphic sequences in basin analysis I: architecture and genesis of flooding-surface bounded depositional units. APPG Bull., **73** (2), 125-142.

Gamberi, F., Rovere, M., Marani, M. 2011. Mass-transport complex evolution in a tectonically active margin (Gioia Basin, Southeastern Tyrrhenian Sea). Mar. Geol., **279**, 98-110.

Gong, C., Wang, Y., Hodgson, D.M., Zhu, W., Li, W., Xu, Q., Li, D. 2014. Origin and anatomy of two different types of mass-transport complexes: a 3D seismic case study from the northern South China Sea margin. Mar. and Petr. Geol., **54**, 198-215.

Gong, C., Wang, Y., Steel, R.J., Olariu, C., Xu, Q., Liu, X., Zhao, Q. 2015. Growth styles of shelf-margin clinoforms: prediction of sand- and sediment-budget partitioning into and across the shelf. J. of Sed. Res., **85**, online publ.

Helland-Hansen, W. and Hampson, G.J. 2009. Trajectory analysis: concepts and applications. Basin Res., **21**,454-483.

Henriksen, S., Hampson, G.J., Helland-Hansen, W., Johannessen, E.P., Steel, R.J. 2009. Shelf edge and shoreline trajectories, a dynamic approach to stratigraphic analysis. Basin Res., **21**, 445-453.

Henriksen, S., Helland-Hansen, W. and Bullimore, S. 2011. Relationships between shelf-edge trajectories and sediment dispersal along depositional dip and strike: a different approach to sequence stratigraphy. Basin Res., **23**, 3-21.

Houseknecht, D.W., Bird, K.J. and Schenk, C.J. 2009. Seismic analysis of clinoform depositional sequences and shelf-margin trajectories in Lower Cretaceous (Albian) strata, Alaska North Slope. Basin Res., **21**, 644-654.

Hunt, D. and Tucker, M.E. 1992. Stranded parasequences and the forced regressive wedge systems tract: deposition during base-level fall. Sed. Geol., **81**, 1-9.

Johannessen, E.P. and Steel, R.J. 2005. Shelf-margin clinoforms and prediction of deepwater sands. Basin Res., **17**, 521-550.

Karner, G.D. and Driscoll, N.W. 1999. Tectonic and stratigraphic development of the West African and eastern Brazilian Margins: insights from quantitative basin modeling. In: The Oil and Gas Habitats of the South Atlantic (Ed. by N.R. Cameron, R.H. Bate and V.S. Clure), Geological Soc. Special Publ., **152**, 11-40.

Lourens, L.J., Sluijs, A., Kroon, D., Zachos, J.C., Thomas, E., Röhl, U., Bowles, J., Raffi, I. 2005. Astronomical pacing of late Palaeocene to early Eocene global warming events. Nature Let., **435**, 1083-1087.

Macedo, J.M. 1989. Evolução tectônica da Bacia de Santos e áreas continentais adjacentes. Bol. de Geoc. da Petrobras, **3**,159-173.

Martinez, J.F., Cartwright, J. and Hall, B. 2005. 3D seismic interpretation of slump complexes: examples from the continental margin of Israel. Basin Res., **17**, 83-108.

Modica, C.J. and Brush, E.R. 2004. Postrift sequence stratigraphy, paleogeography, and fill history of the deep-water Santos Basin, offshore southeast Brazil. AAPG Bull., **88**(7), 923-945.

Mohriak, W.U. and Magalhães, J.M. 1993. Estratigrafia e evolução estrutural da área norte da Bacia de Santos. Atas do III Simp. de Geol. do Sudeste, **1**, 19-26.

Monteverde, D.H., Mountain, G.S. and Miller, K.G. 2008. Early Miocene sequence development across the New Jersey margin. Basin Res., **20**, 249-267.

Moreira, J.L.P. and Carminatti, M. 2004. Sistemas deposicionais de talude e de bacia no Eoceno da Bacia de Santos. Bol. de Geoc. da Petrobras, **12**(1), 73-87.

Moreira, J.L.P., Madeira, C.V., Gil, J.A., Machado, MAP. 2007. Bacia de Santos. Bol. de Geoc. da Petrobras, **15**(2), 531-549.

Moreira, J.L.P., Nalpas, T., Joseph, P., Guillocheau, F. 2001. Stratigraphie sismique de la marge éocène du Nord du Bassin de Santos (Brésil): relations plate-forme/systèmes turbiditiques; distorsion dês séquences de dépôt. Earth and Planetary Sciences., **332,** 491-498.

Moscardelli, L. and Wood, L. 2008. New classification system for mass transport complexes in offshore Trinidad. Basin Res., **20**, 73-98.

Moscardelli, L., Wood, L. and Mann, P. 2006. Mass-transport complexes and associated processes in the offshore area of Trinidad and Venezuela. AAPG Bull., **90** (7), 1059-1088.

Muto, T. and Steel, R.J. 2002. In defense of shelf-edge delta development during falling and lowstand of relative sea level. The J. of Geol., **110**, 421-436.

Mutti, E., Tinterri, R., Magalhaes, P.M., Basta, G. 2007. Deep-water turbidites and their equally important shallower water cousins. Search and Disc. Article, **50057**, online publ.

Mutti, E. 1992. Turbidite Sandstones. *Agip Spec. Publ.*, Milan, 275p.

Olafiranye, K., Jackson, C.A.-L. and Hodgson, D.M. 2013. The role of tectonics and mass-transport complex on upper slope stratigraphic evolution: a 3D seismic case study from offshore Angola. Mar. and Petr. Geol., **44**, 196-216.

Patruno, S., Hampson, G.J. and Jackson, C.A.-L. 2015. Quantitative characterization of deltaic and subaqueous clinoforms. Earth-Sci. Rev., **142**, 79-119.

Petter, A.L., Kim, W., Muto, T., Steel, R.J. 2011. Comment on “Clinoform quantification for assessing the effects of external forcing on continental margin development”. Basin Res., **23**, 118-121.

Plink-Björklund, P. and Steel, R.J. 2002. Sea-fall below the shelf edge, without basin-floor fans. Geology, **30** (2), 115-118.

Plint, A.G. and Nummedal, D. 2000. The falling stage systems tract: recognition and importance in sequence stratigraphic analysis. In: Sedimentary responses to forced regressions (Ed. by D. Hunt and R.L. Gawthorpe). Geological Soc. Spec. Publ., **172**, 1-17.

Porębski, S.J. and Steel, R.J. 2003. Shelf-margin deltas: their stratigraphic significance and relation to deepwater sands. Earth-Science Rev., **62**, 283-326.

Posamentier, H.W. and Allen, G.P. 1999. Siliciclastic sequence stratigraphy – concepts and applications. SEPM, Tulsa, 210p.

Posamentier, H.W. and Erskine, R.D. 1991. Seismic expression and recognition criteria of ancient submarine fans. In: Seismic facies and sedimentary processes of submarine fans and turbidite systems (Ed. by P. Weimer and M.H. Link). Springer, 197-222.

Posamentier, H.W. and Kolla, V. 2003. Seismic geomorphology and stratigraphy of depositional elements in deep-water settings. J. of Sed. Res., **73** (3), 367-388.

Posamentier, H.W. and Martinsen, O.J. 2011. The character and genesis of submarine mass-transport deposits: insights from outcrop and 3D seismic data. SEPM Spec. Publ., **96**, 7-38.

Posamentier, H.W. and Morris, W. 2000. Aspects of the stratal architecture of forced regressive deposits. In: Sedimentary responses to forced regressions (Ed. by D. Hunt and R.L. Gawthorpe). Geological Soc. Spec. Publ., **172**, 19-46.

Posamentier, H.W. and Vail, P.R. 1988. Eustatic controls on clastic deposition II – sequence and systems tract models. In: Sea level changes: an integrate approach (Ed. by C.K. Wilgus, B.S. Hastings, C.G.St.C. Kendall, H.W. Posamentier, C.A. Ross, J.C. van Wagoner). SEPM Spec. Publ., **42**, 125-154.

Ribeiro, M.C.S. 2007. Termocronologia e história denudacional da Serra do Mar e implicações no controle deposicional da Bacia de Santos. Dr. Scient. thesis, UNESP.

Safronova, P.A., Henriksen, S., Andreassen, K., Laberg, J.S., Vorren, T.O. 2014. Evolution of shelf-margin clinoforms and deep-water fans during the middle Eocene in the Sørvestsnaget Basin, southwest Barents Sea. AAPG Bull., **98**(3), 515-544.

Sahy, D. Condon, D.J., Terry Jr., D.O., Fischer, A.U., Kuiper, K.F. 2015. Synchronizing terrestrial and marine records of environmental change across the Eocene-Oligocene transition. Earth and Plan. Sci. Let., **427**, 171-182.

Schlager, W. 1993. Accommodation and supply – a dual control on stratigraphic sequences. Sed. Geol., **86**, 111-136.

Steel, R.J., Carvajal, C., Olariu, C., Petter, A., Plink-Björklund, P., Sanchez, C. 2010. Shelf-margin trajectories: significance for sediment by-pass. Search and Disc. Article, **50297**, online publ.

Steel, R.J. and Olsen, T. 2002. Clinoforms, clinoform trajectories and deepwater sands. In: Sequence stratigraphic models for exploration and production: evolving models and application histories (Ed. by J.M. Armentrout and N.C. Rosen), GCS-SEPM Spec. Publ., 367-381.

Vail, P.R., Mitchum, R.M. and Thompson, S. 1977. Seismic stratigraphy and global changes of sea level: part 4. Global cycles and relative changes of sea level. In: Seismic stratigraphy – Application to hydrocarbon exploration (Ed. by C.E. Payton), AAPG Mem., **26**, 83-98.

Veeken, P.C.H. and van Moerkerken, B. 2013. Seismic stratigraphy and depositional facies models. EAGE, Houten, 494p.

Walker, R.G. 1990. Submarine fan models on seismic studies: a geological perspective. McMaster Univ., Hamilton, 109p.

Zalán, P.V. and Oliveira, J.A.B. 2005. Origem e evolução estrutural do Sistema de Riftes Cenozóicos do Sudeste do Brasil. Bol. de Geoc. da Petrobras, **13**(2), 269-300.

Zecchin, M. and Catuneanu, O. 2013. High-resolution sequence stratigraphy of clastic shelves I: units and bounding surfaces. Mar. and Petr. Geol., **39**, 1-25.

2.3 Seismic expression of buried bottom-current-related comet marks developed in an outer shelf and upper slope – Eocene-Oligocene transition in northern Santos Basin, SE Brazil

2.3.1 ABSTRACT

Bottom-current-related bedforms, such as sediment bodies and erosive features, are good indicatives of the environmental conditions during deposition. The Eocene-Oligocene transition in north Santos Basin is seismically expressed as a high-amplitude surface punctuated by irregular erosive features known as comet marks. This surface truncates shelf-margin deltas and slope-accretion clinoforms from the Eocene, and marks an important change in the stratigraphic architecture of the basin, as the essentially prograding Eocene configuration gives place to extensive Oligocene transgressive deposits. The transgression was a result of regional tectonic and global climatic changes that reduced sediment supply to the basin and allowed the establishment of new bottom currents. Bottom-current-related comet marks are essentially erosive features morphologically described as drop-shaped bedforms with an erosive head and an erosive tail, and the tail is a reliable indicative of the direction of the current. As no buried comet marks have been described, it is important to determine their 2D and 3D seismic character, in order to interpret the conditions of generation of these forms. In the study area, they occur abundantly in the outer shelf and upper slope, with maximum longitudinal extension reaching 1 km, maximum width of 200 m, and up to 20 ms TWT of maximum deepness. These dimensions allow the classification of such bedforms as giant comet marks. They are the result of erosion of the irregular sea floor by strong flows exceeding 0.6 m s^{-1}, in contexts of low sediment availability or sediment starvation. When the bottom currents encounter an obstacle, it creates an erosive shadow to the downstream of the obstruction, where the erosive tail is developed. Sea-floor irregularity was caused by pockmarks formed by gas seeps from the underlying paleodeltas. Comet marks strong alignment toward N68 indicates the action of a NE-oriented shallow bottom current in north Santos Basin.

Keywords: comet marks, bottom currents, pockmarks, north Santos Basin

2.3.2 INTRODUCTION

Bottom currents play an important role in marine geomorphology, acting both in deposition (contourites) and erosion of the sea floor. Although contourite drifts were firstly described in basinal settings (e.g. Heezen *et al*, 1966), current-controlled bedforms in the seafloor are also identified in shallower waters, in the outer shelf or upper slope (e.g. Flemming, 1978; Flemming, 1980; Viana *et al.*, 1998; Carmelenghi *et al.*, 2001; Galloway, 2001; Laberg et al., 2001; Viana, 2002), but the deposits in these areas aren't considered contourites *stricto sensu* (Stow *et al.*, 1998; Viana *et al.*, 1998). However, the shallow-water bedforms show that bottom-current action is not restricted to deep-marine settings. In conditions of low sediment circulation, bottom currents may form mainly erosive features on the shelf and upper slope, with little or no deposition of expressive sediment bodies (e.g. Flemming, 1980; McLean, 1980; Galloway, 2001). Consequently, the identification of ancient erosive bottom-current-related forms may be a key for the understanding of the environmental conditions that affected a basin. Most bottom-current-related seafloor features, as comet marks, are asymmetrical and oriented according to prevailing currents. Their mapping can thus provide information regarding ocean circulation in both modern and ancient open marine settings. Since no buried comet marks has been described before, identification of these structures in the stratigraphic record may be an excellent guide for determination of the conditions of bottom-current action in the past.

In northern Santos Basin, elongated features punctuate the paleo seafloor of a prominent marine flooding surface that overlies progradational, shelf-margin clinoforms of the Eocene. These drop-shaped erosive features are known as comet marks (e.g. Werner and Newton, 1975; Fleming, 1980; Fleming, 1984; Kuijpers et al., 1993). This surface marks the top of the Eocene succession and record a major paleogeographical change in the basin, when the high sediment input related to the paleodrainage of the Paraíba do Sul River was interrupted due to river capture associated to the development of the Serra do Mar range. The scope of this paper is to document these structures, interpret their origin and to discuss potential implications for bottom current circulation patterns during the Eocene-Oligocene transition in the Brazilian continental margin. For this analysis, we use a seismic-geomorphological approach, that allows precise interpretations about the processes that shaped the marine morphology (e.g. Posamentier and Kolla, 2003; Carlotto & Rodrigues, 2009; Jobe et al., 2011; Prather et al., 2012; Sylvester et al., 2012).

2.3.3 GEOLOGICAL SETTING

The Santos Basin is a divergent margin basin located in SE Brazil, bounded in north by the Cabo Frio high, and in the south by the Florianópolis high (fig. C1). The geologic evolution of the basin comprises three main evolutionary phases associated with the crustal stretching during the breakup of Gondwana and opening processes of the South Atlantic Ocean. The three main tectonic phases recognized are: a Barremian to Aptian rift phase, an Aptian to Albian transitional evaporitic-carbonatic phase, and an Albian to modern divergent margin phase (Moreira *et al.*, 2007).

From the Turonian until late Eocene, the Serra do Mar uplift at the Brazilian southeastern margin and the consequent denudation of the mountain chain increased sediment supply and conditionated the development of a strongly progradational phase, known as Juréia progradation (fig. C1; Macedo, 1989). This long-term regressive phase (duration of approximately 60 My) resulted in extensive deltaic progradations during the Upper Cretaceous, Paleocene and Eocene (Mohriak and Magalhães, 1993). The consequent sediment load associated to these high supply periods has contributed to trigger salt movements basinward and to the generation of syn-sedimentary regional faults, structural highs and mini-basins (Assine et al., 2008; Badalini et al., 2010). The main stratigraphic surfaces of the Paleogene are interpreted in a dip-oriented seismic section in Fig. C2.

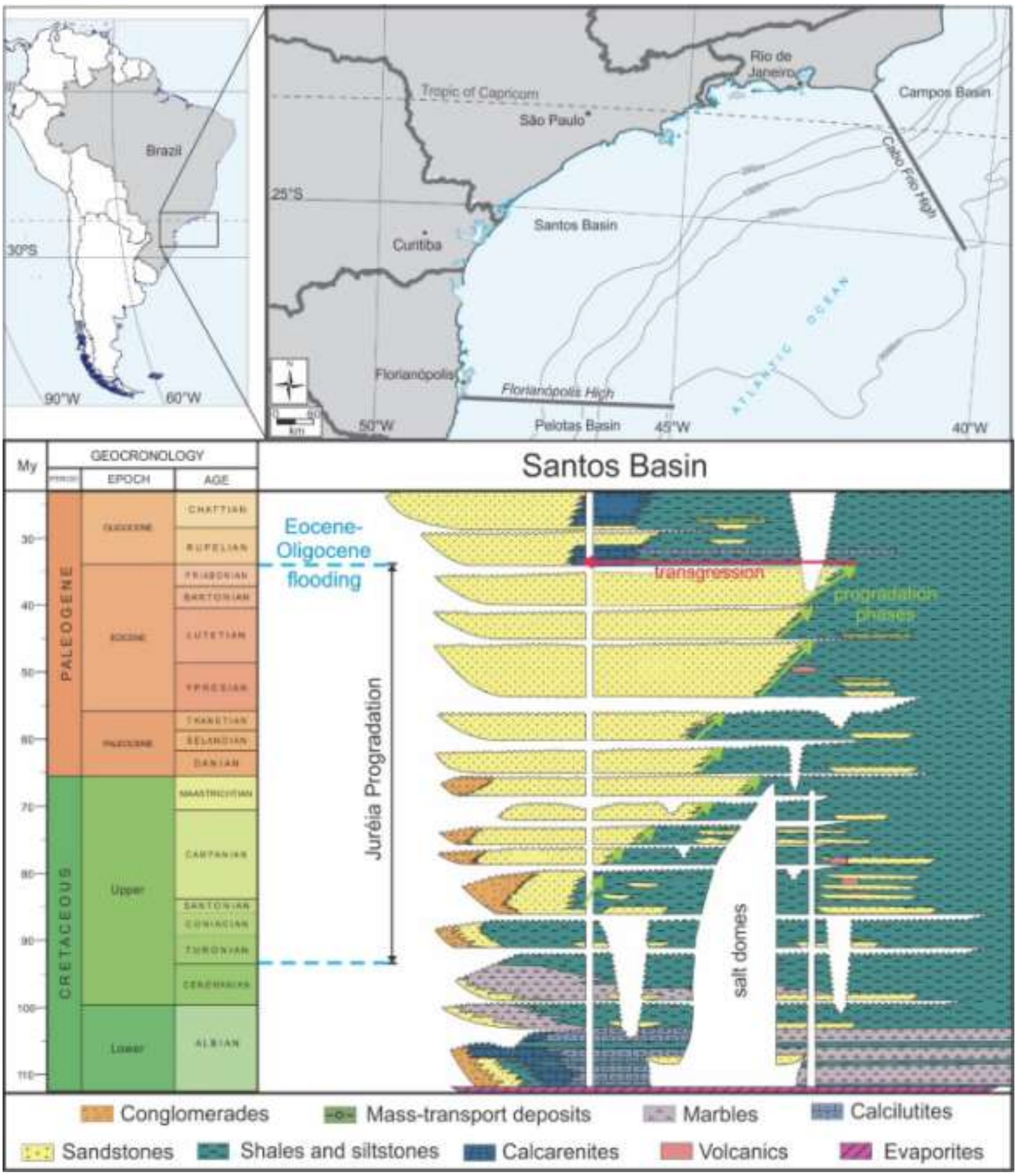

Figure C1: Location map and stratigraphic chart of the Santos Basin (modified from Moreira *et al.*, 2007). Note the Juréia progradation (main progradations indicated by green arrows) ending in an important transgression (red arrow) during the Eocene-Oligocene boundary.

During the Eocene, a global warming event (Eocene Thermal Maximum; Lourens *et al.*, 2005) caused an increase on the pluviosity in the Serra do Mar range, which resulted in a peak of sediment supply to the basin (Zalán and Oliveira, 2005). In this period, sediment influx to northern Santos Basin was controlled by the Paraíba do Sul paleodrainage (Ribeiro, 2007), resulting in a strongly progradational stacking pattern. In seismic sections, the interval is composed by progradational seismic facies, including shelf-margin deltas, slope-accretion clinoforms, mass-transport deposits and sand-rich turbidites. These seismic facies reflect a period of high sediment supply and forced regressions.

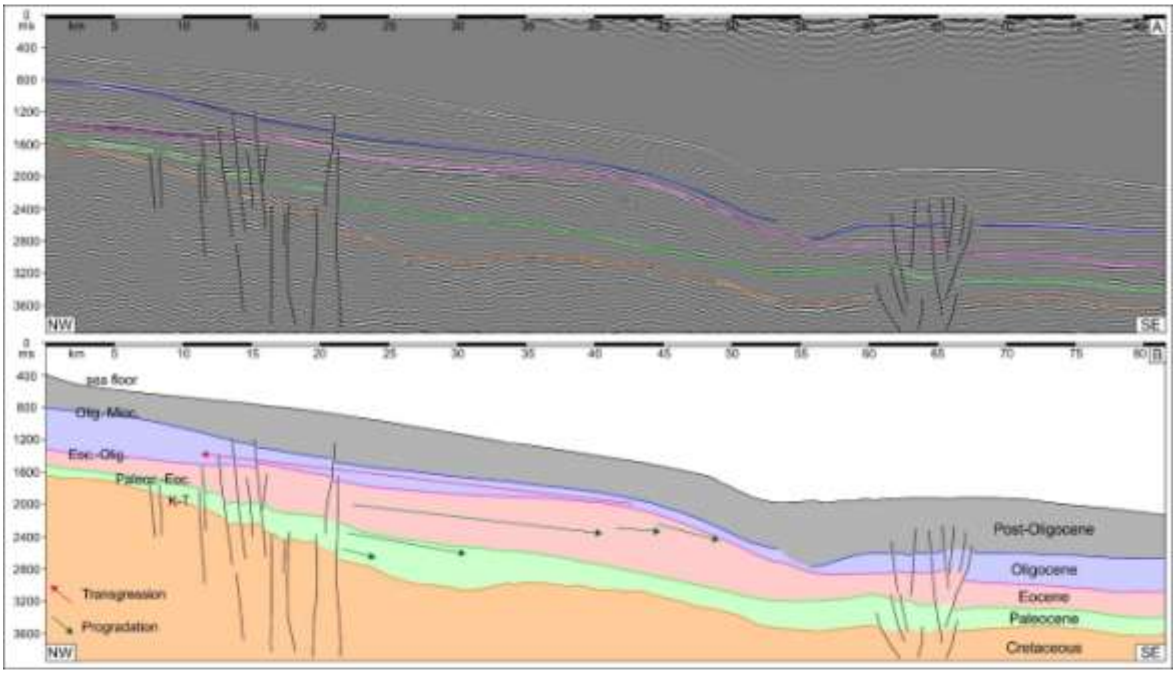

Figure C2: (A) Main depositional intervals and surfaces in northern Santos Basin. (B) Green arrows represent the main progradational trajectories, and the red arrow represents the extensive transgression of the Early Oligocene.

In the transition between Eocene and Oligocene, the beginning of a global cooling event (Sahy *et al.*, 2015) altered the pluviosity regime in the continent and diminished sediment supply to the basin. This phase was also affected by local relief changes associated to tectonic adjustments of the Serra do Mar range, causing a reorganization and migration of the paleodrainage towards Campos Basin (Karner and Driscoll, 1999), as Santos Basin became sediment-starved and experienced an important transgressive event (Moreira *et al.*, 2001; Duarte and Viana, 2007; Assine *et al.*, 2008). A prominent maximum flooding surface materialize this transgressive episode and records a period of strong reworking by recently-established cold thermohaline bottom currents, that acted in the sediment reworking during the Eocene-Oligocene transition (Duarte and Viana, 2007).

2.3.4 DATASET AND METHODS

The study area is located in northern Santos Basin, approximately 150 km offshore from the city of Rio de Janeiro, in the Atlantic Ocean (fig. C3).

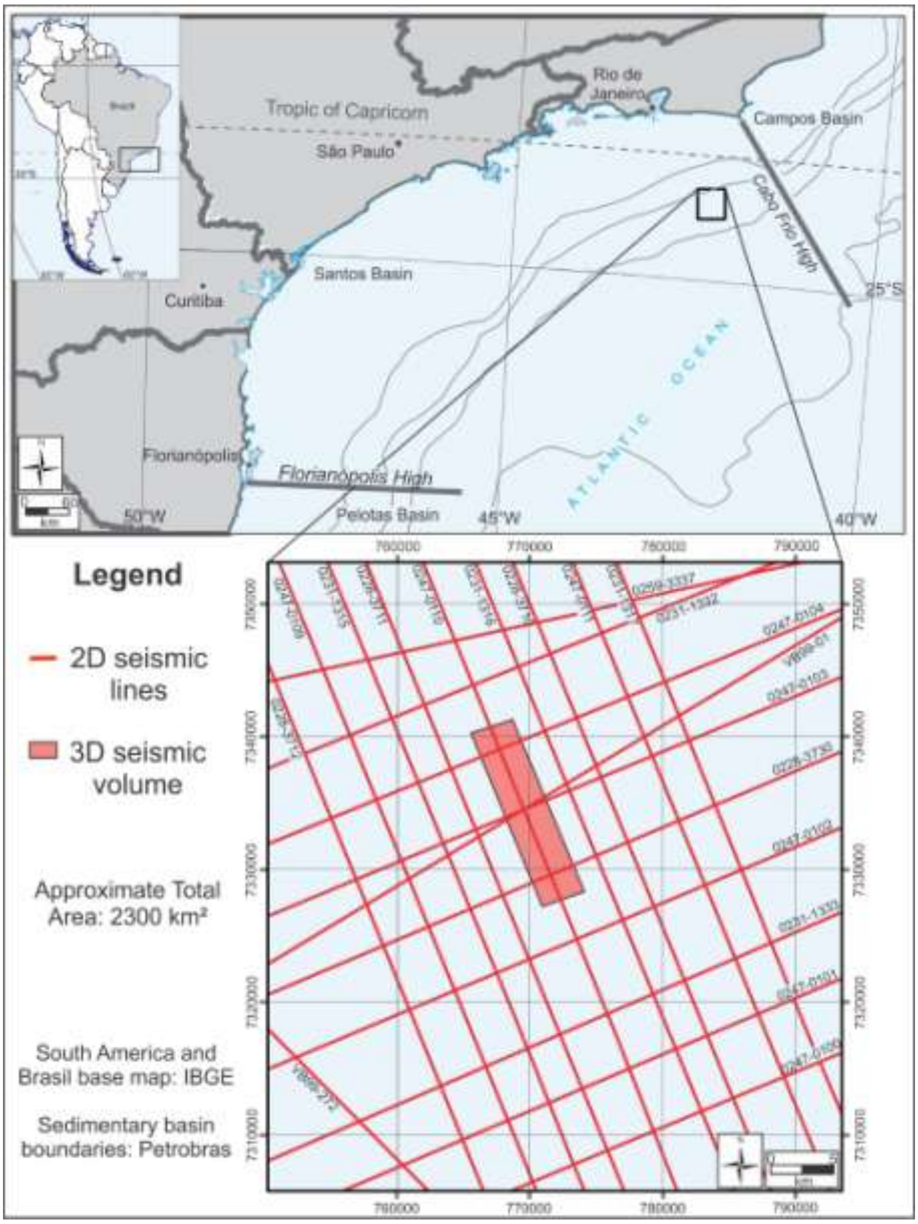

Figure C3: Location of the study area in north Santos Basin, with reference to the seismic data used in the present study.

The public domain database was provided by the Brazilian National Agency of Petroleum, Natural Gas and Biofuels (ANP), and comprises 20 2D seismic lines covering an area of up to 2300 km² and approximately 50 km² of a 3D seismic volume (fig. C3). Seismic data are from surveys performed since the 1990's, including 0228 SANTOS 11A, 0231 Santos 18A, 0247 CABO FRIO 3A, 0261 VB99 2D BMS, and R0003 0259 2D SPP 2Q 1999 (2D), and 0276 BS500 (3D).

The data were interpreted under the scope of seismic geomorphology, to determine the stratigraphic position, morphology and characteristics of the erosive features, and the paleoenvironmental setting of the analyzed interval. Seismic geomorphology consists in the analysis of geomorphic surfaces in subsurface, applying concepts of geomorphology in three-dimensional seismic data (Posamentier *et al.*, 2007). The software used for horizon tracing and interpretation was OpendTect version 4.6 (dGB Earth Sciences, 2012). Characteristics of the bottom-current-related structures such as orientation, depth, width and length were measured using seismic attribute maps of horizons and longitudinal and transversal cross-sections extracted from the 3D volume. In addition, rosette plots generated in the software OpenStereo (Grohmann and Campanha, 2010) were used for paleocurrent analysis, taking into account the direction and asymmetry of the erosive features. Both software are open-source.

2.3.5 SEISMIC EXPRESSION OF COMET MARKS

The analyzed horizon is a regional truncation surface with high seismic amplitude, truncating shelf-margin deltas and prograding high-relief clinoforms from the Eocene interval, and correspondent to an extensive transgressive event in the basin (e.g. Modica and Brush, 2004; Assine et al., 2008; Contreras et al., 2010). The surface is punctuated by erosive features observed in 2D dip-oriented seismic sections as symmetric channel-like forms developed in the shelf and upper slope (fig. C4). The forms are registered both in dip-oriented and strike-oriented sections, although their lateral extent may be wider in the strike-oriented sections. Vertical dimensions reach 20 ms TWT (approx. 10 m), and maximum lateral extension varies from 130 m (dip-oriented seismic sections) to 250 m (strike-oriented seismic sections). When compatible to seismic resolution, the infilling of the erosive structures display a parallel aggradational pattern.

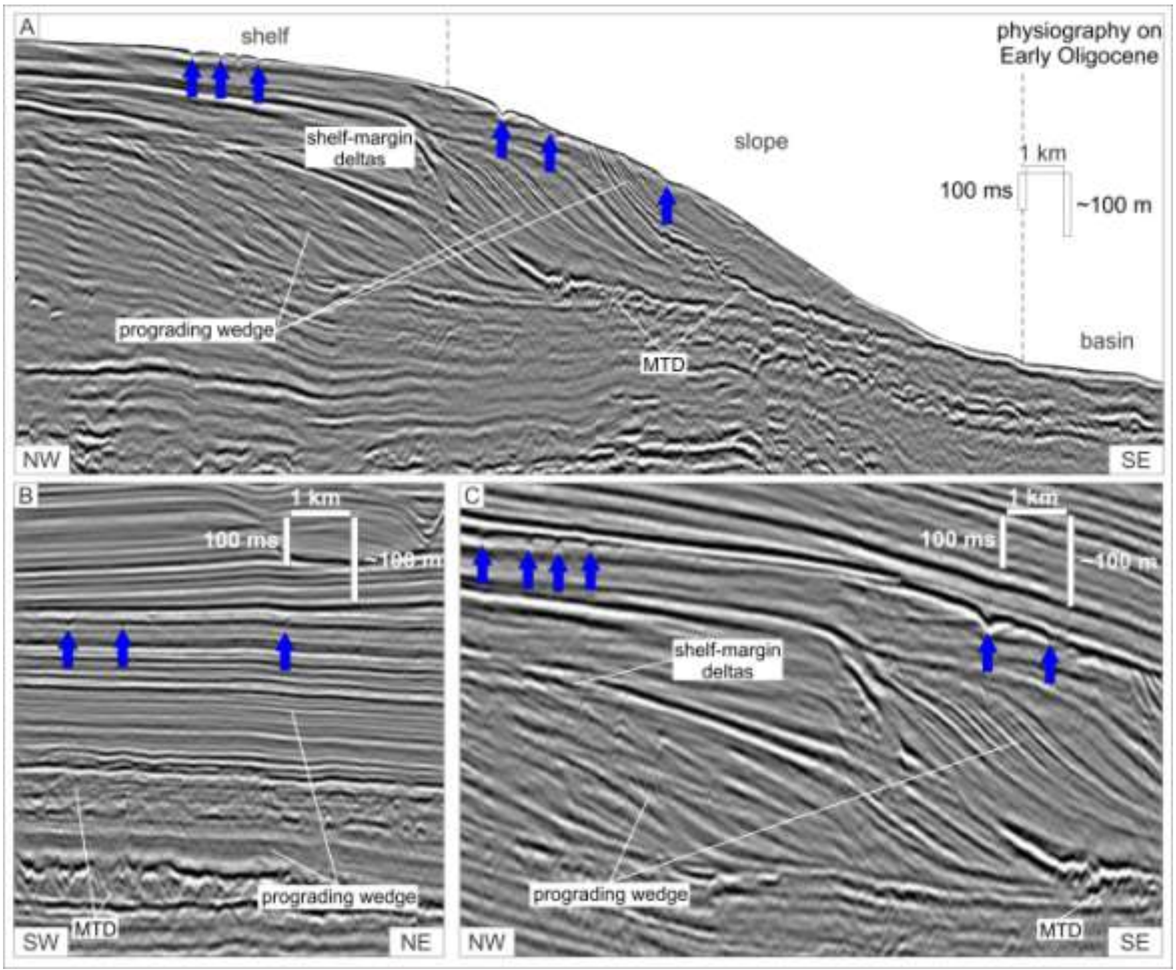

Figure C4: Bottom-current-related erosive features seen in 2D seismic data (blue arrows). In A, general view of a dip section, showing shelf-margin deltas, slope prograding wedges and mass-transport deposits. These features are detailed in strike (B) and dip (C) sections.

In horizon slices the erosive features appear as elongated and discontinuous scour marks with asymmetric shapes if seen in plan view, being comparable to comet marks reported in the literature (e.g. Werner and Newton, 1975; Fleming, 1980; Fleming, 1984;

Kuijpers et al., 1993; Gee et al., 2001; Verdicchio and Trincardi, 2006; Trincardi et al., 2007; fig. C5).

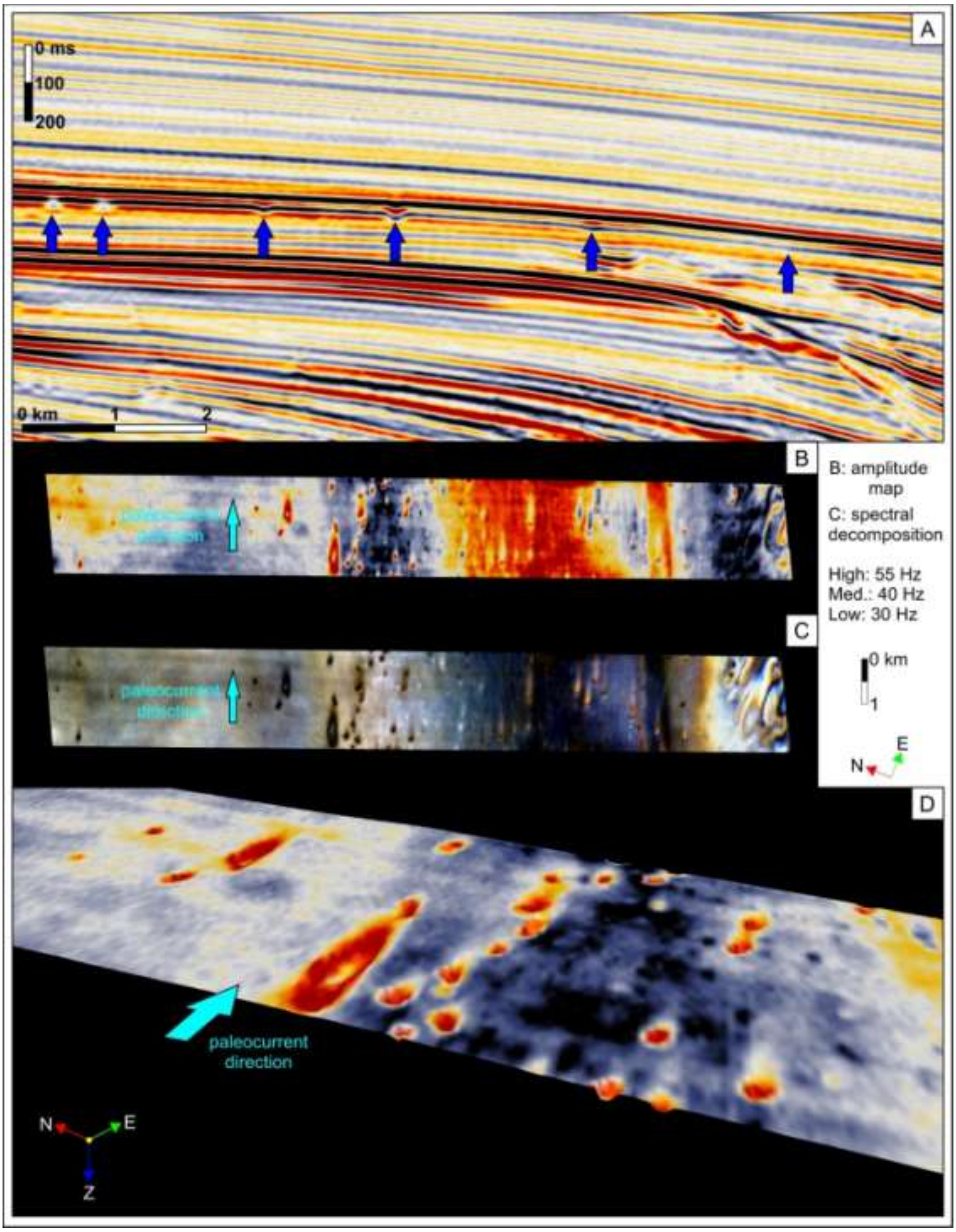

Figure C5: Comet marks in a 3D seismic volume. A) blue arrows indicate comet marks in an inline section. The comet marks are easily interpreted in a seismic horizon in B (amplitude map) and C (spectral decomposition). D) a perspective view allows the evaluation of maximum depth and dimensions of the comet marks. Their geometry indicates paleocurrents towards the NE.

The heads of the forms are circular depressions with a maximum width of 200 m and up to 20 ms TWT of maximum depth, being the deepest part of the comet marks (fig. C6). The tails are smaller and shallower, with width smaller than 40 m and depth gradually reduced to zero (fig. C6). Longitudinal dimensions are variable, generally ranging between 300-500 m, but in some cases reaching 1 km. Length/width ratio ranges from 4.2 to 5.5.

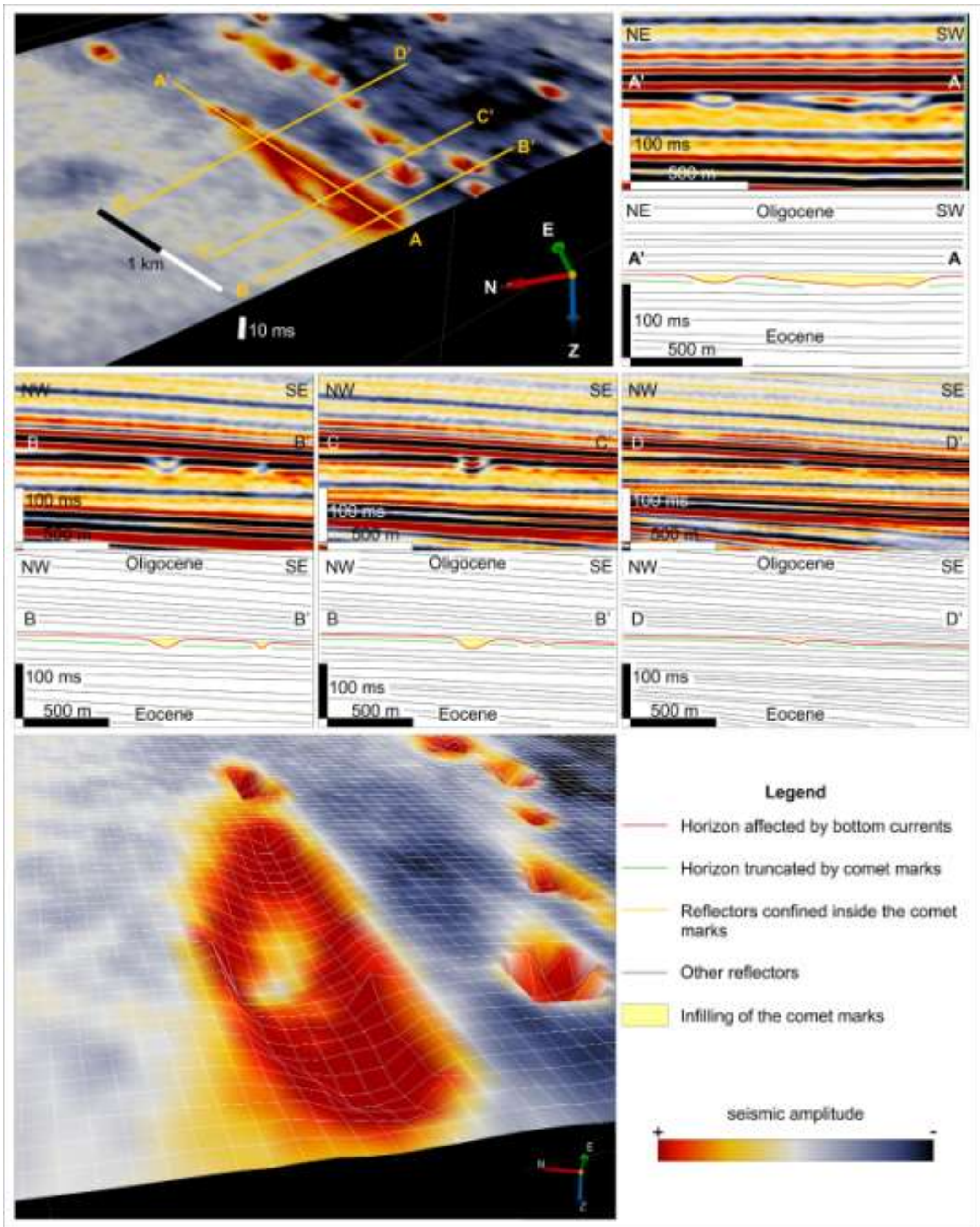

Figure C6: 2-D seismic sections of giant comet marks. A-A’ is a longitudinal section; B-B’ is a transverse section of the head of the feature; C-C’ is a transverse section of the tail of the feature; D-D’ is a transverse section of the terminal part of the tail.

The structures are strongly aligned in the NE-SW direction, with the tails pointing towards NE (fig. C5). The only exception is an E-W aligned feature identified in the upper slope, associated to an increase in dip angles. In this particular case, the tail of the feature points towards E.

2.3.6 GAS-ESCAPE CONDUCTS

Gas-escape conducts are described in seismic data as acoustically transparent vertical features that correspond to gas chimneys with at least some residual gas that make it visible by the disturbance on seismic amplitudes (e.g. Heggland, 1998; Cathles et al., 2010; Petersen et al., 2010; Freire, 2013). Around the main conducts, some low-frequency disturbance may be visible, as a consequence of lower amounts of gas accumulations (Cathles et al., 2010). Such features are locally observed in the 2D seismic data (fig. C7).

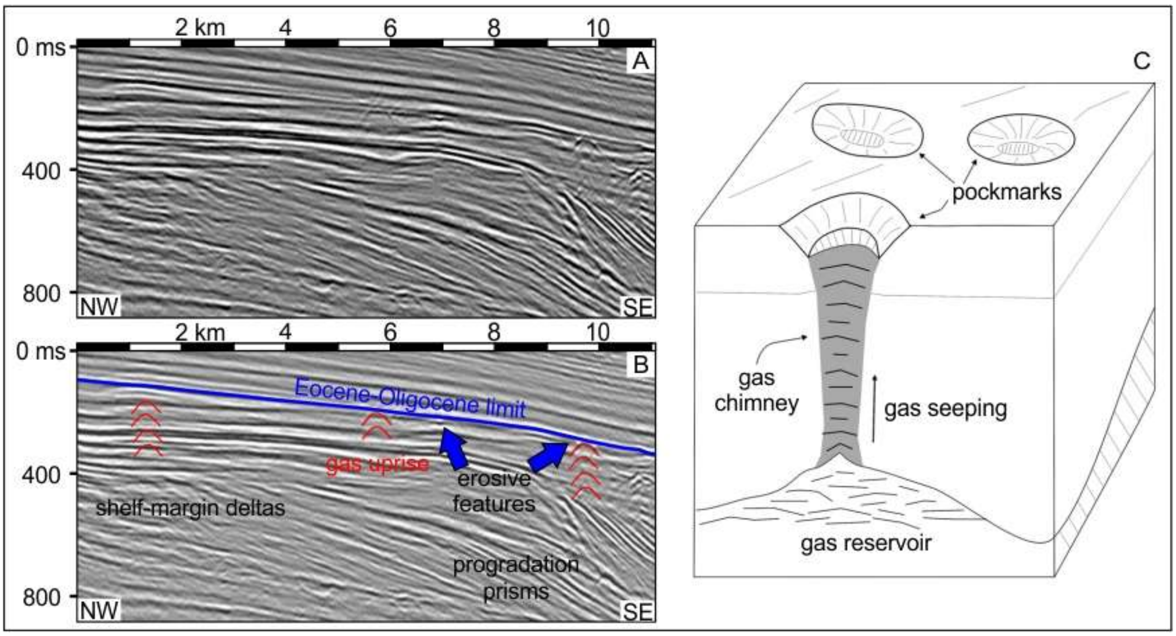

Figure C7: Detail of a 2D dip seismic section (A) with shelf-margin deltas from the Eocene, gas uprising features, and erosive features in the Eocene-Oligocene limit, interpreted in B. C) model for the generation of pockmarks in the sea bottom due to gas escape (adapted from Cathles *et al.*, 2010).

The gas-escape conducts appear to origin from the eocenic shelf-edge deltas, ending in the analyzed horizon (e.g. Clayton, 1992; Evans, 2012; Nuzzo et al., 2012). At least some of the comet marks seem to be related to gas-escape conducts, suggesting that the circular depressions that compose the head of the comet marks were, at the time, pockmarks on the seafloor (e.g. Cathles et al., 2010; Valle & Gamberi, 2011).

2.3.7 DISCUSSION

The erosive features described above are interpreted as bottom-current-related comet marks (e.g. Flemming, 1980; Flemming, 1984; Kuijpers *et al.*, 1993; Viana *et al.*, 1998), developed in the outer shelf and upper slope (e.g. Reineck and Singh, 1980). Comet marks were defined by Werner and Newton (1975) as erosive features with an erosive tail formed when a current reaches an obstacle. Although comet marks were initially related to positive obstacles distributed over the seafloor (e.g. Werner and Newton, 1975; Flemming, 1980; Flemming, 1984), it seems more coherent to consider it an elongated erosive form associated to the action of bottom currents over an irregular seafloor (e.g. Werner et al., 1980; Trincardi et al., 2007).

In the study area, the heads of the comet marks are circular depressions where the maximum deep of the features is located (fig. C6). These depressions are interpreted as pockmarks, probably associated to the gas chimneys interpreted in the 2D seismic data, although no direct connection between the gas chimneys and the pockmarks has been observed (fig. C7). The occurrence of these features is well documented in the seafloor of many basins around the world, generally composing complexes and clusters of pockmarks (e.g. Heggland, 1998; Petersen et al., 2010; Nickel et al., 2012; Luo et al., 2013). Pockmarks developed in areas with strong bottom currents may be rapidly filled with sediment (Cathles et al., 2010), but in the study area these features are associated with the erosive action of the currents, indicating a context of low availability of sediments.

This characteristic, added to the non-association to visible depositional features, suggest that the sediment-starved conditions during the Eocene-Oligocene transition (Duarte and Viana, 2007) prevented pockmark fill and contourite deposition. The linking between comet marks occurrence and circulation of bottom currents in conditions of low sediment availability is well known (e.g. McLean, 1980; Werner et al., 1980; Masson, 2001).

Comet marks are formed when the bottom current encounters an obstacle, creating an erosive shadow to the downstream of the obstruction (Werner *et al*, 1980; Flemming, 1980; Flemming, 1984; Kuijpers *et al.*, 1993). Flume experiments performed by Werner et al. (1980) shows that, when the flow encounters the obstacle, the velocity distribution creates a paired helical flow. This results in an increase of the bottom stresses, as the flow passes around the obstacle (Verdicchio and Trincardi, 2006). Consequently, the orientation of the aligned erosive tails is a reliable indicator of the direction of the currents (e.g. Werner et al., 1980; Gee et al., 2001; Kuijpers et al., 2002; Trincardi et al., 2007). In the same way, paleocurrent analysis based on the alignment of these features is a good tool for the understanding of the environmental conditions during the Eocene-Oligocene transition in north Santos Basin.

The rosette plot of Fig. C8 shows a strong trend towards NE, with mean direction of 68°. Few exceptions have been registered, including an anomalous near-E oriented comet mark in the slope. This indicates that the comet marks in the study area were generated by northeastward-trending paleocurrents during the Oligocene transgression. This paleocurrent direction differs from the SW-trending erosive features and lineaments described by Duarte and Viana (2007), which are related to an upper-slope current that acted in the Early Oligocene, and is similar to the present-day Brazil Current. Instead, the reported flow direction coincides with a NE-trending paleocurrent identified by the same authors in the lower slope domain. Thus, results of the present paper indicate the presence of another NE-trending bottom current that was active during Early Oligocene in the shelf and upper slope.

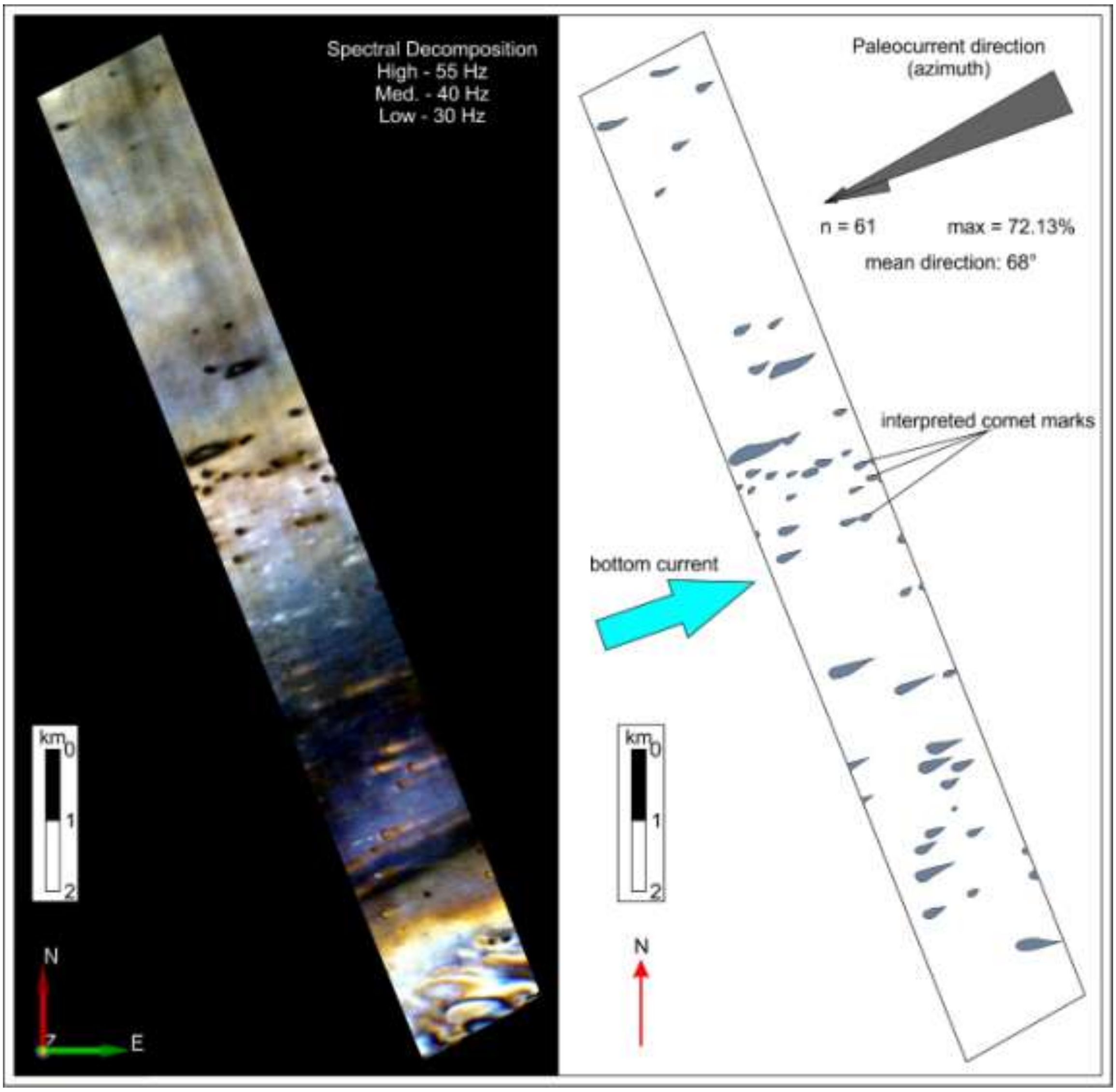

Figure C8: Interpretation of comet marks and rosette plot showing a NE-oriented general trend. The strong orientation of the comet marks indicate the presence of a strong bottom current.

Flume experiments showed that, in sediment-starved conditions, morphology of the marks are not reliable indicators of current velocity (Werner et al., 1980). However, many authors consider comet mark formation in a range of current velocities from 0.6 m s^{-1} to more than 1.0 m s^{-1} (e.g. Kenyon, 1986; Masson, 2001; Kuijpers et al., 2002; Verdicchio and Trincardi, 2006; Trincardi et al., 2007; Wynn and Masson, 2008). Length/width ratio of the erosive tails are the main indicators for the intensity of the current (e.g. Kuijpers et al., 2002; Verdicchio and Trincardi, 2006), although it must be considered that comet marks are a result of peaks on the velocities of the currents (e.g. Masson, 2001; Trincardi et al., 2007). Under the action of long-duration strong currents, the erosive tails may tend to a quasi-infinite length, forming structures similar to sand ribbons (e.g. McLean, 1980; Kuijpers et al., 2002). In the study area, comet marks have a relatively moderate length/width ratio, suggesting bottom-current velocities around 0.6 m s^{-1} (e.g. Kuijpers et al., 2002; Verdicchio and Trincardi, 2006).

Formation of such exceptionally large-shaped comet marks (e.g. Flemming, 1984; Gee et al., 2001; Verdicchio and Trincardi, 2006; Trincardi et al., 2007) seems to be related to gas escapes from the Eocene prograding wedges (fig. C9).

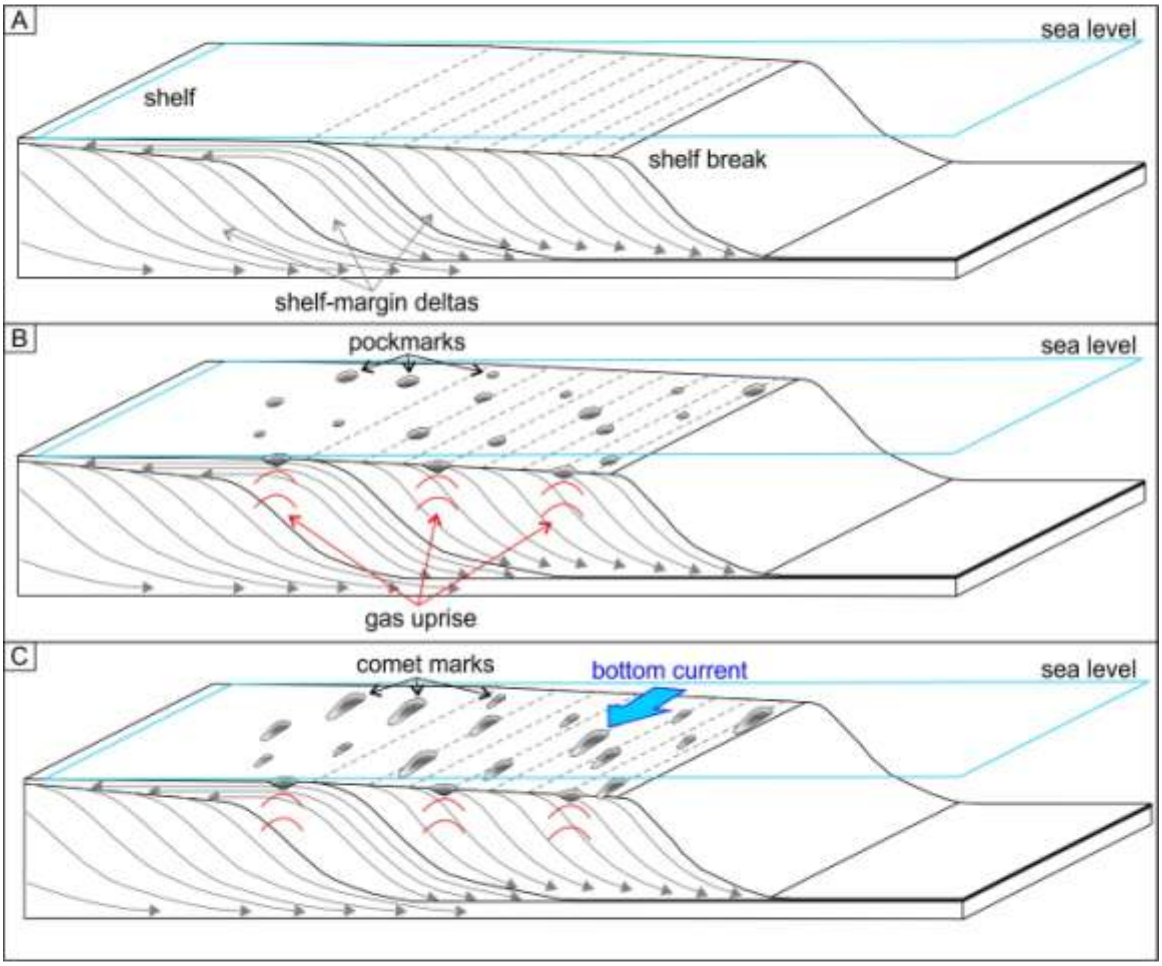

Figure C9: General scheme for development of comet marks from pockmarks in the shelf, in a sediment-starved system. In A, an extensive shelf is developed above older shelf-margin clinoforms. In B, biogenic gas ascends from shelf-margin deltas, creating pockmarks in the sea floor. In C, a relatively shallow bottom-current system creates an erosive tail from the pockmarks, originating comet marks.

The biogenic gas from underlying paleodeltas (e.g. Clayton, 1992; Evans, 2012; Nuzzo et al., 2012) travelled towards the Oligocene paleosea-floor, originating pockmarks in the surface (e.g. Cathles *et al.*, 2010; Valle and Gamberi, 2011). These pockmarks configured negative obstacles, as bottom-current erosive action over the irregular seafloor created the erosive tails, originating comet-mark-shaped features. This sequence of events is represented in Fig. C9. Although we find no previous pre-Quaternary registers of such structures, it seems plausible to consider that they are present in other basins where conditions as described above prevailed during a time interval.

2.3.8 CONCLUSIONS

As a synthesis, the development of comet marks in the study area can be explained as a combination of factors:

- sediment starvation as a result of the migration of the Paraíba do Sul paleodrainage system from north Santos Basin;
- enhanced thermohaline circulation promoted by a global cooling;
- creation of pockmarks on the shelf as a result of biogenic gas ascending from underlying deltas;
- bottom-current modulation of the pockmarks, creating an erosive tail and forming comet marks.

These factors reflect the extreme changes in environmental conditions in north Santos Basin during the Eocene-Oligocene transition. The strong orientation of these erosive features is a good indicator for a shelf-to-upper slope bottom current activity, with velocity of the flows around 0.6 m s^{-1}. The present paper shows that the identification and analysis of buried comet marks using seismic geomorphology can be a good guide for paleocurrent analysis.

2.3.9 ACKNOWLEDGEMENTS

The authors thank Universidade Federal do Paraná (UFPR) and the Laboratório de Análise de Bacias (LABAP) for the infrastructure and institutional support to the research. The Programa Interdisciplinar em Engenharia de Petróleo e Gás Natural (PRH-24) is acknowledged for providing scholarship to F.B. F.F.V. thanks the Conselho Nacional de Desenvolvimento Científico e Tecnológico (CNPq) for financial support (grants: 461628/2014-7). Seismic and well data were provided by the Agência Nacional do Petróleo, Gás Natural e Biocombustíveis (BDEP-ANP).

2.3.10 REFERENCES

Assine, M.L., Corrêa, F.S. & Chang, H.K. 2008. Migração de depocentros na Bacia de Santos: importância na exploração de hidrocarbonetos. Rev. Bras. de Geoc., **38**(2), 111-127.

Badalini, G., Browner, F., Bourque, R., Blight, R., de Bruin, G. 2010. Seismic-sequence stratigraphic analysis of regional 2D lines in the Santos Basin, offshore Brazil. Search and Disc. Article, **40538**, *online publ*.

Carlotto, MA & Rodrigues, L.F. 2009. O escorregamento Maricá – anatomia de um depósito de fluxo gravitacional de massa do Maastrichtiano, Bacia de Santos. Bol. de Geoc. da Petrobras, **18**(1), 51-67.

Carmelenghi, A., Domack, E., Rebesco, M., Gilbert, R., Ishman, S., Leventer, A., Brachfeld, S., Drake, A. 2001. Glacial morphology and post-glacial contourites in northern Prince Gustav Channel (NW Weddell Sea, Antarctica). Mar. Geoph. Res., **22**, 417-443.

Cathles, L.M., Su, Z. & Chen, D. 2010. The physics of gas chimney and pockmark formation, with implications for assessment of seafloor hazards and gas sequestration. Mar. and Petr. Geol., **27**, 82-91.

Clayton, C. 1992. Source volumetrics of biogenic gas generation. In: *Bacterial gas* (Ed. by R. Vially). Editions Technip, Paris, FRA, 191-204.

Contreras, J., Zühlke, R., Bowmann, S., Bechstädt, T. 2010. Seismic stratigraphy and subsidence analysis of the southern Brazilian margin (Campos, Santos and Pelotas basins). Mar. and Petr. Geol., **27**, 1952-1980.

dGB Earth Sciences. 2012. OpendTect version 4.6. Nijverheidstraat, NED, dGB Earth Sciences. Downloaded from http://opendtect.org/index.php/download.html, in October 22th, 2013.

Duarte, C.S.L. & Viana, A.R. 2007. Santos drift system: stratigraphic organization and implications for late Cenozoic palaeocirculation in the Santos Basin, SW Atlantic Ocean. *In*: *Economic and Palaeocenographic Significance of Contourite Deposits* (Ed. by A.R. Viana & M. Rebesco), Geological Soc. Special Publ., **276**, 171-198.

Evans, G. Deltas: the fertile dustbins of the continents. Proc. of the Geol. Assoc., **123**, 397-418.

Flemming, B.W. 1978. Underwater sand dunes along the southeast African continental margin – observations and implications. Mar. Geol., **26**, 177-198.

Flemming, B.W. 1980. Sand transport and bedform patterns on the continental shelf between Durban and Port Elizabeth (Southeast African continental margin). Sed. Geol., **26**, 179-205.

Flemming, B.W. 1984. Giant comet marks. Geo-Mar. Letters, **4**, 113-115.

Freire, A.F.M. 2013. Controle estrutural-estratigráfico na distribuição de hidratos e gases livres do anticlinal Umitaka, Bacia Joetsu, margem leste do Mar do Japão. Bol. de Geoc. da Petrobras, **21**(1), 63-84.

Galloway, W.E. 2001. Seismic expressions of deep-shelf depositional and erosional morphologies, Miocene Utsira Formation, North Sea Basin. Mar. Geoph. Res., **22**, 309-321.

Gee, M.J.R., Masson, D.G., Watts, A.B., Mitchell, N.C. 2001. Passage of debris flows and turbidity currents through a topographic constriction: seafloor erosion and deflection of flow pathways. Sedimentology, **48**, 1389-1409.

Grohmann, C.H. & Campanh, G.A. 2010. OpenStereo: open source, cross-platform software for structural geology analysis. *Abstracts from the 2010 AGU Fall Meeting*.

Heezen, B.C., Hollister, C.D. & Ruddiman, W.F. 1966. Shaping of the continental rise by deep geostrophic contour currents. Science, **152**, 502-508.

Heggland, R. 1998. Gas seepage as an indicator of deeper prospective reservoirs. A study based on exploration 3D seismic data. Mar. and Petr. Geol., **15**, 1-9.

Jobe, Z.R., Lowe, D.R. & Uchytil, S.J. 2011. Two fundamentally different types of submarine canyons along the continental margin of Equatorial Guinea. Mar. and Petr. Geol., **28**, 843-860.

Karner, G.D. & Driscoll, N.W. 1999. Tectonic and stratigraphic development of the West African and eastern Brazilian Margins: insights from quantitative basin modeling. *In*: *The Oil and Gas Habitats of the South Atlantic* (Ed. by N.R. Cameron, R.H. Bate & V.S. Clure), Geological Soc. Special Publ., **152**, 11-40.

Kenyon, N.H. 1986. Evidence from bedforms for a strong poleward current along the upper continental slope of northwestern Europe. Mar. Geol., **72**, 187-198.

Kuijpers, A., Hansen, B., Hühnerbach, V., Larsen, B., Nielsen, T., Werner, F. 2002. Norwegian Sea overflow through the Faroe-Shetland gateway as documented by its bedforms. Mar. Geol., **188**, 147-164.

Kuijpers, A., Werner, F. & Rumohr, J. 1993. Sandwaves and other large-scale bedforms as indicators of non-tidal surge currents in the Skagerrak off northern Denmark. Mar. Geol., **111**, 209-221.

Laberg, J.S., Dahlgren, T., Vorren, T.O., Haflidason, H., Bryn, P. 2001. Seismic analyses of Cenozoic contourite drift development in the northern Norwegian Sea. Mar. Geoph. Res., **22**, 401-416.

Luo, M., Chen, L., Wang, S., Yan, W., Wang, H., Chen, D. 2013. Pockmark activity inferred from pore water geochemistry in shallow sediments of the pockmark field in southwestern Xisha Uplift, northwestern South China Sea. Mar. and Petr. Geol., **48**, 247-259.

Macedo, J.M. 1989. Evolução tectônica da Bacia de Santos e áreas continentais adjacentes. Bol. de Geoc. da Petrobras, **3**,159-173.

Masson, D.G. 2001. Sedimentary processes shaping the eastern slope of the Faeroe-Shetland Channel. Cont. Shelf Res., **21**, 825-857.

McLean, S.R. 1980. The role of non-uniform roughness in the formation of sand ribbons. Mar. Geol., **42**, 49-74.

Modica, C.J. & Brush, E.R. 2004. Postrift sequence stratigraphy, paleogeography, and fill history of the deep-water Santos Basin, offshore southeast Brazil. AAPG Bull., **88**(7), 923-945.

Mohriak, W.U. & Magalhães, J.M. 1993. Estratigrafia e evolução estrutural da área norte da Bacia de Santos. *Atas do III Simp. de Geol. do Sudeste*, **1**, 19-26.

Moreira, J.L.P., Madeira, C.V., Gil, J.A., Machado, MAP. 2007. Bacia de Santos. Bol. de Geoc. da Petrobras*,* **15**(2), 531-549*.*

Moreira, J.L.P., Nalpas, T., Joseph, P., Guillocheau, F. 2001. Stratigraphie sismique de la marge éocène du Nord du Bassin de Santos (Brésil): relations plate-forme/systèmes turbiditiques; distorsion dês séquences de dépôt. Earth and Planetary Sciences, **332,** 491-498.

Nickel, J.C., di Primio, R., Mangelsdorf, K., Stoddart, D., Kallmeyer, J. 2012. Characterization of microbial activity in pockmark fields of the SW-Barents Sea. Mar. and Petr. Geol*.*, **334**, 152-162.

Nuzzo, M., Elvert, M., Schmidt, M., Scholz, F., Reitz, A., Hinrichs, K.-U., Hensen, C. 2012. Impact of hot fluid advection on hydrocarbon gas production and seepage in mud volcano sediments of thick Cenozoic deltas. Earth and Plan. Sci. Let*.*, **344**, 139-157.

Petersen, C.J., Bünz, S., Hustoft, S., Mienert, J., Klaeschen, D. 2010. High-resolution P-Cable 3D seismic imaging of gas chimney structures in gas hydrated sediments of an Arctic sediment drift. Mar. and Petr. Geol*.*, **27**, 1981-1994.

Posamentier, H.W., Davies, R.J., Cartwright, J.A., Wood, L. 2007. Seismic geomorphology – an overview. In: *Seismic geomorphology: applications to hydrocarbon exploration and production*. Ed. by R.J. Davies, H.W. Posamentier, L.J. Wood, J.A. Cartwright. Geol. Soc. Spec. Publ., **277**, 1-14.

Posamentier, H.W. & Kolla, V. 2003. Seismic geomorphology and stratigraphy of depositional elements in deep-water settings. J. of Sed. Res*.*, **73** (3), 367-388.

Prather, B.E., Deptuck, M.E., Mohrig, D., van Hoorn, B., Wynn, R.B. 2012. Application of the principles of seismic geomorphology to continental-slope and base-of-slope systems: case studies from seafloor and near-seafloor analogues. SEPM Spec. Publ., **99**, 5-9.

Reineck, H.-E. & Singh, I. B. 1980. *Depositional sedimentary environments with reference to terrigenous clastics*. Springer-Verlag, Berlin, GER, 551 p.

Ribeiro, M.C.S. 2007. Termocronologia e história denudacional da Serra do Mar e implicações no controle deposicional da Bacia de Santos. Dr. Scient. thesis, UNESP.

Sahy, D., Condon, D.J., Terry Jr., D.O., Fischer, A.U., Kuiper, K.F. 2015. Synchronizing terrestrial and marine records of environmental change across the Eocene-Oligocene transition. Earth and Plan. Sci. Lett., **427**, 171-182.

Stow, D.A.V., Faugères, J.-C., Viana, A., Gonthier, E. 1998. Fossil contourites: a critical review. Sed. Geol., **115**, 3-31.

Sylvester, Z., Deptuck, M.E., Prather, B., Pirmez, C., O'Byrne, C. 2012. Seismic stratigraphy of a shelf-edge delta and linked submarine channels in the northeastern Gulf of Mexico. SEPM Spec. Publ., **99**, 31-59.

Trincardi, F., Verdicchio, G. & Miserocchi, S. 2007. Seafloor evidence for the interaction between cascading and along-slope bottom water masses. J. of Geoph. Res., **112**, *online publ*.

Valle, G.D. & Gamberi, F. 2011. Pockmarks and seafloor instability in the Olbia continental slope (northeastern Sardinian margin, Tyrrhenian Sea). Mar. Geoph. Res., **32**, 193-205.

Verdicchio, G. & Trincardi, F. 2006. Short-distance variability in slope bed-forms along the southwestern Adriatic Margin (Central Mediterranean). Mar. Geol., **234**, 271-292.

Viana, A.R. 2002. Seismic expression of shallow- to deep-water contourites along the south-eastern Brazilian margin. Mar. Geoph. Res., **22**, 509-521.

Viana, A.R., Faugères, J.-C. & Stow, D.A.V. 1998. Bottom-current-controlled sand deposits – a review of modern shallow- to deep-water environments. Sed. Geol., **115**, 53-80.

Werner, F. & Newton, R.S. 1975. The pattern of large-scale bed forms in the Langeland Belt (Baltic Sea). Mar. Geol., **19**, 29-59.

Werner, F., Ünsold, G., Koopmann, B., Stefanon, A. 1980. Field observations and flume experiments on the nature of comet marks. Sed. Geol., **26**, 233-262.

Wynn, R.B. & Masson, D.G. 2008. Sediment waves and bedforms. Developments in Sedimentology, **60**, 289-300.

3. CONSIDERAÇÕES FINAIS

O intervalo eoceno no norte da Bacia de Santos é um estudo de caso ideal para a avaliação dos controles do aporte sedimentar e das variações do nível de base sobre a arquitetura estratigráfica e a deposição marinha profunda. O alto aporte sedimentar resultou em um empilhamento essencialmente progradacional, expresso nos dados sísmicos em deltas de margem de plataforma e clinoformas de talude. Os rebaixamentos do nível de base contribuíram para que depósitos de *topset*, formados em períodos de regressão normal, sejam exceção no intervalo. Geralmente os *topsets* são truncados, associados a trajetórias de margem de plataforma fortemente descendentes.

Este contexto é preferencial para o transporte de sedimentos para o mar profundo, na forma de turbiditos arenosos e depósitos de transporte em massa. De fato, os turbiditos são comuns no intervalo eoceno, e os DTMs formam depósitos de ampla distribuição na área de estudo. Ainda que os fatores atuantes na geração destes depósitos sejam os mesmos, sua história evolutiva se mostra diferente. Os turbiditos arenosos se encontram distribuídos ao longo de todo intervalo, destacando-se os grandes volumes de turbiditos associados aos deltas de margem de plataforma nas sequências E31 e E32. Isto demonstra que o principal controle para sua deposição foi o alto aporte sedimentar associado à denudação da Serra do Mar durante o máximo termal do Eoceno (ETM), ainda que as regressões forçadas tenham sido períodos preferenciais ao transporte de areia para o mar profundo.

Os DTMs apresentam controle maior dos rebaixamentos do nível de base. Neste caso, o alto aporte de sedimentos contribuiu para a sobrecarga da margem da plataforma durante as regressões normais, em fases de agradação na plataforma. Entretanto, os gatilhos para os escorregamentos submarinos que originaram os DTMs foram rebaixamentos do nível de base que alteraram o perfil de equilíbrio submarino. Esta sequência de eventos implica em um *timing* de disparo de escorregamentos submarinos em algum momento da transição de regressão normal para regressão forçada. Consequentemente, na escala de trabalho da sismoestratigrafia, a cicatriz de escorregamento e a superfície basal de descolamento do DTM configuram uma superfície basal de regressão forçada (BSFR). Gradiente acima, a superfície é truncada pela discordância subaérea formada durante o rebaixamento do nível de base, enquanto em direção à bacia se torna uma concordância correlata.

O final do período Eoceno foi marcado por mudanças ambientais que reduziram o aporte sedimentar para a bacia. Estas mudanças, que incluem um evento de resfriamento global no Oligoceno e a reorganização dos sistemas de drenagem da Serra do Mar, ocasionaram a mudança da arquitetura regressiva do Eoceno para um arranjo transgressivo. A redução do aporte sedimentar suprimiu a geração de turbiditos e DTMs neste período, predominando processos erosivos relacionados à ação de correntes de fundo recém estabelecidas em consequência das mudanças climáticas. Na área de estudo, foram formadas *comet marks* na região da plataforma e talude superior, indicativas de baixa disponibilidade de sedimentos e ação de correntes de fundo de alta energia com fluxo para NE.

Estas conclusões demonstram a importância de uma abordagem de múltiplos métodos na sismoestratigrafia, para uma caracterização mais detalhada da evolução estratigráfica de um intervalo estratigráfico. Técnicas e conceitos clássicos da estratigrafia de sequências (e.g. determinação de padrões de terminações de refletores; diagramas de Wheeler) se mostraram mais confiáveis quando utilizados em conjunto com técnicas alternativas (e.g. trajetórias de migração da margem da plataforma; mapeamento da quebra da plataforma). Em adição, informações provenientes da análise de fácies sísmicas e da geomorfologia sísmica permitiram maior detalhamento de elementos deposicionais e feições erosivas em subsuperfície, e consequentemente, interpretações a respeito das condições de formação destas feições.

REFERÊNCIAS BIBLIOGRÁFICAS

Alves, T.M., Kurtev, K., Moore, G.F., Strasser, M. 2014. Assessing the internal character, reservoir potential, and seal competence of mass-transport deposits using seismic texture: a geophysical and petrophysical approach. AAPG Bull., **98**(4), 793-824.

Arienti, L., Mucelini, H., Gontijo, R.C., Voelcker, H.E. 2009. Turbidite systems and their stratigraphic evolution in the Oligomiocene and Miocene of Campos Basin – Brazil. *AAPG Int. Conf. and Exhibit.*, Rio de Janeiro, 2009.

Burgess, P.M. & Hovius, N. 1998. Rates of delta progradation during highstands: consequences for timing of deposition in deep-marine systems. J. of the Geol. Soc., **155**, 217-222.

Carminatti, M., Guardado, L.R., Martins, C.C., D'Ávila, R.S.F., Spadini, A.R., Appi, C.J. 2000. The contribution of sedimentological studies on deep-water deposits in the Petrobras exploration process. *In*: *Deep-water sedimentation: technological challenges for the next millenium*. 2000. Ed. by C.J. Appi. ABGP, Rio de Janeiro, RJ, 81-84.

Carvajal, C.R. & Steel, R.J. 2006. Thick turbidite successions from supply-dominated shelves during sea-level highstand. Geology, **34**(8), 665-668.

Carvajal, C.R., Steel, R.J. & Petter, A. 2009. Sediment supply: the main driver of shelf-margin growth. Earth-Sci. Rev., **96**, 221-248.

Catuneanu, O. 2002. Sequence stratigraphy of clastic systems: concepts, merits, and pitfalls. J. of African Earth Sci., **35,** 1-43.

Catuneanu, O. 2006. *Principles of sequence stratigraphy*. Elsevier, Amsterdan, ND, 375p.

Catuneanu, O., Abreu, V., Bhattacharya, J.P., Blum, M.D., Dalrymple, R.W., Eriksson, P.G., Fielding, C.R., Fisher, W.L., Galloway, W.E., Gibling, M.R., Giles, K.A., Holbrook, J.M., Jordan, R., Kendall, C.G.St.C., Macurda, B., Martinsen, O.J., Miall, A.D., Neal, J.E., Nummedal, D., Pomar, L., Posamentier, H.W., Pratt, B.R., Sarg, J.F., Shanley, K.W., Steel, R.J., Strasser, A., Tucker, M.E., Winker, C. 2009. Towards the standardization of sequence stratigraphy. Earth-Science Rev., **92**, 1-33.

Chang, H.K., Assine, M.L., Corrêa, F.S., Tinen, J.S., Vidal, A.C., Koike, L. 2008. Sistemas petrolíferos e modelos de acumulação de hidrocarbonetos na Bacia de Santos. Rev. Bras. de Geoc., **38**(2), 29-46.

Contreras, J.; Zühlke, R.; Bowman, S.; Bechstädt, T. 2010. Seismic stratigraphy and subsidence analysis of the southern Brazilian margin (Campos, Santos and Pelotas basins). Mar. and Petr. Geol., **27**, 1952-1980.

Della Fávera, J.C. 2000. History of interpretation of deep-water sandstones in Brazil. *In*: *Deep-water sedimentation: technological challenges for the next millenium*. 2000. Ed. by C.J. Appi. ABGP, Rio de Janeiro, RJ, 12-15.

Dias, J.L. 2008. Estratigrafia e sedimentação dos evaporitos neo-aptianos na margem leste brasileira. *In*: *Sal: geologia e tectônica*. 2008. Org. by W.U. Mohriak, P. Szatman & S.M.C. Anjos. Beca, São Paulo, BR, 220-229.

Dixon, J.F., Steel, R.J. & Olariu, C. 2012. Shelf-edge delta regime as a predictor of deep-water deposition. J. of Sed. Res. **82,** 681-687.

Dixon, J.F., Steel, R.J. & Olariu, C. 2013. A model for cutting and healing of deltaic mouth bars at the shelf edge: mechanism for basin-margin accretion. J. of Sed. Res., **83**, *online publ.*

Duarte, C.S.L. & Viana, A.R. 2007. Santos drift system: stratigraphic organization and implications for late Cenozoic palaeocirculation in the Santos Basin, SW Atlantic Ocean. *In*: *Economic and Palaeocenographic Significance of Contourite Deposits*. 2007. Ed. by A.R. Viana & M. Rebesco. Geological Soc. Special Publ., **276**:171-198.

Gamberi, F., Rovere, M. & Marani, M. 2011. Mass-transport complex evolution in a tectonically active margin (Gioia Basin, Southeastern Tyrrhenian Sea). Mar. Geol., **279,** 98-110.

Helland-Hansen, W. & Hampson, G. J. 2009. Trajectory analysis: concepts and applications. Basin Res., **21**, 454-483.

Johannessen, E.P. & Steel, R.J. 2005. Shelf-margin clinoforms and prediction of deepwater sands. Basin Res., **17**, 521-550.

Karner, G.D. & Driscoll, N.W. 1999. Tectonic and stratigraphic development of the West African and eastern Brazilian Margins: insights from quantitative basin modeling. *In*: *The oil and gas habitats of the South Atlantic*. 1999. Ed. by N.R. Cameron, R.H. Bate & V.S. Clure. Geol. Soc. Spec. Publ., London, **153**, 11-40.

Lourens, L.J., Sluijs, A., Kroon, D., Zachos, J.C., Thomas, E., Röhl, U., Bowles, J., Raffi, I. 2005. Astronomical pacing of late Palaeocene to early Eocene global warming events. Nature Let., **435,** 1083-1087.

Macedo, J.M. 1989. Evolução tectônica da Bacia de Santos e áreas continentais adjacentes. Bol. de Geoc. da Petrobras, **3**, 159-173.

Modica, C.J.; Brush, E.R. 2004. Postrift sequence stratigraphy, paleogeography, and fill history of the deep-water Santos Basin, offshore southeast Brazil. AAPG Bull, **88**(7), 923-945.

Mohriak, W.U. 2003. Bacias sedimentares da margem continental brasileira. *In*: *Geologia, tectônica e recursos minerais do Brasil*. 2003. Ed. by L.A. Bizzi, C. Schobbenhaus, R.M. Vidotti, H. Gonçalves. CPRM, Brasília, DF, 87-165.

Mohriak, W.U. 2012. Bacias de Santos, Campos e Espírito Santo. *In*: *Geologia do Brasil*. 2012. Org. by Y. Hasui, C.D.R. Carneiro, F.F.M. de Almeida, A. Bartorelli. Beca, São Paulo, BR, 481-496.

Mohriak, W.U. & Magalhães, J.M. 1993. Estratigrafia e evolução estrutural da área norte da Bacia de Santos. *Atas do III Simp. de Geol. do Sudeste*, **1**, 19-26.

Monteverde, D.H., Mountain, G.S. & Miller, K.G. 2008. Early Miocene sequence development accross the New Jersey margin. Basin Res., **20**, 249-267.

Morais Júnior, J.J. & Toledo, J.B. 1993. A exploração de petróleo na Bacia de Santos. *Atas do III Simp. de Geol. do Sudeste*, **1,** 27-32.

Moreira, J.L.P., Madeira, C.V., Gil, J.A., Machado, M.A.P. 2007. Bacia de Santos. *Bol*. de Geoc. da Petrobras, **15**(2), 531-549.

Moscardelli, L. & Wood, L. 2008. New classification system for mass transport complexes in offshore Trinidad. Basin Res., **20**, 73-98.

Muto, T. & Steel, R. J. 2002. In defense of shelf-edge delta development during falling and lowstand of relative sea level. The J. of Geol., **110**, 421-436.

Mutti, E., Tinterri, R., Magalhaes, P.M., Basta, G. 2007. Deep-water turbidites and their equally important shallower water cousins. Search and Disc. Article, **50057**, *online publ.*

Pereira, M.J., Barbosa, C.M., Agra, J., Gomes, J.B., Aranha, L.G.F., Saito, M., Ramos, M.A., de Carvalho, M.D., Stamato, M., Bagni, O. 1986. Estratigrafia da Bacia de Santos: análise das sequências, sistemas deposicionais e revisão litoestratigráfica. *Anais do XXXIV Congr. Bras. de Geol.*, Goiânia. **1**, 65-79.

Pereira, M.J. & Macedo, J.M. 1990. A Bacia de Santos: perspectivas de uma nova província petrolífera na plataforma continental sudeste brasileira. Bol. de Geoc. da Petrobras, **4**(1), 3-11.

Plink-Björklund, P. & Steel, R.J. 2002. Sea-fall below the shelf edge, without basin-floor fans. Geology, **30**(2),115-118.

Posamentier, H.W., Allen, G.P. 1999. *Siliciclastic sequence stratigraphy – concepts and applications*. SEPM, Tulsa, USA, 210p.

Posamentier, H.W. & Martinsen, O.J. 2011. The character and genesis of submarine mass-transport deposits: insights from outcrop and 3D seismic data. SEPM Spec. Publ., **96**:7-38.

Posamentier, H.W. & Vail, P.R. 1988. Eustatic controls on clastic deposition II – sequence and systems tract models. *In*: *Sea level changes: an integrate approach*. 1988. Ed. by C.K. Wilgus, B.S. Hastings, C.G.St.C. Kendall, H.W. Posamentier, C.A. Ross, J.C. van Wagoner. SEPM Spec. Publ., **42**, 125-154.

Ribeiro, M.C.S. 2007. *Termocronologia e história denudacional da Serra do Mar e implicações no controle deposicional da Bacia de Santos*. Tese de Doutoramento, Rio Claro, Instit. de Geoc. e Ciên. Exat. da Univ. Estad. Paul., 227p

Safronova, P.A., Henriksen, S., Andreassen, K., Laberg, J.S., Vorren, T.O. 2014. Evolution of shelf-margin clinoforms and deep-water fans during the middle Eocene in the Sørvestsnaget Basin, southwest Barents Sea. AAPG Bull., **98**(3), 515-544.

Sahy, D., Condon, D.J., Terry Jr., D.O., Fischer, A.U., Kuiper, K.F. 2015. Synchronizing terrestrial and marine records of environmental change across the Eocene-Oligocene transition. Earth and Plan. Sci. Lett., **427**, 171-182.

Schlager, W. 1993. Accommodation and supply – a dual control on stratigraphic sequences. Sed. Geol., **86**, 111-136.

Sombra, C.L., Arienti, L.M., Pereira, M.J., Macedo, J.M. 1990. Parâmetros controladores da porosidade e da permeabilidade nos reservatórios clásticos profundos do campo de Merluza, Bacia de Santos, Brasil. Bol. de Geoc. da Petrobras, **4**(4), 451-466.

Vail, P.R., Mitchum, R.M. & Thompson, S. 1977. Seismic stratigraphy and global changes of sea level: part 4. Global cycles and relative changes of sea level. *In*: *Seismic stratigraphy – application to hydrocarbon exploration*. 1977. Ed. by C.E. Payton. AAPG Mem., **26**:83-98.

Walker, R.G. 1990. *Submarine fan models on seismic studies: a geological perspective.* McMaster Univ., Hamilton, CAN, 109p.

Williams, B.G., Hubbard, R.J. 1984. Seismic framework and depositional sequences in the Santos Basin. Mar. and Petr. Geol., **1,** 90-104.

Zalán, P.V. & Oliveira, J.A.B. 2005. Origem e evolução estrutural do Sistema de Riftes Cenozóicos do Sudeste do Brasil. Bol. de Geoc. da Petrobras, **13**(2), 269-300.